AD-A246 022

AD_____

EVALUATION OF NO_X-INDUCED TOXICITY

ANNUAL REPORT

DTIC
ELECTE
FEB 03 1992
S B D

BRUCE E. LEHNERT
DOUGLAS M. STAVERT

NOVEMBER 20, 1991

Supported by

U.S. ARMY MEDICAL RESEARCH AND DEVELOPMENT COMMAND
Fort Detrick, Frederick, Maryland 21702-5012

91MM1509

Los Alamos National Laboratory
Los Alamos, New Mexico 87545

Approved for public release; distribution unlimited.

The findings in this report are not to be construed as an official Department of the Army position unless so designated by other authorized documents

92-02587

Best
Available
Copy

REPORT DOCUMENTATION PAGE

Form Approved
OMB No. 0704-0188

Public reporting burden for this collection of information is estimated to average 1 hour per response, including the time for reviewing instructions, searching existing data sources, gathering and maintaining the data needed, and completing and reviewing the collection of information. Send comments regarding this burden estimate or any other aspect of this collection of information, including suggestions for reducing this burden to Washington Headquarters Services, Directorate for information Operations and Reports, 1215 Jefferson Davis Highway, Suite 1204, Arlington, VA 22202-4302, and to the Office of Management and Budget, Paperwork Reduction Project (0704-0188), Washington, DC 20503

1. AGENCY USE ONLY (Leave blank)	2. REPORT DATE	3. REPORT TYPE AND DATES COVERED
	November 20, 1991	Annual 25 Oct 90 - 30 Sep 91

4. TITLE AND SUBTITLE
Evaluation of NO_x-Induced Toxicity

5. FUNDING NUMBERS
91MM1509
61102A
3M161102BS15 CG
DA335695

6. AUTHOR(S)
Bruce E. Lehnert
Douglas M. Stavert

7. PERFORMING ORGANIZATION NAME(S) AND ADDRESS(ES)
Los Alamos National Laboratory
Los Alamos, New Mexico 87545

8. PERFORMING ORGANIZATION REPORT NUMBER

9. SPONSORING/MONITORING AGENCY NAME(S) AND ADDRESS(ES)
U.S. Army Medical Research & Development Command
Fort Detrick
Frederick, Maryland 21702-5012

10. SPONSORING/MONITORING AGENCY REPORT NUMBER

11. SUPPLEMENTARY NOTES

12a. DISTRIBUTION/AVAILABILITY STATEMENT
Approved for public release; distribution unlimited

12b. DISTRIBUTION CODE

13. ABSTRACT *(Maximum 200 words)*

This report summarizes experimental approaches and the results of investigations of the pulmonary toxicity of NO_x that were conducted at the Los Alamos National Laboratory during FY91. Herein we describe: 1) how ventilatory patterns are altered by the inhalation of high concentrations of nitrogen dioxide [NO_2], 2) how the ventilatory response(s) to CO_2 are altered by the concurrent inhalation of high concentrations of NO_2, 3) the results of studies of the relative severities of pulmonary injury caused by NO_2 when inhaled under resting and CO_2-driven minute ventilations, 4) assessments of the severity of NO_2-induced lung injury in the context of actual inhaled doses, 4) findings obtained about the relationship of the severity of NO_2-induced injury in terms of

14. SUBJECT TERMS
RA 3; Nitrogen oxides; Toxicity

15. NUMBER OF PAGES

16. PRICE CODE

17. SECURITY CLASSIFICATION OF REPORT	18. SECURITY CLASSIFICATION OF THIS PAGE	19. SECURITY CLASSIFICATION OF ABSTRACT	20. LIMITATION OF ABSTRACT
Unclassified	Unclassified	Unclassified	Unlimited

13. ABSTRACT (CONTINUED)

exposure mass concentration and duration, 5) how post-exposure exercise can potentiate lung injury caused by short burst, high concentration NO_2 exposure, 6) the kinetics of lung free cell and biochemical changes in lavage fluids following exposure to a high concentration of NO_2, and 7) further refinements that have been made in our mathematical model that describes the accumulation and elimination of methemoglobin during and after exposure to nitric oxide [NO], respectively.

Accession For
NTIS GRA&I
DTIC TAB
Unannounced
Justification
By
Distribution/
Availability Codes
Dist | Avail and/or Special
A-1

FOREWORD

In conducting research using animals, the investigator(s) adhered to the "Guide for the Care and Use of Laboratory Animals," prepared by the Committee on Care and Use of Laboratory Animals of the Institute of Laboratory Animal Resources Commission on Life Sciences, National Research Council (DHHS, PHS, NIH Publication No. 86-23, Revised 1985).

Citations of commercial organizations and trade names in this report do not constitute an official Department of the Army endorsement or approval of the products or services of these organizations.

ANNUAL REPORT

PRINCIPAL INVESTIGATORS:

Bruce E. Lehnert, Ph.D.
Douglas M. Stavert, M.A.

INSTITUTION:
Cell Growth, Damage and Repair Group, LS-1
Life Sciences Division, MS M888
Los Alamos National Laboratory
Los Alamos, New Mexico 87545

Scientific Accomplishments/Progress

Severity of NO_x-Induced Lung Injury Relative to Minute Ventilation (VE)

We have shown in previous studies (Toxicologist 9:a746,1989) that a general reduction of minute ventilation (VE) occurs during the inhalation of high concentrations of NO_2 (>100 ppm). This reduction in VE potentially could serve to protect the lower respiratory tract by lowering the mass of inhaled NO_2 entering the lung. Little experimental attention, however, has been given to characterizing the effects of increased ventilation during exposure to NO_2 exposure. The objectives of this component of the project were: 1) to further characterize the ventilatory response(s) to the inhalation of relatively high concentrations of NO_2, 2) to examine how the ventilatory response to CO_2, a major gas constituent in many typical combustion atmospheres, is altered by the concurrent inhalation of high concentrations of NO_2, 3) to investigate the relative severities of pulmonary injury caused by NO_2 when inhaled under "normal" VE and "CO_2-driven" VE conditions, 4) to examine the severity of NO_2-induced lung injury in the context of actual inhaled dose, and 5) to assess the relationship of NO_2-induced lung injury in terms of mass concentration and exposure duration.

Fischer-344 rats (SPF) were trained (3 days) to occupy partial body

flow plethysmographs. On the day of exposure, the animals were placed into the plethysmographs and they were provided clean filtered air for 5 min while pre-exposure ventilatory parameters were measured. Exposure atmospheres consisting of either filtered air with or without 5% CO_2 (controls), or 100, 300, or 1000 ppm NO_2 with or without 5% CO_2 were then delivered to the rats for various durations ranging from 1 min to 20 min with the ventilatory parameters being measured over these exposure periods. For the 1000 ppm short-duration exposures, the animals were pre-exposed to 5% CO_2 before the NO_2 exposure. After cessation of the exposures, clean air was again delivered to the animals for 5 to 15 min while post-exposure ventilatory parameters were measured. After the exposures, the animals were returned to animal housing and sacrificed 24 hrs after the exposures for histologic analyses of their lower respiratory tracts and for lung gravimetric measurements.

NO_2 exposure atmospheres were generated by mixing pure NO_2 with anhydrous HEPA filtered air within a quartz glass mixing chamber. CO_2 was added and adjusted to 5% immediately upstream of the exposure chamber. As previously indicated the animals were exposed to the atmospheres while in a flow plethysmograph, Figure 1. A Teflon head piece with 2 rubber dams effectively sealed the body of the animal within the plethysmograph. A neck brace stabilized the animal during exposure. Rat sacrifices were initiated by I.P injections of 50 mg pentobarbital sodium. The trachea and lungs were excised, and the heart, extra-pulmonary mediastinal tissue, and the esophagus were removed. The lungs were blotted and weighed (Lung Wet Weight, LWW). The bronchus leading to the right cranial lobe (RCL) was ligated with fine suture and the RCL was removed and weighed (Right Cranial Lobe Wet Weight, RCLWW). Following the gravimetric measurements, the trachea and lungs, minus the RCL, was cannulated with an 18-ga. needle that was secured with ligature and the lungs were subsequently infused and fixed at a constant pressure of 30 cm H_2O with 10% formalin in phosphate buffered saline. The RCLs were oven dried to a constant weight at 100°C for 36 hrs and reweighed (Right Cranial Lobe Dry Weight, RCLDW). Inasmuch as the RCLWW generally scaled with LWW values, only the LWW and RCLDW will be summarized herein. Histopathologic assessments focused on the appearance of fibrin, accumulations of PMN and alveolar macrophages (AM), the extravasation of erythrocytes, vascular congestion, and alveolar cuboidal cell hyperplasia, i.e. Type II cell hyperplasia. With the exception of vascular congestion, a grading scale was used to quantitatively describe the relative severity of each of the above pathologic features in terms of their: (1) distribution, i.e., relative number of terminal bronchioles showing a lesion in associated alveolar structures, (2) severity, or the relative number of periterminal bronchiolar alveolar structures affected, and (3) intensity,

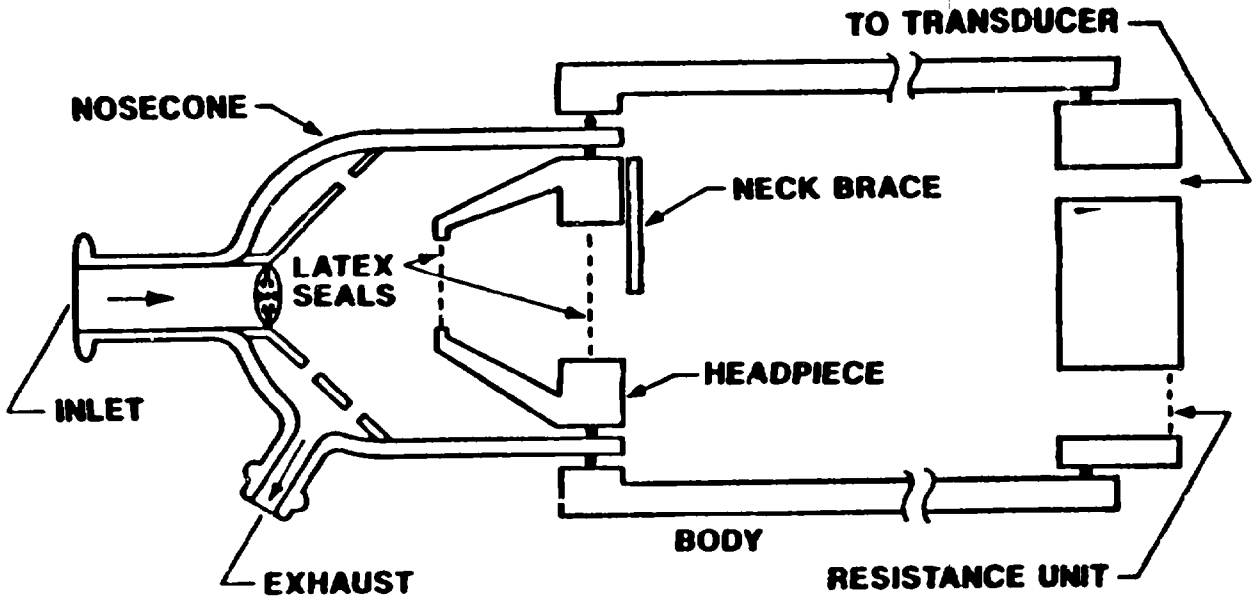

Figure 1. Illustration of a partial body flow plethysmograph used for the ventilatory measurements in this study. The nose cone is the front portion of a LANL quartz glass exposure tube. The headpiece is designed to hold the head of the rat in position during an exposure as well as to seal the animal within the body portion of the plethysmograph. The body portion and resistance unit allow for the measurement of pressure fluctuations within the plethysmograph, which are proportional to volume changes.

the relative amount of material or relative alterations of cells in the alveoli. The distribution index for a given pathologic feature ranged from 0-4 with 0 = not observed, 1=single or focal in appearance, 2=few but multifocal, 3= moderate number to many involved terminal airway structures, and 4=all or essentially all alveolar structures were affected, i.e., diffuse. The relative severity index for a given pathologic feature ranged from 0-3 with 0=no abnormality, 1=the focal appearance of the abnormality in the periterminal alveolar structures, 2=focal to multifical appearance, 3= several affected alveolar structures, and 4=many to all periterminal alveolar structures demonstrated the abnormality. The relative intensity index ranged from 0 to 4 with 0=no abnormality, 1=trace but detectable alterations in the amount of abnormal material, 2=mild amount of small changes in cell numbers, 3=moderate amount of abnormal material or abnormal number of cells, and 4=large amounts of intra-alveolar material of large changes in cell numbers.

In general, VE was reduced upon the inhalation of most NO_2 atmospheres, Figure 2, compared to the VE measured from air control exposed animals. The reduction in VE was greatest with the higher concentrations of inhaled NO_2. Overall VE reductions of approximately 7% and 15% were measured during the 100 ppm NO_2 x 15 min and 20 min exposures, respectively, while greater reductions in VE of ~20% and ~28% we e measured during inhalation of 1000 ppm NO_2 x 1 and 2 min exposures. Exposures to 100 ppm NO_2 x 10 min did not produce significant changes in VE. These reductions of VE were primarily due to reductions in VT, Figures 2, 3 and 4. While breathing frequency (f) increased slightly during during most NO_2 exposures compared to f measurements on air exposed animals, VT decreased by as much as 40%. The greatest reductions in VT were measured during the exposures to the highest NO_2 concentrations studied. The ventilatory response to CO_2 during air breathing was a VE increase of ~65% primarily due to increases in VT (42%), as compared to increases in f (21%). The ventilatory response to CO_2 during concurrent NO_2 inhalation was greatly reduced, Figure 2. Increases in VE averaged only ~40% during the 100 to 300 ppm NO_2 + 5% CO_2 exposures compared to only a ~25% increase of VE during 1000 ppm NO_2 x 2 min exposure. No significant increase in VE occurred during the 1000 ppm NO_2 x 1 min exposure. The increased VE measured during NO_2 + CO_2 exposures was primarily related to increases in VT and to a lesser extent to increases in f. Breathing frequency actually fell during the 1000 ppm NO_2 + CO_2 exposure levels.

Lung wet weights (LWW), Figure 5, and right cranial lobe dry weights (RCLDW), Figure 6, measured 24 hr after the NO_2 exposure regimens used in this study were all significantly greater compared to values measured with animals exposed to air only. LWW and RCLDW increased with

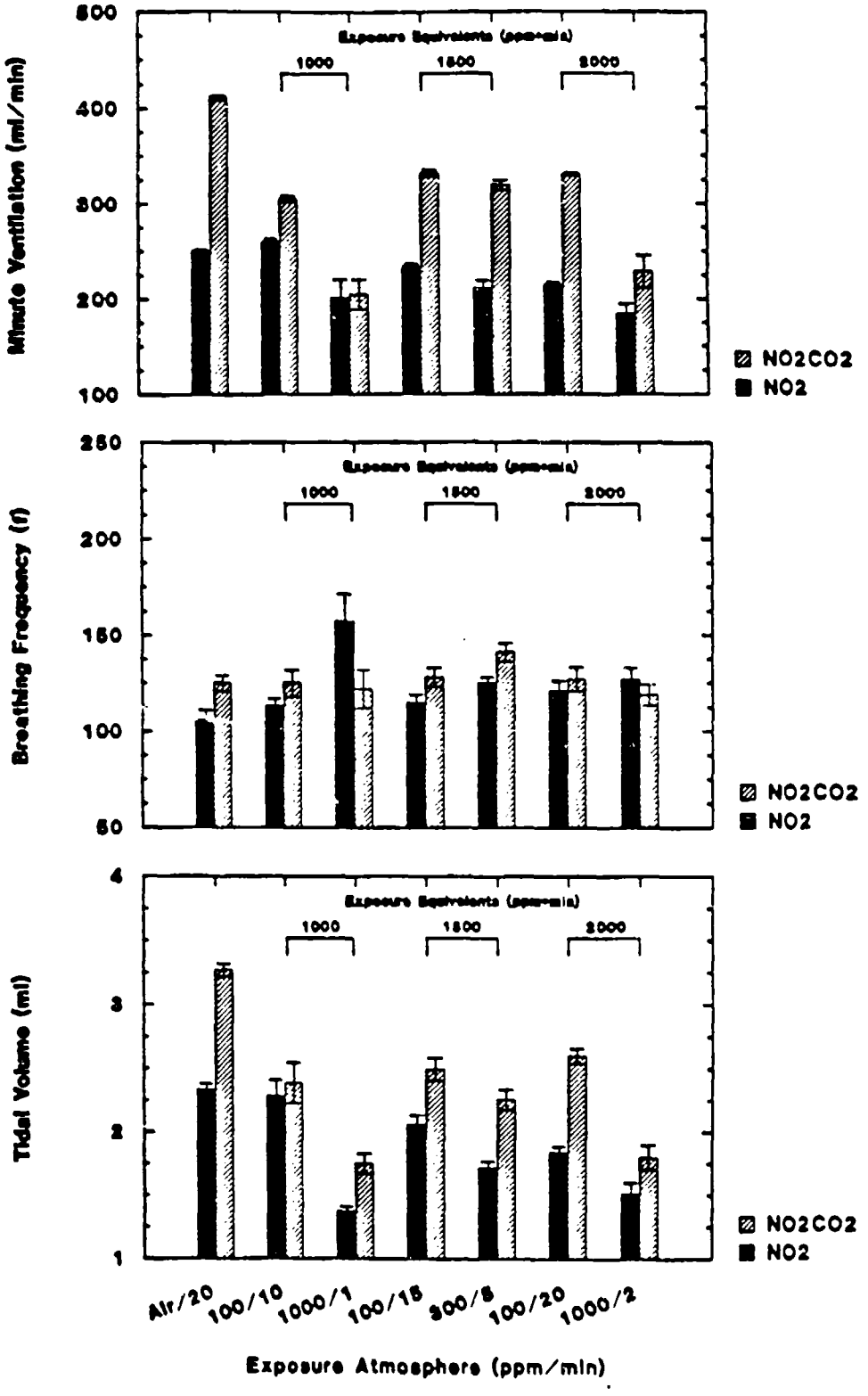

Figure 2. Minute ventilation (V_E), breathing frequency (f), and tidal volume (V_T) of awake rats during exposures to air, or to NO_2 at different concentrations (ppm) and durations (min). Also represented are the ventilatory responses during identical exposure scenarios with the addition of 5% CO_2. Each bar represents the mean and S.E.M. for N = 6 to 12 animals.

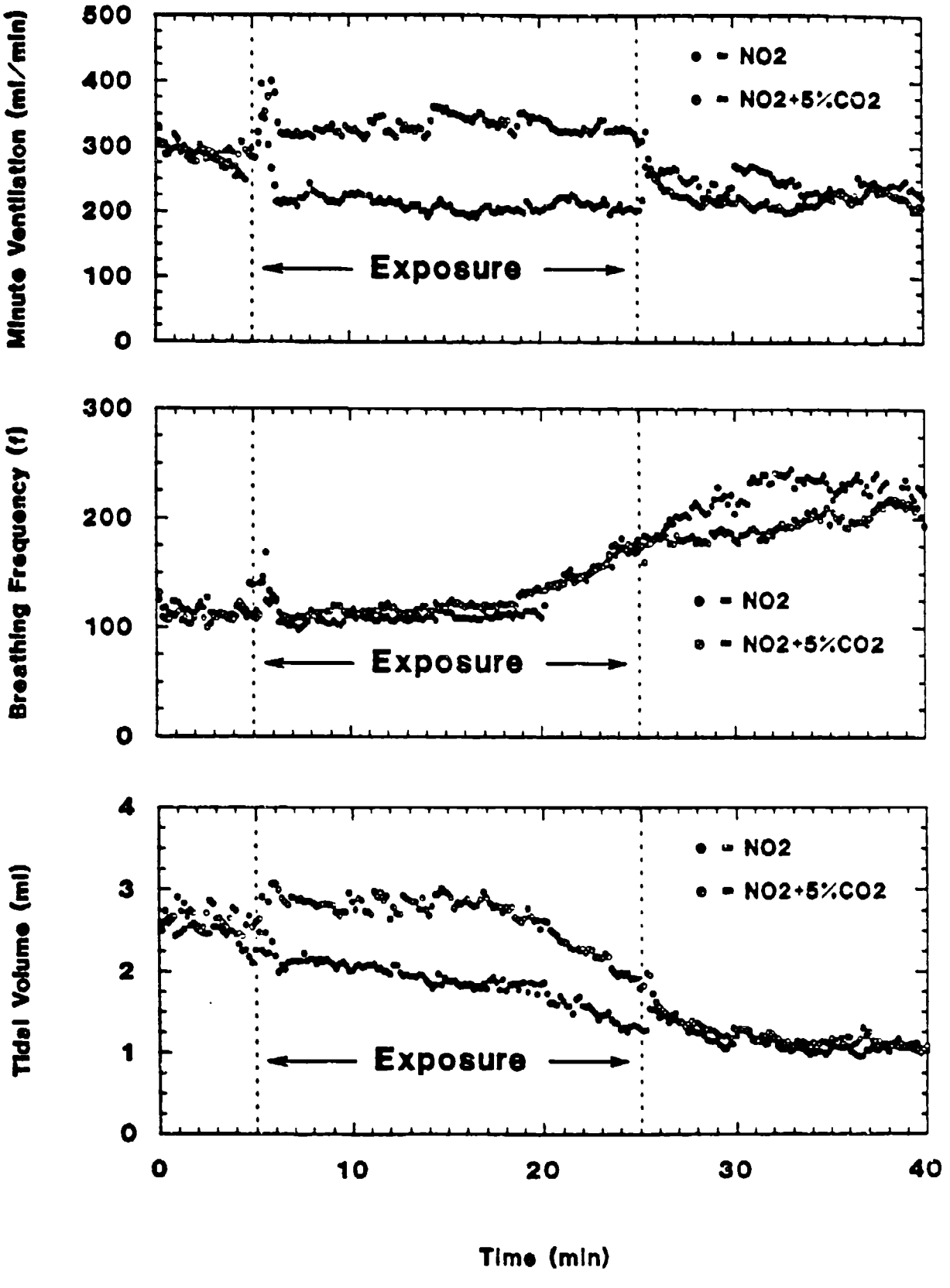

Figure 3. Minute ventilation (V_E), breathing frequency (f) and tidal volume (V_T) measurements during the pre-exposure, exposure, and post exposure phase of the 100 ppm x 20 min exposure scenario with and without 5% CO_2. Each point represents the mean values of breath by breath ventilatory measurements over a 10 second period for N= 12 animals.

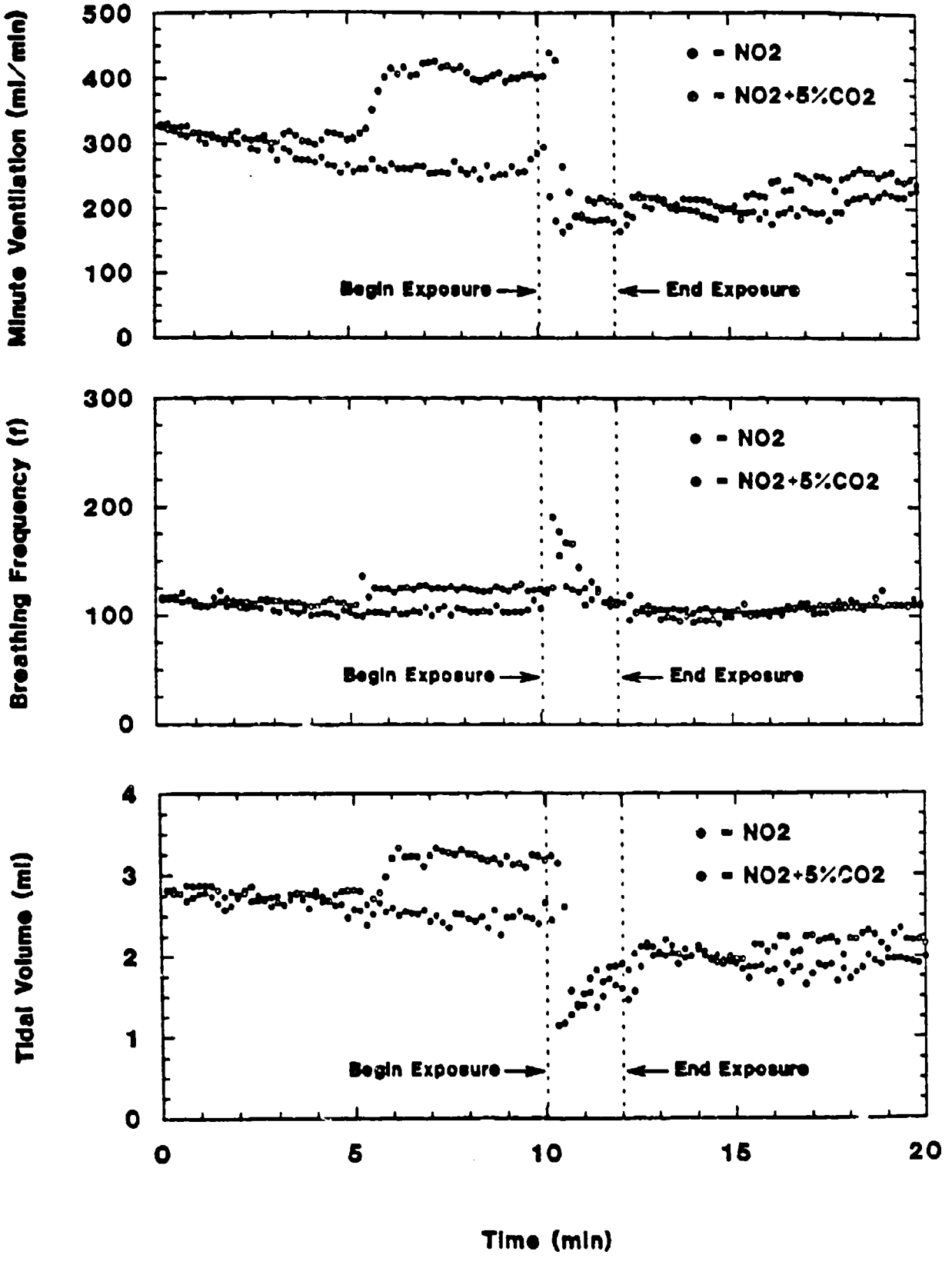

Figure 4. Minute ventilation (V_E), breathing frequency (f) and tidal volume (V_T) measurements during the pre-exposure, exposure and post exposure phase of the 1000 ppm x 2 min exposure scenario with and without 5% CO_2. The NO_2 + CO_2 group of animals were preloaded with 5% CO_2 during the last 5 minutes of the pre-exposure data collection period. Each point represents the mean values of breath by breath ventilatory measurements over a 10 second period for N= 9 to 11 animals.

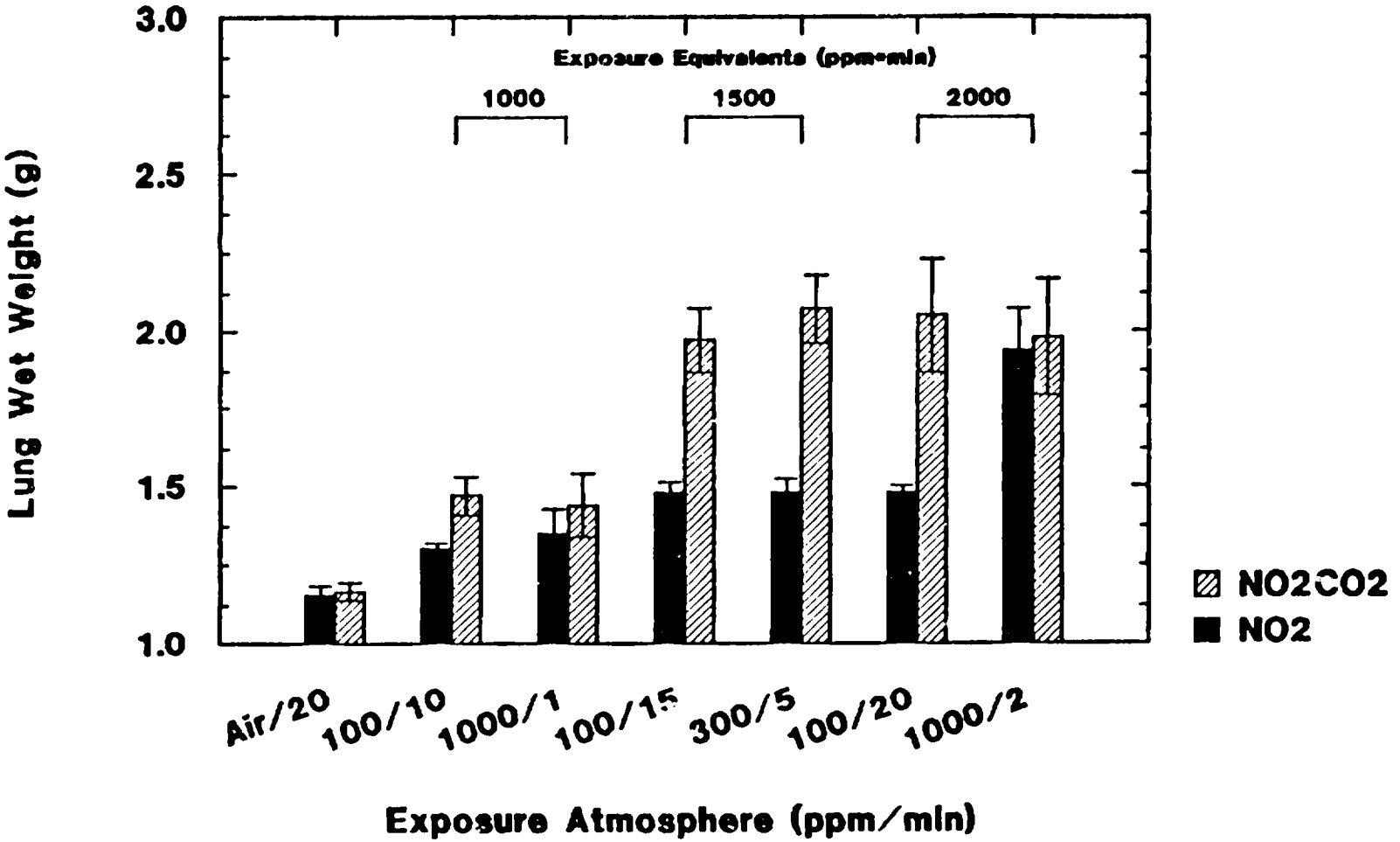

Figure 5. Lung wet weight (LWW) of rats 24 hr after exposure to the various air or NO_2 exposure regimens with and without CO_2 during the exposures. Each bar represents the mean and S.E.M of N= 6 to 12 animals.

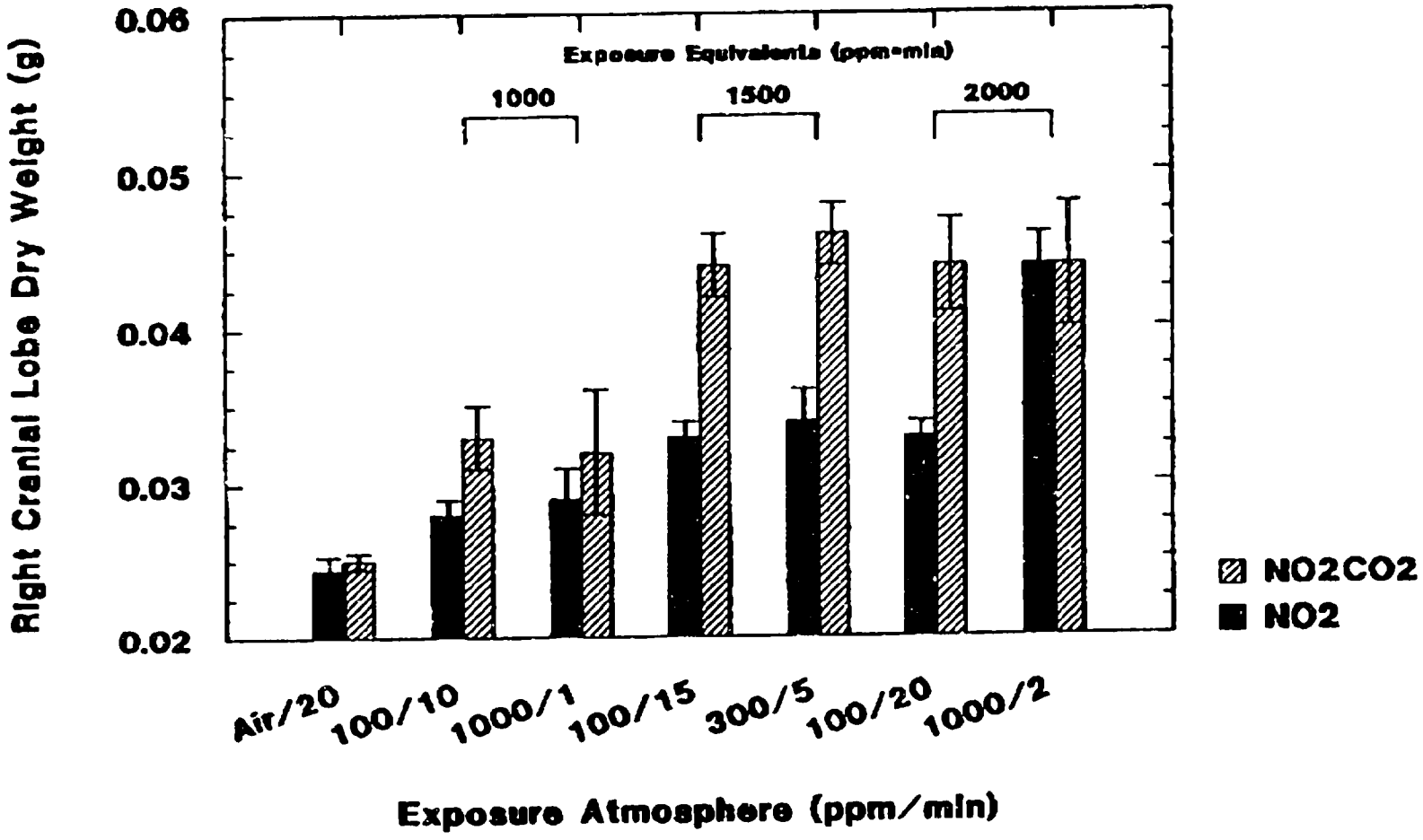

Figure 6. Right cranial lobe dry weight (RCLDW) of rats 24 hr after exposure to the various air or NO_2 exposure scenarios with and without CO_2 during the exposure. Each bar represents the mean and S.E.M of N= 6 to 12 animals.

increasing NO_2 exposure equivalents (ppm X minutes). The LWW and RCLDW of animals exposed to the 100 ppm and 300 ppm NO_2 + 5% CO_2 atmospheres were also significantly increased above values measured on animals exposed to the various concentrations of NO_2 alone. Values of LWW and RCLDW from animals exposed to the 1000 ppm NO_2 + 5% CO_2 atmospheres, however, were not significantly different from values obtained from animals exposed to NO_2 alone. The estimated inhaled dose of NO_2 was calculated as the sum of the VE (ml) times the exposure concentration of NO_2 (mg/L), Figure 7. Generally, the lung gravimetric parameters correlated with the calculated dose of inhaled NO_2. Notable exceptions were that the LWW and RCLDW values for animals exposed to the 1000 ppm NO_2 atmospheres were greater than expected from the estimated inhaled dose.

In conclusion, the results of this study component indicate: 1) minute ventilation (VE) is reduced with increasing NO_2 concentrations, 2) VE progressively falls as the duration of exposure to NO_2 increases, and this progressive reduction is exclusively related to a reduction in tidal volume (VT), 3) CO_2-induced increases in VE are attenuated by the concurrent inhalation of high concentrations of NO_2 and they are essentially eliminated at very high concentrations of NO_2, 4) the diminished VE response to CO_2 during high concentration NO_2 exposure are exclusively due to decreases in VT, 5) the severity of acute lung injury increases with increasing exposure equivalents to NO_2 even though VE decreases as NO_2 concentration increases, 6) generally, the severity of acute lung injury in response to NO_2 inhalation is increased by an increase in VE during exposure, 7) the severity of acute lung injury for a given concentration of NO_2 tends to scale proportionally with inhaled dose of NO_2, and 8) with or without CO_2, the highest NO_2 concentration studied, (1000 ppm) caused a greater than expected injurious response.

Short Burst, High NO_2 Concentration-Response Studies

Another ongoing objective for this project has been to examine NO_2 concentration-time response relationships using short burst exposures to relatively high NO_2 concentrations. We have continued these studies in FY91 with short term exposures (1 to 2 min durations) to high mass concentrations (500 ppm to 2000 ppm) NO_2 using lung gravimetric and histopathologic endpoints to assess pulmonary injury. As we have reported before (The Toxicologist 8(1):557a,1988), pulmonary injury after exposure to a particular NO_2 exposure equivalent (concentration x time) is greater in animals exposed to higher concentrations of NO_2 for a shorter duration than that observed with animals exposed to lesser concentrations of NO_2 for longer durations. In other words, concentration rather than exposure duration is the more important exposure variable in NO_2-induced

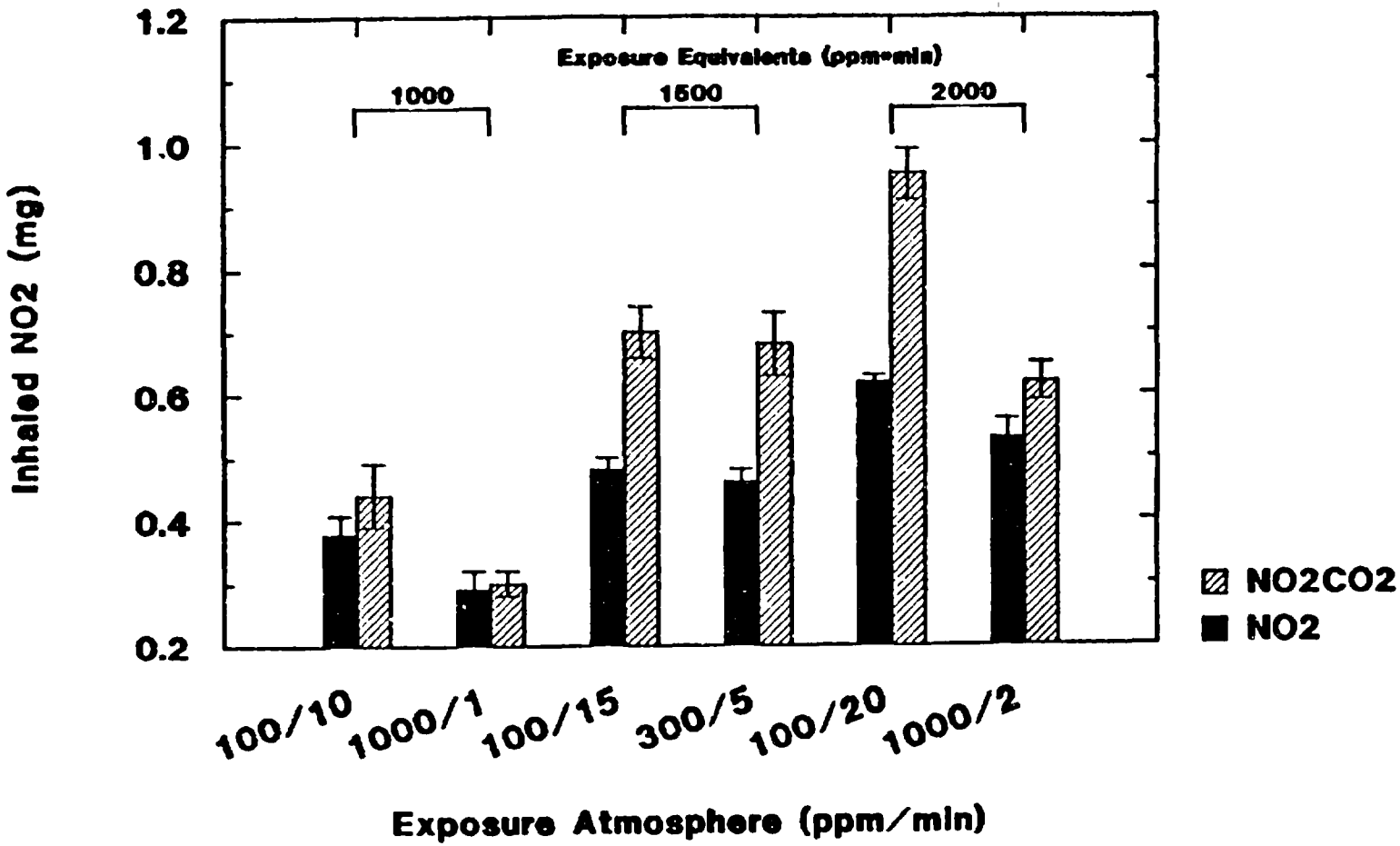

Figure 7. Inhaled NO_2 was calculated as: (exposure atmosphere concentration (mg/L)) X (sum of the mean minute ventilations over the exposure duration). Nominal exposure concentrations were used in this calculation but measured exposure concentrations did not vary more than 2% of nominal concentrations.

acute lung injury. The present studies with short burst NO_2 atmospheres confirm these earlier findings. Figure 8 represents the percent change of Lung Wet Weight (LWW) 24 hrs after exposure to various concentration x time NO_2 exposure regimens. In this figure, we grouped the data from the experimental animals into exposure concentration families of low concentration, long duration (25 ppm to 50 ppm, 15 to 30 min), medium concentration, medium duration (75 ppm to 200 ppm, 5 to 15 min) and the short burst, high concentration group (500 ppm to 2000 ppm, 1 to 2 min). As illustrated in Figure 8, at any particular exposure equivalent, the higher the concentration and shorter duration the NO_2 exposure was, the greater the resulting pulmonary edema. Histopathologic evaluation of the animals exposed to high concentration NO_2 atmospheres is nearing completion.

Short Burst, High Concentration NO_2 and Post-Exposure Exercise

Another objective relating to the pulmonary injury of animals exposed to short burst high concentration NO_2 atmospheres is to assess exercise as a potentiator of expression of NO_2-induced lung injury following these exposure scenarios. Figure 9 summarizes the percentage increases in LWW values obtained with groups of animals that were subjected to various high concentration, short duration exposures and then rested after until they were sacrificed 24 hr after exposure (solid line). Also shown in Figure 9 are the responses of groups of animals exposed in an identical manner but exercised within 1 hr after exposure and then sacrificed 24 hr after exposure. Exercise shortly after short burst NO_2 exposure can potentiate the resulting pulmonary edema. Also, for any particular exposure equivalent, the animal group exposed to the lower NO_2 concentration (of this high NO_2 concentration family) for the longer duration had a much greater response to the potentiating effects of exercise. For example, the group of animals exposed to 1000 ppm NO_2 x 1.5 minutes experienced 80% mortality after exercise compared tc no mortality and only ~10% increase in LWW compared to identically exposed and rested control animals. Animals exposed to 1000 ppm NO_2 x 2 minutes experienced 100% mortality compared to the group of anima s exposed to 2000 ppm NO_2 x 1 min in which 60% mortality occurred.

Kinetics of Lung Free Cell and Biochemical Changes in Lavage Fluid Following Exposure to a Relatively High Mass Concentration of NO_2

Little is known about the kinetic course of development of permeability changes that occur in the lung or the kinetic course of inflammatory cell changes that occur in the lung's alveoli and conducting airways following exposure to a high concentration of NO_2. Conceivably,

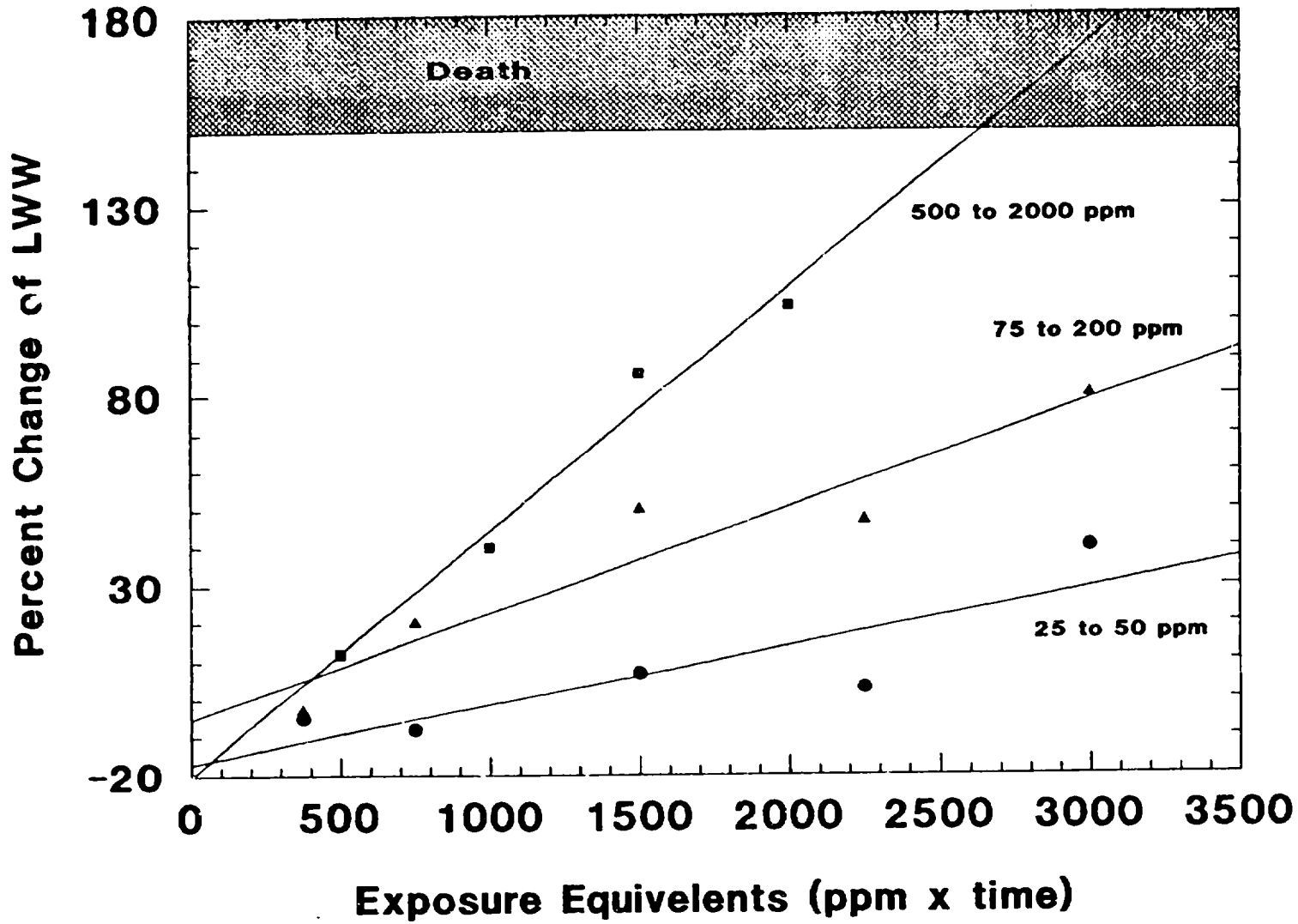

Figure 8. Percent change of Lung Wet Weight (LWW) of groups of animals exposed to various concentrations of NO_2 for various periods of time and sacrificed 24 hr after exposure. Animals have been grouped into the NO_2 exposure concentration families of Low, circles, (25 to 50 ppm for 15 to 30 minutes), Medium, triangles, (75 to 200 ppm for 5 to 15 minutes) and High, squares, (500 to 1000 ppm for 1 to 2 minutes). Each point represents mean values of N = 6 to 18 animals. Lines were fitted to each NO_2 concentration family. LWW increase over 150% generally result in death.

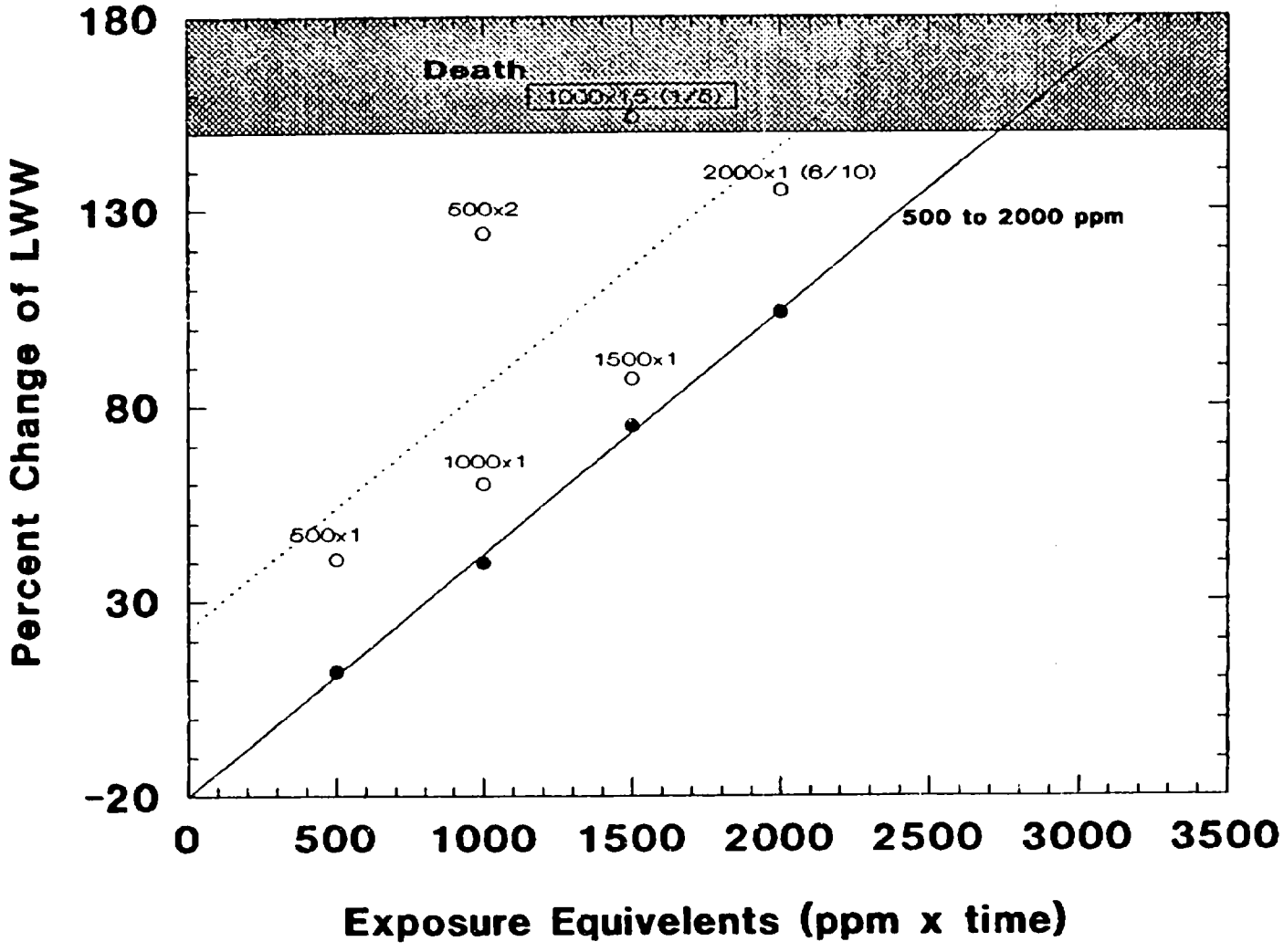

Figure 9. Percent change of Lung Wet Weight (LWW) of groups of animals exposed to high concentrations of NO_2 (500 to 2000 ppm) for short duration (1 to 2 minutes) and either rested after exposure (solid circle, solid line) or exercised within 1 hr after exposure (open circle, dashed line). The exercised groups are identified with concentration and time labels as well some groups are labeled as to number of survivors in parathensies. Each point represents the mean of N=5 to 12 animals. LWW increase over 150% generally result in death.

these responses may be related. In order to investigate this possiblity, Fischer-344 rats (SPF) were exposed to 100 ppm NO_2 for 15 min, and they were subsequently sacrificed 8, 24, 48, 72, and 96 hrs. Their lungs were lavaged by a standardized protocol, free cell numbers and types were determined, and the lavaged fluids were analyzed using a new ion exchange-HPLC technique to quantitate various proteins that translocate from the lung's vasculature into the airspace compartment when the permeability status of the lung's air-blood barrier is breached. This work was undertaken by a Masters Degree candidate (Timothy Ellis) working in our laboratory under the mentorship of Drs. L.R. Gurley and B.E. Lehnert. Briefly, one outcome from this study was the observation that the excessive occurrence of polymorphonucleated leukocytes (PMN) in the air space compartment occurs well after the pulmonary edematous response to inhaled high NO_2 is in place. A copy of this thesis work/investigation follows.

DEVELOPMENT AND ASSESSMENT OF A NEW HPLC APPROACH FOR QUANTIFYING CHANGES IN BRONCHOALVEOLAR LAVAGE FLUID CONSTITUENTS DURING PULMONARY EDEMA

By
Timothy M. Ellis

A Thesis

Submitted to the Graduate School
Jackson State University
in Partial Fulfillment of the Requirements
for the Degree of
MASTER OF SCIENCE

October, 1990

Major Subject: Biology

TABLE OF CONTENTS

	LIST OF TABLES	vii
	LIST OF FIGURES	viii
I.	**INTRODUCTION**	1
II.	**BACKGROUND**	2
	A. The Alveolar Region, Lung Free Cells, and the Extracellular Lining Fluid	2
	B. Approaches for Characterizing ELF Changes that Result from Lung Injury	4
	C. Hypothesis	6
III.	**MATERIALS AND METHODS**	7
	A. Overview of Experimental Design	7
	B. Animals and Animal Exposures	7
	C. Animal Sacrifices and Bronchoalveolar Lavage Preparations	8
	D. Cell Differentials of Lavaged Cells	10
	E. Protein Analysis with High Performance Liquid Chromatography (HPLC)	11
	F. Data Analysis	14
IV.	**RESULTS**	14
	A. Development of an Ion Exchange HPLC Method for Analysis of Lavage Fluid Constituents from Healthy Rats	14

B. Ion Exchange HPLC Using Blood Protein Standards 21

C. Alterations in Lavage Fluid Constituents Following NO_2-Induced Pulmonary Edema 25

D. Kinetics of the Free Cell Response to NO_2 35

V. DISCUSSION AND SIGNIFICANCE OF STUDY 41

A. Usefulness of HPLC Technique Compared to Other Techniques for Characterizing Pulmonary Edema 41

B. Current Shortcomings and Advantages of the Technique and Areas Requiring Further Study 42

C. Insight that the New Technique Has Provided in Characterizing the Kinetics of NO_2-Induced Pulmonary Edema 43

VI. CONCLUSIONS 44

VII. REFERENCES 45

VITA 48

LIST OF TABLES

Table I: Solvent Delivery Schedule for the Elution of BALF Component from a Protein-Pak DEAE-5PW Ion Exchange Column 17

Table II: Lavaged Cell Viabilities 36

Table III: Total Numbers of Lavaged Cells ($x10^{-7}$) 36

Table IV: Absolute Cell Population 40

LIST OF FIGURES

Figure 1: Schematic Representation of the Gas Delivery System and Associated Components used to Administer the Test Atmospheres 9

Figure 2: Cross-sectional Diagram of a Non-avoidance, Non-constraining Animal Exposure Tube 9

Figure 3: Water 600 Multisolvent Delivery System 13

Figure 4: Water 600E Fluid Components 13

Figure 5: Ion Exchange Chromatography of the Constituents of Normal BALF Eluted from the Protein-Pak DEAE Column 16

Figure 6: The Linear Relationship Between Sample Load and Quantity of Each Fraction Recovered from the Protein Pak DEAE Col 18

Figure 7: A Single Sep-Pak Was Used as a Means to Concentrate Lavage Protein Constituents While Removing Electrolytic Components from the Lavage Sample 19

Figure 8: Double Sep-Paks and lyolphilization were Used to Concentrate the Lavage Protein Constituents and to Increase Sample Load 20

Figure 9: Rat Albumin was Eluted from a Protein-Pak DEAE Column with an Increasing NaCl Gradient and a Decreasing Gradient pH 22

Figure 10: Rat Transferrin was Eluted from the Protein-Pak DEAE Column Using the Same Gradient as in Figure 5 23

Figure 11: Rate Immunoglobulin-G from the Protein-Pak DEAE Column in a Broad Unresolvable Pattern 24

Figure 12: This Chromatography Shows the Elution of BALF Components 8 Hours After NO_2 Exposure 26

Figure 13: Kinetic Response of IEC Fractions of BALF Following Exposure of Rats to 100 ppm NO_2 for 15 Minutes 27

Figure 14: Kinetic Response of Fraction 4 (which contains transferrin) to NO_2 Exposure 28

Figure 15: Kinetic Response of Fractoins 3, 4, 5, and 7 to NO_2 Exposure 30

Figure 16: Kinetic Response of Fraction 6 to NO_2 Exposure 31

Figure 17: Kinetic Response of Fraction 7 to NO_2 Exposure 32

Figure 18: The Kinetic Response of Fraction 4, 6, and 7 After Exposure to NO_2 33

Figure 19: Kinetic Response of Fraction 8 and Fraction 9 to Exposure to 100 ppm NO_2 for 15 Minutes 34

Figure 20: Shows the Changes in the Percentages of AM After Exposure to 100 ppm NO_2 for 15 Minutes 37

Figure 21: Shows the Response of PMN Cells to 100 ppm NO_2 for 15 Minutes 39

I. INTRODUCTION

A hallmark feature of acute lung injury caused by the inhalation of toxic agents is a breach in the integrity of the air-blood barrier in the gas exchange region of the lung (Lehnert and Stavert, 1988). In such instances, blood fluid phase constituents that are otherwise generally well retained in the vascular compartment of the lung gain access to the lung's interstitial compartment and the alveolar space compartment, i.e., pulmonary edema. Information about the quality and quantity of the blood compartment constituents in the alveolar space compartment following a toxic insult to the lung can provide useful information about the magnitude and severity of permeability changes associated with the injurious response. One widely accepted method for sampling constituents in the lung's terminal air spaces is bronchoalveolar lavage. Many investigators assess for increases in total protein or albumin in lavage fluids following toxic insults to the lung as a means to characterize the severity of resulting pulmonary edema, a condition which usually involves the passage of blood-derived proteins into the alveoli. *Values for total protein or albumin in lavage fluids alone, however, fail to provide more detailed information about the underlying nature of the "leak" between the pulmonary vascular and alveolar space compartments, e.g., "effective pore sizes". Moreover, such simple measurements preclude the detection of the numerous blood compartment constituents that may translocate into the alveoli during pulmonary edema and subsequently be involved in further injury or repair processes.* The research described herein focuses on the development and application of a new approach for obtaining qualitative and quantitative information about protein changes that occur in the lung's extracellular fluid lining during pulmonary edema.

II. BACKGROUND

II. A. The Alveolar Region, Lung Free Cells, and The Extracellular Lining Fluid

The respiratory tract is composed of approximately 40 different cell types (Kuhn, 1976; Crapo et al, 1982; and Burri, 1983). Of these, the Type I pneumocytes and the Type II pneumocytes are the main cell types that line the epithelial surfaces of the alveoli where gas exchange occurs. The Type I pneumocytes normally account for ~90% of the alveolar surface area (Evans et al, 1978), and these cells are generally more susceptible to the injurious effects of inhaled materials than are the Type II pneumocytes (Rombout et al., 1986). In the healthy lung, the Type I and Type II cells form tight junctions with one another (Schneeberger and Karnovsky, 1968). These junctions limit the paracellular passage of larger soluble substances, e.g., proteins, from the lung's interstitial region into the alveolar spaces (Barrios, et al., 1977). Coursing through the alveolar septa are extensive capillary beds that bring blood in close proximity to the alveolar space compartment so that gas exchange can efficiently occur. These capillaries are lined by endothelial cells, which account for ~50% of all cell types in the alveolar region of the lung (Inoue et al., 1976). The pulmonary endothelial cells are also attached to one another via tight junctions (Humbert, et al., 1976), which serve to limit the passage of larger blood fluid phase components to extravascular sites. Like the Type I pneumocytes, the pulmonary endothelial cells are known to be sensitive to the damaging effects of numerous toxic agents (Sorokin, 1966).

The air-blood barrier is composed of three distinct tissue layers. These are the alveolar surface epithelium, the alveolar capillary endothelium, and the interstitial space that is bound by the basement membranes of the epithelium and endothelium. Damage to the endothelial cells can result in profound changes in the permeability characteristics of the endothelial cell barrier (Schneeberger and Karnovsky, 1968). The term "lung free cells" refers to those cells that are found on the luminal surfaces of the conducting airways and on alveolar surfaces. Because of their location, the lung free cells can be harvested from the lung by bronchoalveolar lavage. Under healthy conditions, most of the lung

free cells are alveolar macrophages, with the remaining balance of cells being mainly lymphocytes and polymorphonuclear leukocytes (PMN). The types and numbers of lung free cells can be affected by inhaled oxidant-gas and other foreign agents. A general hallmark feature of acute lung injury caused by the inhalation of a variety of toxic materials is the recruitment of PMN from the pulmonary vasculature into the alveoli (Stavert and Lehnert, 1989). Further studies are required to elucidate potential relationship(s) between the kinetics of the PMN response and the expression of toxic substance-induced pulmonary edema.

The epithelial cells lining the airways and peripheral air spaces are covered with a complex fluid called the extracellular lining fluid (ELF), which can be sampled by bronchoalveolar lavage. The ELF is principally composed of a chemical mixture of lipids and proteins (George and Hooks, 1984). A major function of the ELF is to stabilize the patency of the alveoli and terminal airways during lung deflation by lowering the surface tension at the tissue-air interface (Brown, 1957; Macklem,1970). The ELF is also thought to play a defensive role against microorganisms and other inhaled agents either directly or by augmenting cell-mediated defense mechanisms (Hoffman, 1987; LaForce and Boose, 1981; Juers et al, 1976). Additionally, it is likely that the ELF serves to protect the lung's various epithelial cell populations from the direct effects of some types of toxic gases (Green et al., 1977).

The proteins in ELF have not been studied as well as the ELF's lipid constituents (Gurley et al., 1988). One source of proteins can be the lung epithelial cells themselves, as well as other cell types that reside in the alveoli, e.g., alveolar macrophages, lymphocytes (Gurley et al., 1989). It is also possible that some constituents in the ELF may be derived from cellular and acellular components in the lung's interstial compartment. Another major source of proteins in ELF is the lung's vascular compartment. Even though the alveolar epithelial and pulmonary vascular barriers consist of cells with tight junctions, some blood fluid phase components, e.g., albumin, in one manner or another gain access to the alveolar space compartment in relatively low amounts. One mechanism that may underlie this normally low level of passage of materials from the pulmonary vasculature onto the alveolar surface is the active vesicular transport of substances across

endothelial and epithelial cells (Solomon, 1965). The normal occurrence of blood compartment constituents on the alveolar surface may also reflect less than totally efficient junctional barriers between the lung's endothelial and epithelial cells. Overall, the passage of substances across the blood-air barrier can be conceptually depicted as occurring through "effective pores" of varying sizes.

It is well recognized that proteins in the lung's ELF can undergo marked qualitative and quantitative changes during the lung's response to environmental insults (George and Hook, 1984). Specifically, acute lung injury usually is accompanied by a breach in the normal integrity of the air-blood barrier. In such instances, blood compartment fluid phase constituents and water translocate in abnormal abundance into the alveolar interstitial region and into the alveoli, i.e., pulmonary edema. An outcome of this permeability disturbance is extensive alveolar flooding with fluid, which in turn diminishes the gas exchange function of the lung.

II. B. Approaches To Characterize ELF Changes As a Result of Lung Injury

Investigators have attributed macromolecular transport across the blood-air barrier entirely to vesicular exchange or to a system of different effective pore sizes (Renkin, 1985). Normally, the capillary walls are freely permeable to water, salts, and dissolved gases, but they are far less permeable to larger materials like proteins (Starling, 1896). One important factor governing the diffusion of a material across a semi-permeable membrane is its molecular size. When the vessel walls are injured by agents such as oxidant gases, the capillary endothelium becomes permeable to larger substances including proteins (Curry and Michel, 1980). A major detrimental result of this permeability change is the passage of more osmotically active molecules with attendant water into extravascular sites, i.e., edema.

Conventional approaches for quantifying the severity of pulmonary edema often times are limited in scope. For example, many investigators assess the total protein content or total

albumin content in bronchoalveolar lavage fluid (BALF) to index the severity of lung damage (Warren, et al., 1986). While these simple approaches can usefully serve to demonstrate generalized permeability changes in the lung, they do not provide significant information about the underlying nature of the permeability disturbances. For example, it is possible that a given toxic agent can cause the formation of an effective pore size through which albumin (MW:~69 kDa) may freely translocate across the air-blood barrier, while effective pores that can accommodate blood solutes of the size of albumin may be sufficiently small enough to preclude the passage of larger blood constituents such as immunoglobulin G (MW:~150 kDa). Indeed, some recent lines of evidence do suggest that different toxic insults to the lung can bring about different profiles in the effective pore sizes and/or increase the numbers of effective pores with a given pore size range (Gurley et al, 1989). Additionally, conventional measurements of total protein or albumin only in BALF provide no information about other translocating constituents that may be involved in subsequent lung injury or repair processes, e.g., transferrin (MW: ~85 kDa), fibrinogen (MW: ~ 340 kDa) (Jacobs, 1977).

Recently, a reverse phase HPLC method for resolving numerous proteins and other constituents in BALF has been developed as a means to more completely characterize changes in ELF that occur as a result of acute lung injury (Gurley et al, 1989; Gurley et al, 1989). Two shortcomings of this technique are that each sample run requires ~200 min, and the quantitative resolution of immunoglobulins has yet to be optimized.

Thus, new investigative approaches are clearly needed to characterize the biochemical changes that occur in the lung's ELF during pulmonary edematous responses to the inhalation of toxic agents. *The main objectives of the present study, accordingly, were: 1) to develop a more rapid quantitative HPLC method for measuring various proteins in BALF, and 2) to evaluate the utility of the new approach for determining changes in these constituents during pulmonary edema.* A specific driving goal underlying the development of the new HPLC technique was to establish an approach by which albumin, transferrin, and immunoglobulin G in lavage fluids could be quantitatively resolved. The decision to develop a new technique to specifically quantitate

these proteins in BALF was not arbitrary. The molecular weights of albumin and transferrin are substantially different from that of immunoglobulins of the G series. It was envisioned that these differences may be ultimately exploited in future studies to further investigate how effective pore sizes vary in different states of environmentally-induced lung injury and pulmonary edema. Moreover, transferrin, which has a molecular weight similar to that of albumin, was included as a specific constituent of interest because this iron-carrying substance may be involved in the further promotion of lung injury via lipid peroxidation once it enters the alveolar space compartment (Wills, 1965).

II. C. Hypothesis

A review of the literature regarding HPLC techniques for quantitatively resolving blood protein constituents was undertaken. The results from this search indicated that ion exchange chromatography (IEC) may be useful for rapidly resolving blood proteins in BALF inasmuch as such an approach has been used previously for resolving protein constituents in other complex body fluids, e.g., peritoneal ascites fluid (Styla, et al., 1984). Thus, *I hypothesized that a HPLC approach involving IEC could be developed to resolve and quantify various blood protein constituents in BALF. I also hypothesized that the new approach could experimentally serve to characterize quantitative changes in the aforementioned protein constituents in BALF during pulmonary edema caused by the inhalation of a toxic substance, i.e., nitrogen dioxide (NO_2). In addition to examining these hypotheses, I also investigated the lung's free cell inflammatory response following the inhalation of NO_2 in order to determine how such cellular changes may relate to the kinetics of expression of pulmonary edema.*

III. MATERIALS And METHODS

III. A. Overview of Experimental Design

A new HPLC approach was initially developed to examine the various protein constituents in lavage fluids with emphasis on the quantitative resolution of albumin, transferrin, and immunoglobulin G. Upon completion of this phase of the study, laboratory rats were exposed to 100 ppm nitrogen dioxide (NO_2) for 15 min to bring about a condition of acute lung injury (Stavert and Lehnert, 1989; Stavert and Lehnert, 1990). This lung injury model was used to evaluate the utility of the new HPLC approach for quantitatively detecting changes in ELF constituents, specifically albumin, transferrin, and immunoglobulin G, that can occur during pulmonary edema. Sham-air exposed rats sacrificed served as controls, as previously described (Stavert and Lehnert, 1989; Stavert and Lehnert, 1990). Animals exposed to NO_2 or air were sacrificed at 8 hr, 24 hr, 48 hr, 72 hr, 96 hr after exposure, and ELF in their lungs were sampled by bronchoalveolar lavage. BALF from control and NO_2 exposed rats were then analyzed and compared using the new HPLC approach. Additionally, lavaged free cell numbers and cell types were also analyzed at the above sacrifice times.

III. B. Animals and Animal Exposures

Male Fischer-344 rats (Specific Pathogen Free; Harlon Sprague Dawley) weighing between 200-300 g, were used in this study. Nitrogen dioxide was generated from dinitrogen tetraoxide (Stavert et al, 1986) and delivered, as shown in figure 1, to the rats via a quartz-glass exposure system (Wilson et al, 1987; Stavert and Lehnert, 1990), as shown in figure 2. Exposure concentrations were monitored by a dual channel ir-uv spectrophotometer (Binos Inficon, FRG) calibrated with primary gas standards, as previously described (Stavert and Lehnert, 1989; Stavert and Lehnert, 1990). Control animals consisted of rats that were exposed to filtered air only. Following the NO_2 or air exposures, the animals were returned to their cages until further used at the designated post-exposure times.

III. C. Animal Sacrifice and Bronchoalveolar Lavage Preparations

The rats were anesthetized by intraperitoneal injections of 50 mg phentobarbital sodium. Prior to total apnea, the rats were exsanguinated via carotid artery transection, and the trachea was cannulated with a blunt, 18-gauge needle secured with ligature. Following perforation of the diaphragm, the lungs and trachea were removed *en bloc* from the thoracic cavity. The heart and the esophagus were then removed from the trachea-lung preparation.

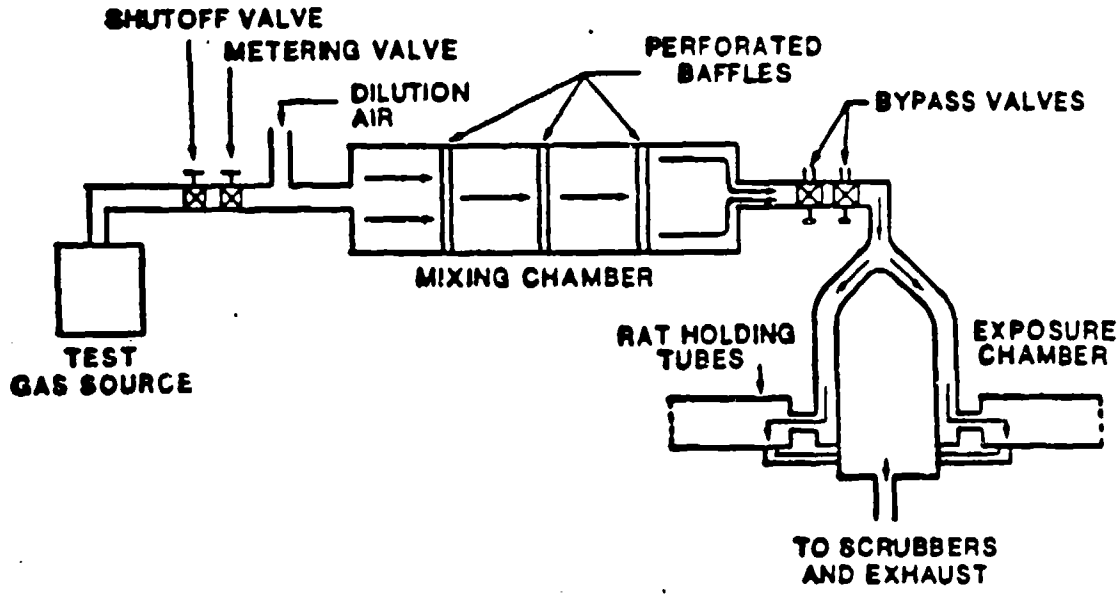

Figure 1: Schematic representation of the gas delivery system and associated components used to administer the test atmospheres.

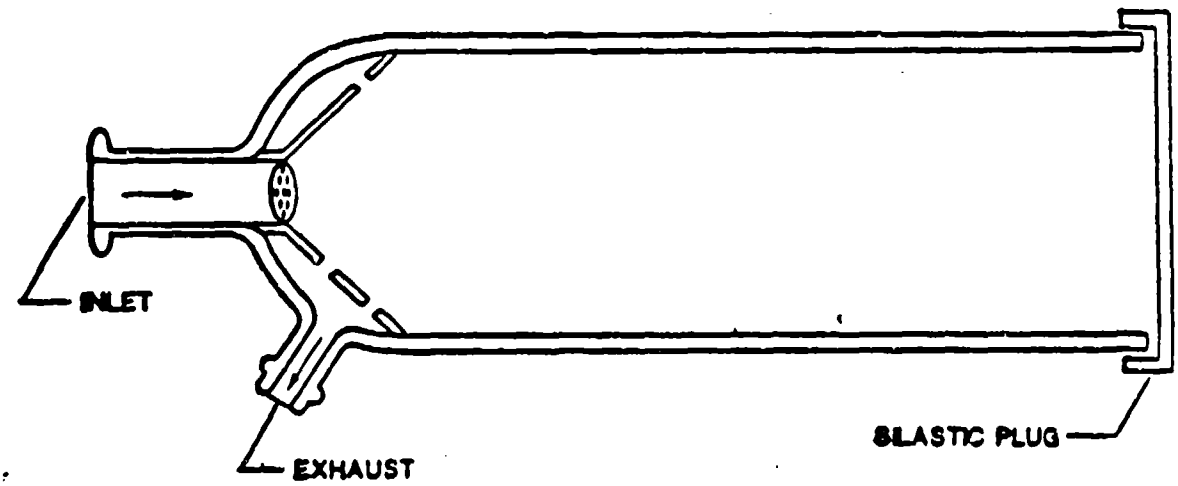

Figure 2: Cross-sectional diagram of a non-avoidance, non-constraining animal exposure tube. The tubes have been designed to provide the continual passage of an exposure atmosphere over the facial region of a rat.

A bronchoalveolar lavage procedure was used to harvest the ELF and lung free cells. The lavage protocol consisted of six sequential lung wash cycles with 8 ml of room temperature, divalent cation-free, phosphate-buffered saline (PBS; made with HPLC grade water) being used for each lung wash cycle. The lavage was performed with gentle massage of the lungs during the infusion and aspiration of the PBS. The retrieved lavage fluid obtained from this protocol was pooled in a centrifuge tube and maintained in ice (Lehnert and Morrow,1984). On average, > 96% of the instilled lavage fluid was recovered from the lungs of the control and NO_2 exposed animals. The lavage fluid was centrifuged at 300 g for 10 min at 4°C to sediment the lung free cells (Gurley et al., 1988). The supernate above the cell pellet was then removed by aspiration and placed in another centrifuge tube and centrifuged at 2300 g for 10 min at 4°C (Gurley et al, 1988) to remove remaining particulate material. The fluid retrieved after the latter centrifugation was designated as the bronchoalveolar lavage fluid (BALF) inasmuch as bronchoalveolar lavage washes the ELF from the conducting airways and alveolated regions of the lungs. The BALF was then stored in a glass tube and frozen at -70°C until used in the HPLC studies.

III. D. Cell Differentials of Lavaged Cells

Cytocentrifuged slide preparations of lung free cells pelleted from the recovered lavage fluid were made with a cytocentrifuge (Shandon Southern Cytospin, Shandon Southern Products, Ltd., Cheshire, UK). Cell differentials of each slide preparation were performed by examining a minimum of 200-400 cells stained with Camco Quik Stain®(Cambridge Chemical Products, Inc., Ft. Lauderdale, FL) using a light microscope. The lavaged lung free cells were categorized as alveolar macrophages (AM), polymorphonuclear leukocytes (PMN), and small mononuclear cells according to their morphologic characteristics and staining features. Because of difficulties in distinguishing between newly recruited blood monocytes, newly recruited pulmonary interstitial macrophages, and some types of lymphocytes, the small mononuclear cell category was used as a general category for both small mononuclear phagocytes and lymphocytes in the cell differential analysis. Eosinophils and epithelial cells were not

included in these cell differential counts because they were rarely observed in slide preparations.

III. E. Protein Analysis with High Performance Liquid Chromatography (HPLC)

A high performance ion exchange HPLC protocol was developed and evaluated with standards with the goal being to resolve, and measure various protein constituents present in ELF, and to quantify alterations in the protein constituents of ELF during pulmonary edema. The system used a Protein-Pak DEAE-5PW (7.5 mm x 7.5 cm) column (Waters Associates, Milford, MA). This ion exchange packing is prepared by introducing diethylaminoethyl groups onto a hydrophilic rigid gel. The large pore size of the packing material (1000 Angstroms) allows for the resolution and recovery of biomolecules, such as proteins, enzymes, and nucleic acids up to a molecular weight of ~10^6. The column was shipped filled with distilled water.

All solvents were prepared with HPLC grade water(J.T. Baker Chemical Co., Phillipsburg, NJ). Buffer A: 20 mM Tris, pH 8.5; Buffer B: 20 mM Tris, pH 7.0 + 0.3 M NaCi; Elution Conditions: linear gradient from 100%A/0%B to 0%A/100%B in 30 min. at a flow rate of 1 ml/min; Detection: UV absorption at 280nM with recorder sat at 0.025 AUFS. Before each HPLC run, the column was equilibrated with solvent A at a flow rate of 1 ml/min until the absorbance of the column effluent was constant, which required ~15 min per run.

The elution solvents were pumped through the column at a flow rate of 1 ml/min using a Waters 600E multisolvent delivery system capable of delivering up to four different solvents. Solvent metering and mixing in this system takes place on the low pressure side of the solvent delivery pump, with additional mixing on the high pressure side of the pump. The Waters 600E is divided into two modules. One module contains fluid related devices including a sparge unit, solvent proportioning valve, pump, sample injector, and HPLC column. The other module contains the system

controller which includes the power supply, electronics and computer (Figure 3). Figure 4 shows the relationships between the major components of the Waters 600E.

Solvent valve A delivered 20 mM Tris, pH 8.5; valve B delivered 20 mM Tris, pH 7.0 + 0.3M NaCl; valve C delivered HPLC grade water; valve D delivered methanol. At the end of the day the ion exchange column was stored in HPLC grade water (delivered by solvent valve C). The solvent series (Table I), which constitutes the standard running conditions optimized in preliminary experiments, was programmed into the Waters 600E multisolvent delivery system controller before each HPLC run.

The fractions eluted from the column were detected by uv absorbance at 280 nM using a Waters 484 tunable absorbance detector. To record the resolved HPLC fractions, the Waters 484 detector was attached directly to the Waters Model 745B Data Module (Figure 4). From this stripchart, all chromatography fractions were quantified by measuring the area under the various resolved peaks.

To identify the different protein constituents, standards for the proteins of major interest were evaluated. The standards consisted of: rat albumin; (Organon Treknika Corp., West Chester, PA); rat transferrin; (Organon Treknika Corp., West Chester, PA); rat immunoglobulin-G; (Organon Treknika Corp., West Chester, PA). All standards were prepared with phosphate buffered saline (PBS). The standards were manufactured by a combination of a variety of purification techniques including: multi-stage fractionation procedures involving serum dilapidation, sequential salt fractionation, gel filtration, affinity chromatography, and ion exchange. All of the purified standard materials were originally derived from rat serum. These products were lyophilized in 0.01M sodium phosphate buffered (pH 7.3) and 0.07M sodium chloride. No preservatives were added to the standard reagents by the supplier.

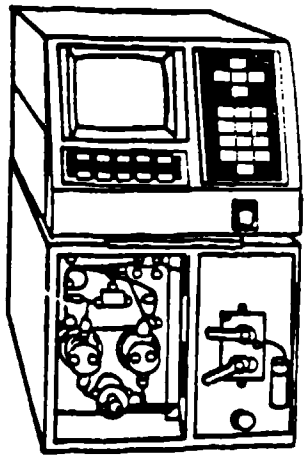

Figure 3: Waters 600 Multisolvent Delivery System

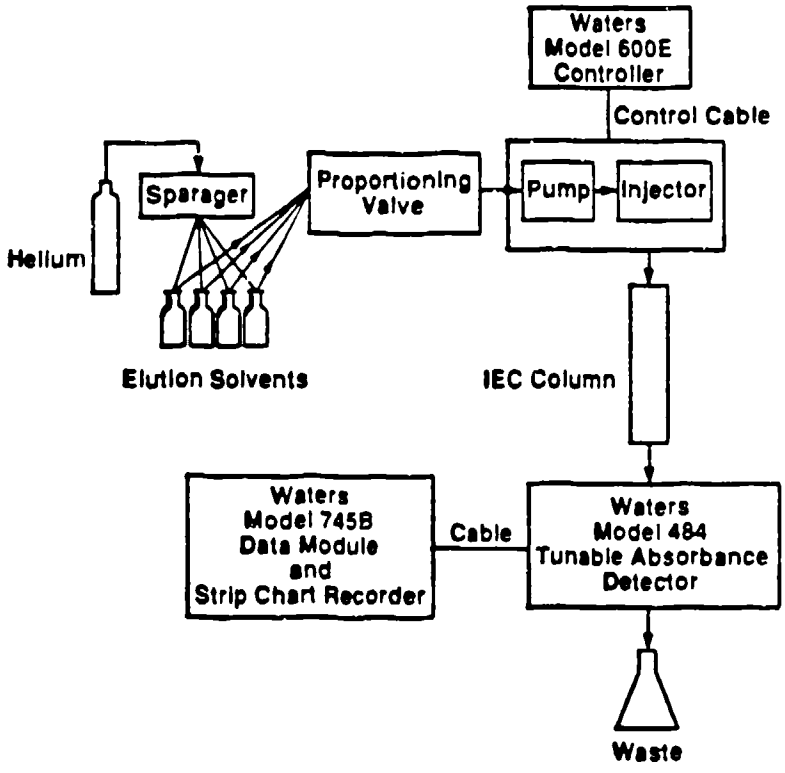

Figure 4: Waters 600E Fluid Components

Standards were prepared in PBS. After standards were prepared, a 300 µl sample was then injected onto the IEC. To load BALF samples onto the IEC, the lavage fluid from each rat was thawed at room temperature. Subsequentialy, a 300 µl sample was removed from the ~40 ml stock BALF and injected onto the column. Preliminary attempts were made to cross reference BALF constituents resolved by the ion exchange column with those constituents that have been previously resolved by using a C-18 column and reverse phase chromatography (Gurley et al, 1988; Gurley et al, 1989).

III. F. Data Analysis

In some experiments , statistical significance of results were determined by using one-way analysis and variance (ANOVA) and, if the F value indicated differences, the Tukey HSD test for multiple comparisons was performed. All values expressed in the text and figure represent the mean ± standard error of the mean, unless otherwise indicated.

IV. RESULTS

IV. A. Development of an Ion Exchange HPLC Method for the Analysis of Lavage Fluids from Healthy Rats

A reversed-phase HPLC system has been previously developed at the Los Alamos National Laboratory to analyze lavage fluid constituents (Gurley, et al, 1989). This technique requires 200 min per sample run, and the resolution of immunoglobulins has not been optimized. Since it has been demonstrated that IonExchange chromatography (IEC) is useful for rapidly resolving protein components in peritoneal ascites fluid, experiments were designed to see if IEC could also be adapted for the analysis of the complex protein mixture found in BALF. Experiments using IEC demonstrated that several components of the lavage fluid could be resolved during a 30 min period of elution with a NaCl and pH gradient (figure 5). In these studies the lavage fluid was pumped through a DEAE IonExchange column that had been equilibrated with buffer A: 20 mm

Tris, pH 8.5. This allowed the lavage fluid to be adsorbed and concentrated at the top of the IEC column.

It was found that if 300 µl or more of lavage fluid was pumped onto the IEC column, PBS was immediately eluted from the column and appeared as the first two components in the chromatogram, (Figure 5). Thereafter, a series of fractions of BALF components were both resolved during the remaining 30 min of the run. These experiments showed that four fractions could be eluted with a gradient increasing in NaCl concentration at a flow rate of 1 ml/min (Figure 5).

In order to quantify the fractions resolved by IEC it is necessary that the HPLC system respond linearly with respect to the amount of BALF loaded on the column. To test this aspect of the new technique, a series of volumes ranging from 0.5 ml to 2 ml of BALF from an untreated animal were injected onto the column and eluted with the solvent gradient,shown in Table I. Each of the fractions were quantified by measuring the area of the peaks detected by uv absorption at 280 nm. The linear relationship between sample load and the quantity response of the fractions was linear for all seven fractions detected in the experiments,(Figure 6). The resolution and quantification of the fractions obtained by IEC could be improved if the BALF sample was more concentrated. A series of experiments were performed to determine if the concentration of BALF was applicable. In one experiment BALF was desalted by acrodisc filtration with water and concentrated by lyophilization. The results of this experiment was the loss of the proteins concurrent with the reduction of PBS. In another experiment the proteins were concentrated and desalted by adsorbing them on a reversed phase Sep-pak C18 cartridge (Waters Association, Milford, MA) and then eluted with a small volume of acetonitrile containing 0.2% trifluoroacetic acid. When these samples were lyophilized and subjected to IEC, most of the proteins were found to be lost (Figure 7). To determine if the proteins were lost because the Sep-pak capacity was exceeded,

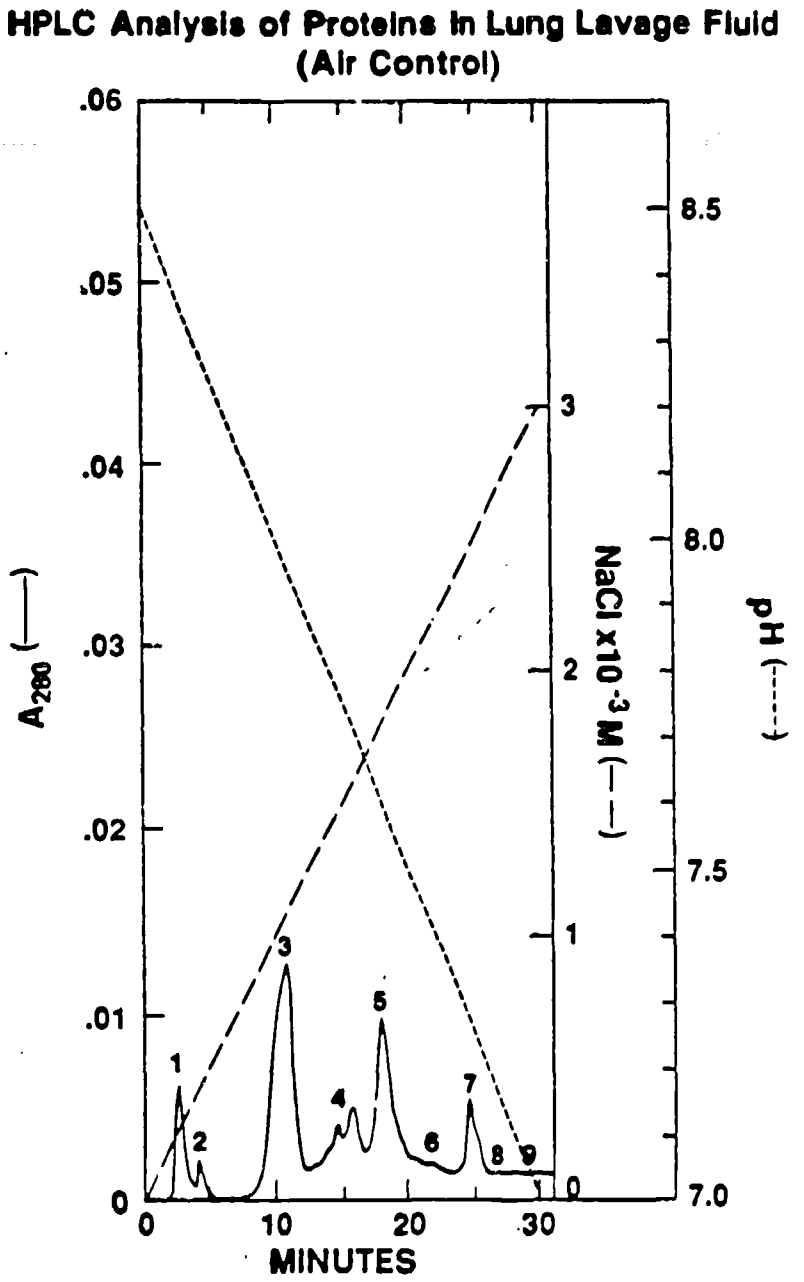

Figure 5: Ion Exchange chromatography of the constituents of normal BALF eluted from the Protein-Pak DEAE column. Fractions 1 and 2 result from the injections of PBS. Fractions 3-7 result from BALF constituents during the remaining 30 min. All fractions were eluted using an increasing NaCl gradient with a decreasing pH from 8.5 to 7.0.

a sample was passed through 2 Sep-paks. When the proteins were then eluted form both Sep-paks, lyophilized, and subjected to IEC, even more protein was found to be lost (figure 8) than was lost when one Sep-pak was used (figure 7). From this it was concluded that the BALF proteins were not being eluted from the Sep-paks and that this procedure was not applicable for BALF studies.

Table I: Solvent Delivery Schedule* for the Elution of BALF Component from a Protein-Pak DEAE-5PW Ion Exchange Column

Elapsed time (min)	Percentage A valve	Percentage B valve	Percentage C valve
0.00	100	0	0
30.00	0	100	0
32.00	0	100	0
32.10	0	100	0

* Total flow rate of solvent delivered to column was 1 ml/min with the pump valves programmed for linear gradient delivery.

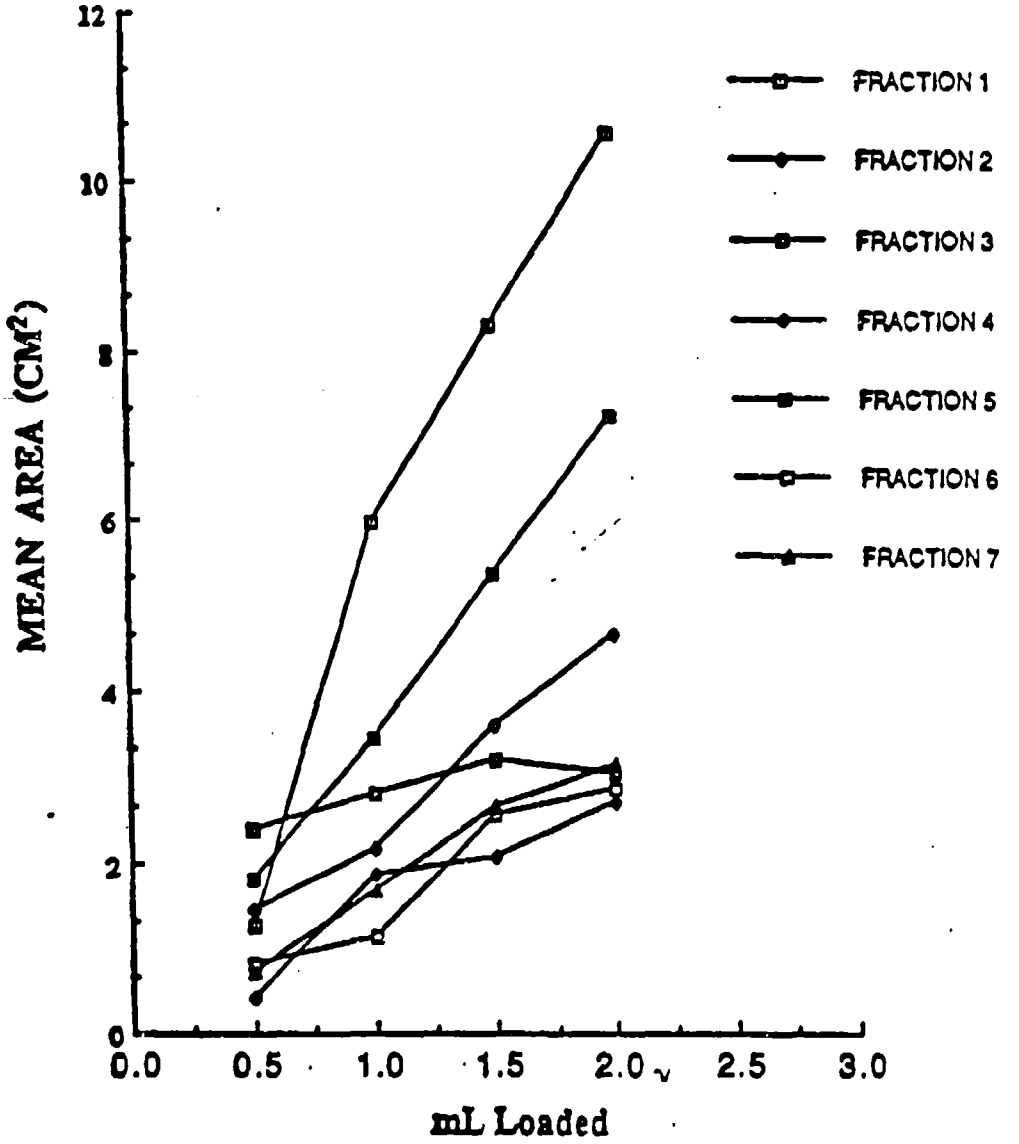

Figure 6: The linear relationship between sample load and quantity of each fraction recovered from the Protein-Pak DEAE column. Volume of lung lavage loaded on the column ranged from 0.5 to 2.0 ml. Each of the seven fractions was quantified by measuring the area of the eluted peaks detected by uv absorption at 280 nm.

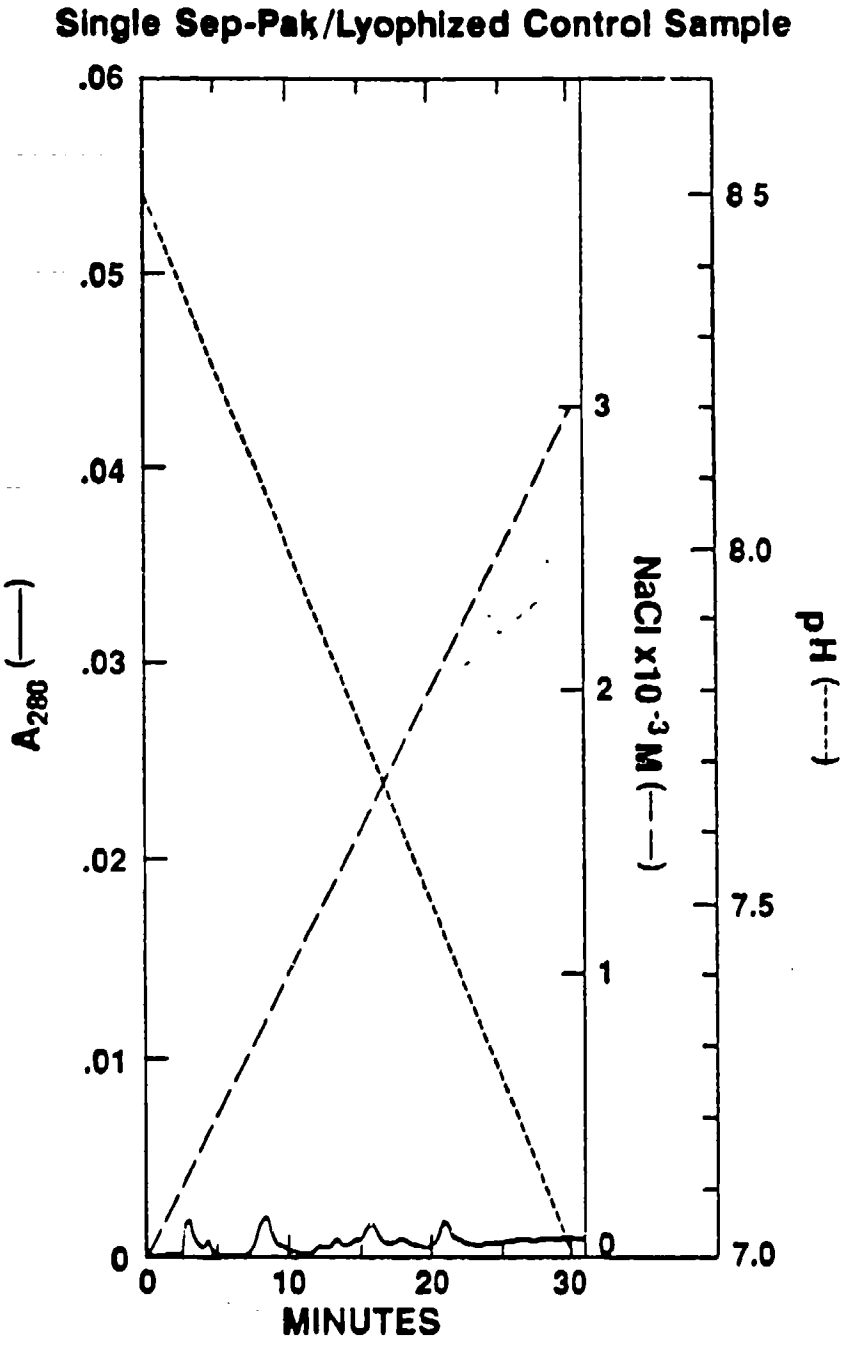

Figure 7: A single Sep-pak was used as a means to concentrate lavage protein constituents while removing electrolytic components form the lavage sample This lavage sample was also exposed to lyophilization, in order to load a larger volume onto the Protein-Pak DEAE column. The end results of these experiments were the loss of important protein constituents and a reduction of PBS.

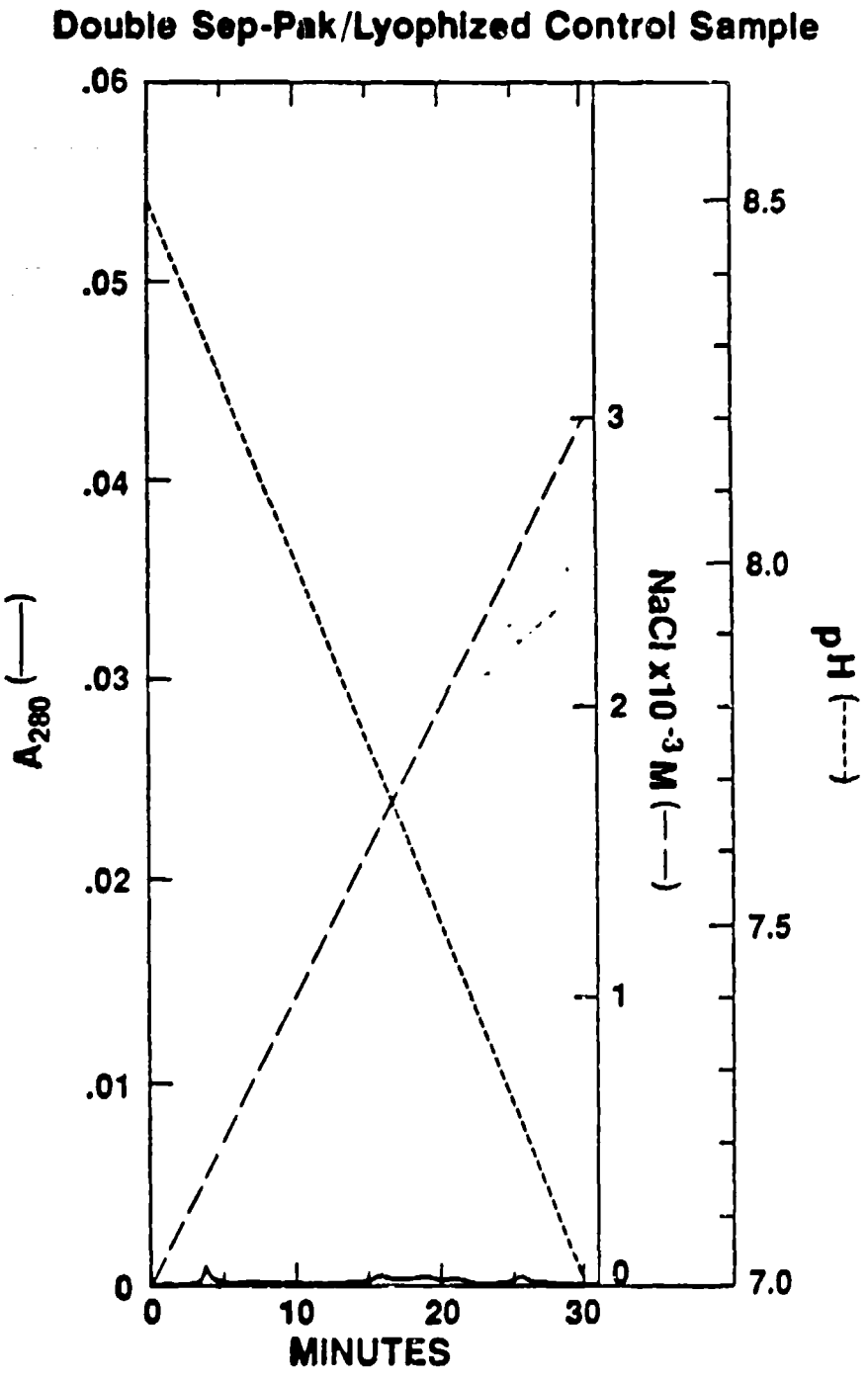

Figure 8: Double Sep-Paks and lvophilization were used to concentrate the lavage protein constituents and to increase sample load. The results of these experiments were also the loss of important protein constituents and a reduction of PBS.

IV. B. Ion Exchange HPLC Using Blood Protein Standards

The constituents found in BALF are derived from two main sources with the largest amount being derived from the plasma and a smaller quantity being derived from the lung tissue. To determine which fractions in the IEC profile of BALF were derived from the blood compartment , a series of plasma protein standards from commercial preparations were subjected to IEC and comparisons were made against rat lung lavage fluid constituents. Commercial standards of albumin, transferrin and immunoglobulin-G were prepared in PBS as previously described. These experiments indicated that the plasma protein, albumin (the most abundant constituent in the BALF), should elute relatively late (Figure 9). A comparison between commercially prepared albumin (Figure 9) and rat lung lavage fluid (Figure 5) indicated that fraction seven would be expected to represent albumin. Another protein standard, transferrin, which has a molecular weight similar to albumin, eluted at an earlier time point than did albumin, (Figure 10), and appears to be a part of fraction four in rat lung lavage (Figure 5). The Immunoglobulin-G standard differed from the albumin and transferrin standards in that it produced only a broad unresolvable elution pattern which eluted from 10-30 min (Figure 11). This observation suggests that the immunoglobulin G reference material was heterogeneous containing many different protein subclasses. It is concluded that IEC is not effective in separating IgG from other blood proteins.

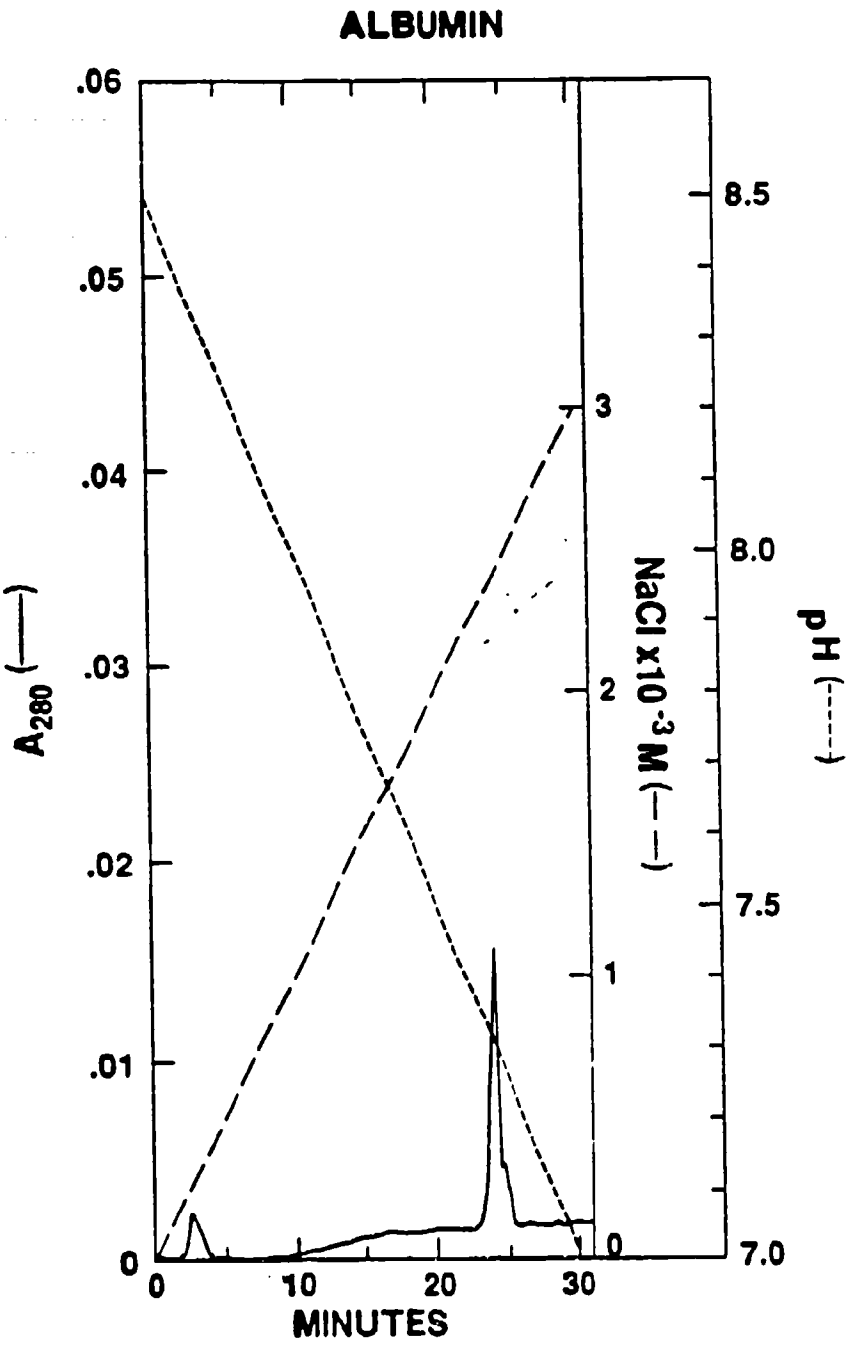

Figure 9: Rat albumin was eluted from a Protein-Pak DEAE column with an increasing NaCl gradient and a decreasing gradient pH. Comparison between the albumin standard and BALF indicated that BALF fraction seven (Figures 10 and 12) would be expected to contain the plasma protein albumin.

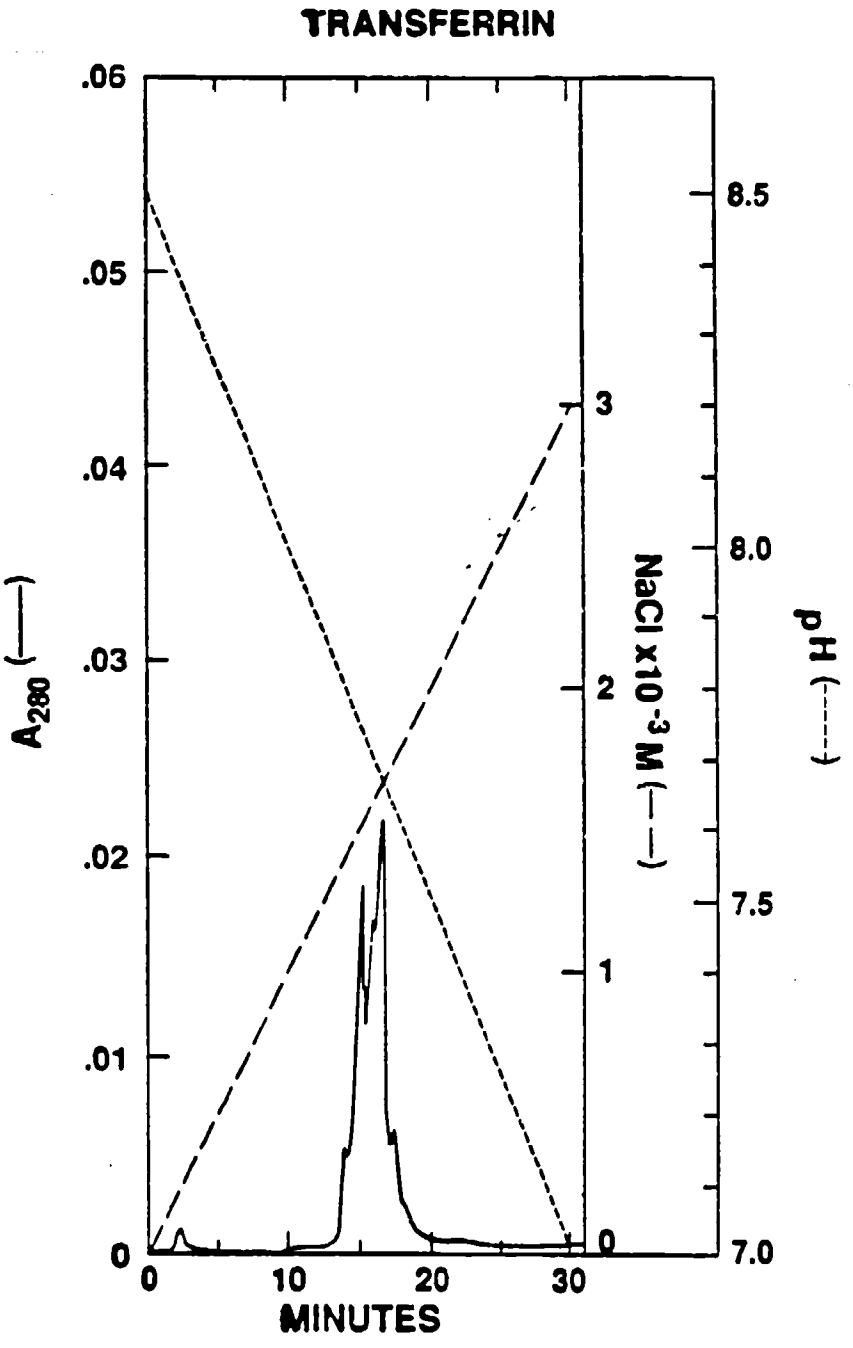

Figure 10: Rat transferrin was eluted from the Protein-Pak DEAE column using the same gradient as in Figure 5. This plasma protein eluted from the column at an earlier time point than albumin and appeared to be a part of fraction four in BALF (Figures 10 and 12).

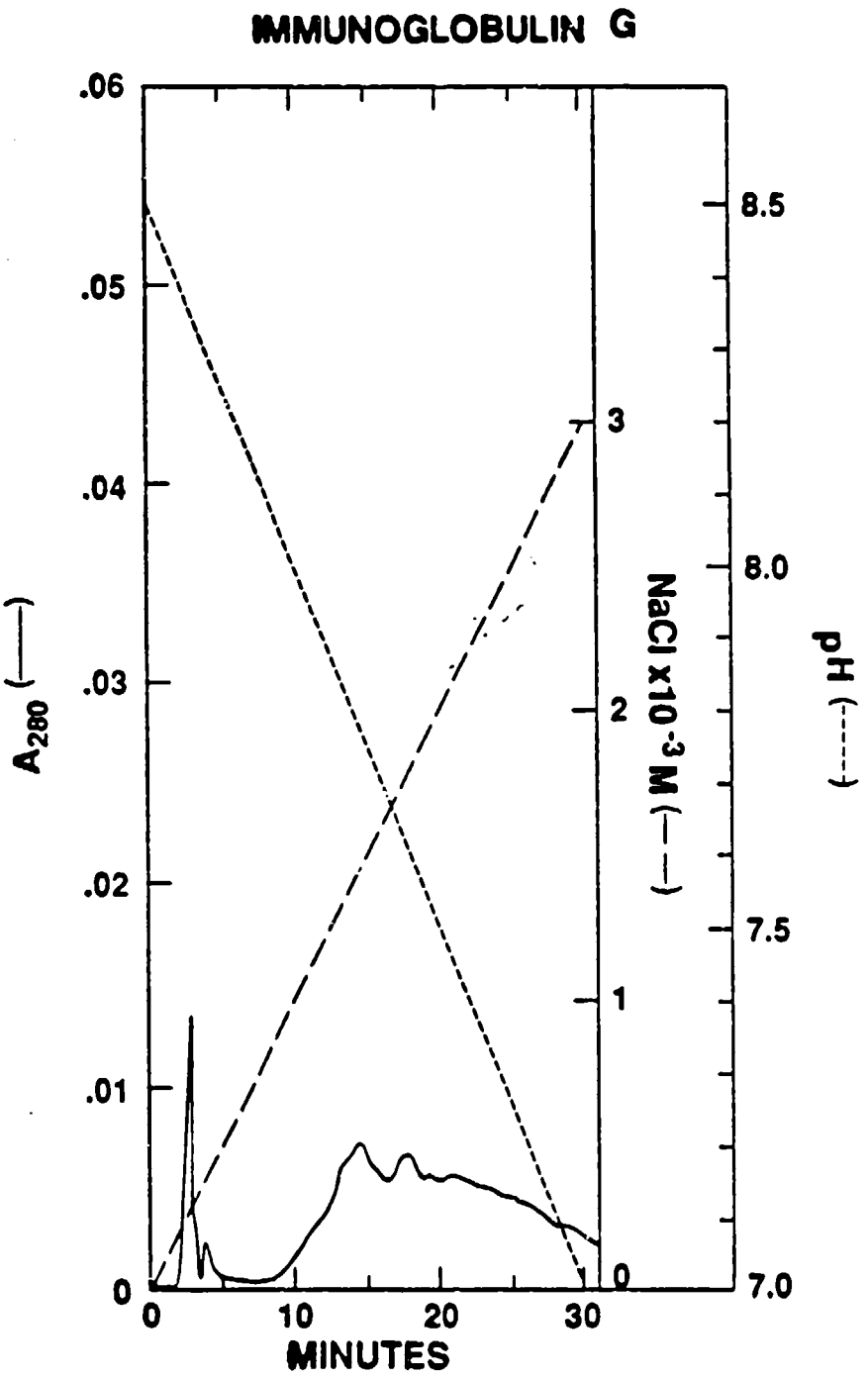

Figure 11: Rat Immunoglobulin-G eluted from the Protein-Pak DEAE column in a broad unresolvable pattern. This observation suggested that the immunoglobulin-G reference material contained a heterogeneous collection of protein subclasses.

IV. C. Alterations In Lavage Fluid Constituents Following NO_2 Exposure and the Kinetic Course of NO_2-Induced Pulmonary Edema

In this phase of the study, rats were exposed to 100 ppm nitrogen dioxide (NO_2) for 15 min and then sacrificed 8 hr, 24 hr, 48 hr, 72 hr, and 96 hr later for lung lavage. Sham air exposed animals served as controls. The lavage fluids were then analyzed for constituents using the new IEC technique. N[illegible] fractions were eluted from the new IEC system (Figure 12). The [illegible]lative changes in these fractions over 96 hours following ex[illegible]ure are shown in figure 13. Statistical analysis of these results indicated that there was no significant difference in fraction 1 after 8 hr post exposure, although there were significant differences at the 24 hr and 48 hr time points ($P<0.010$, $P<0.007$). Fraction 1 was elevated ~7-fold by 24 hr NO_2 post-exposure and remained elevated through 48 hr, but as of 72 hr and 96 hr this fraction had started to return to the level of the control animals. The second fraction results showed no significant difference between air control and NO_2 values at 8-48 hr, but did indicate a slight elevation above controls at 72 hr post-exposure ($P< 0.042$). By 96 hr post-NO_2, fraction 2 had returned to control level. Fraction number 3 increased more slowly than other lavage constituents and showed no significant changes after exposure to NO_2 (Figure 13). The fourth fraction, which most likely contains the plasma protein transferrin and other constituents, increased significantly at the 8 hr post-NO_2 exposure time point. This fraction reached a maximal ~5 -fold increase at the 24 hr time point, and by 48 hr time point this constituent had started to subside, but did not reach control levels until 72 hr and 96 hr NO_2 post-exposure (Figure 14). Fraction number 5 responded similarly to NO_2 as did fraction 3, but showed an increase that was significant by 24 hr post-exposure. This response was much slower than responses

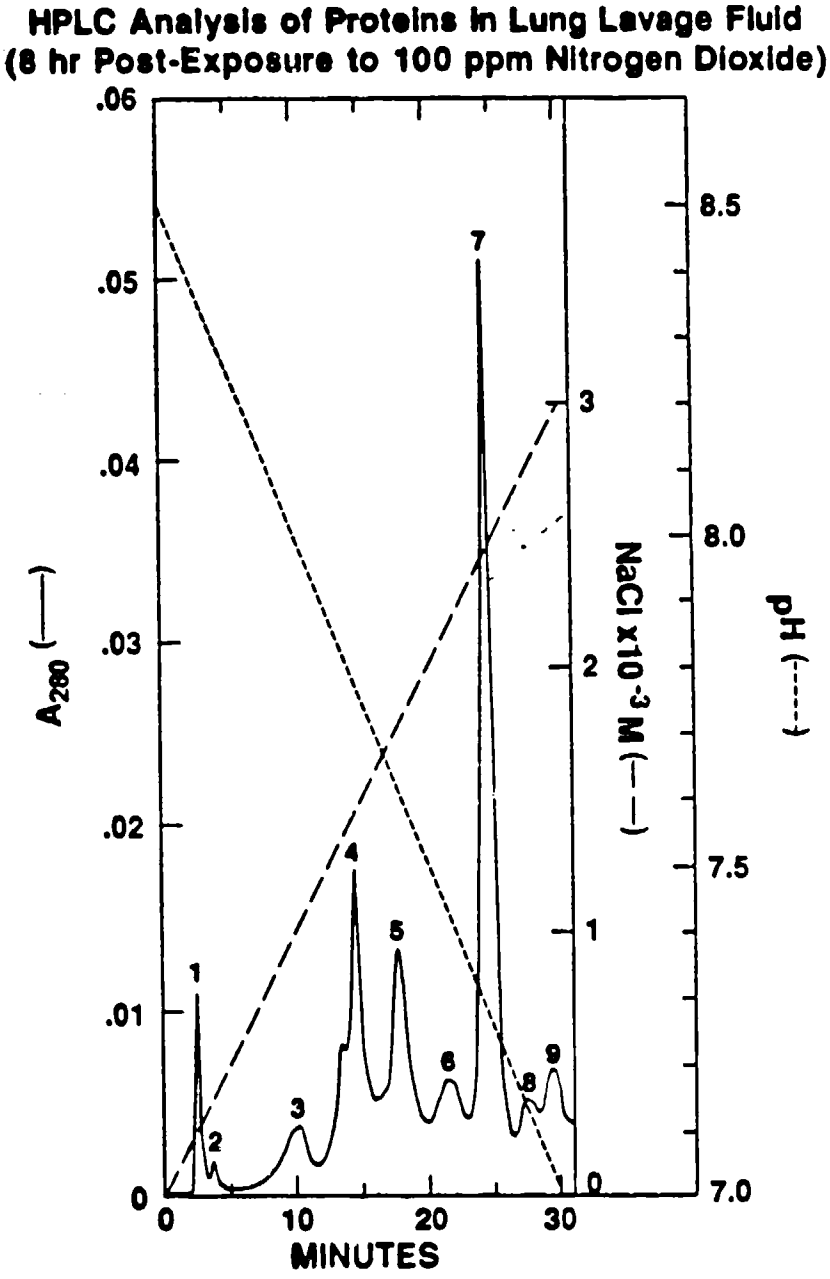

Figure 12: This chromatography shows the elution of BALF components 8 hours after NO_2 exposure. A total of nine fractions were eluted with a flow rate of 1 ml/min. All the fractions were eluted using an increasing NaCl gradient with a decreasing pH from 8.5 to 7.0.

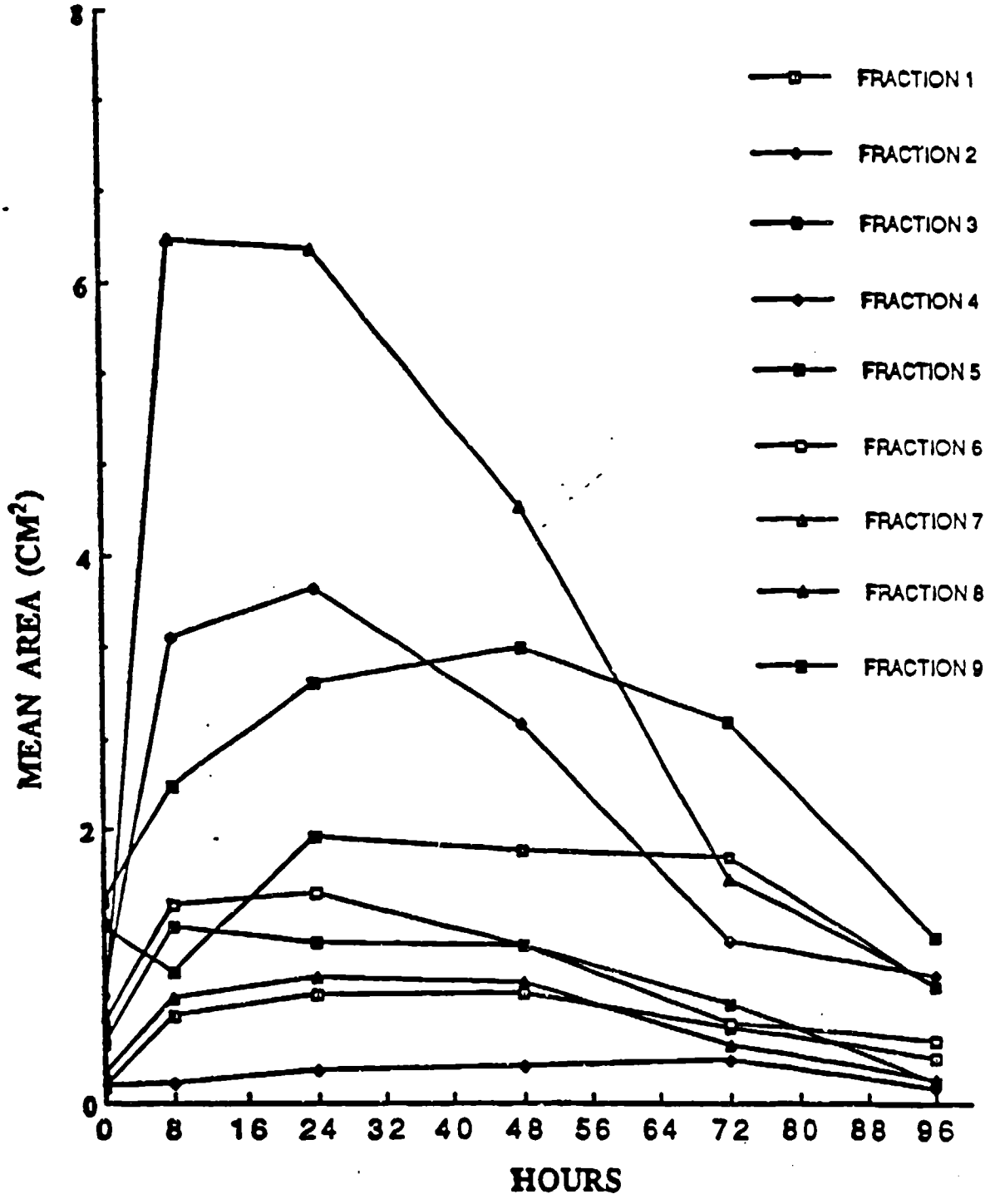

Figure 13: Kinetic response of IEC fractions of BALF following exposure of rats to 100 ppm NO_2 for 15 min. Unexposed control animals are plotted at 0 hr.

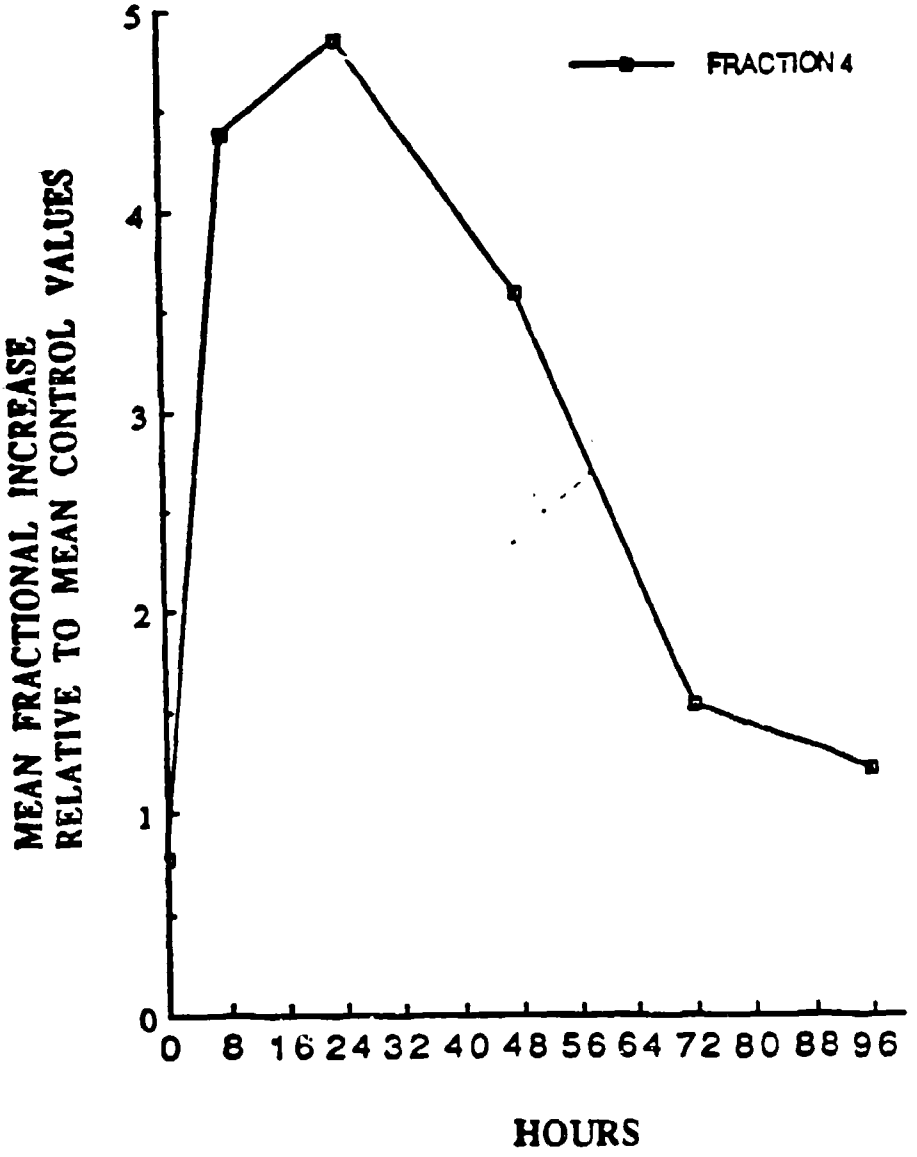

Figure 14: Kinetic response of Fraction 4 (which contains transferrin) to NO_2 exposure. Fraction 4 increased greater than ~4 -fold over controls values after 8 hr NO_2 post-exposure and as of 24 hr this fraction had reached a maximal of ~ 5 -fold, but at 72 hr this component of the BALF had subsided to near control levels.

seen in fractions 4 and 7. Subsequently, fraction 5 remained elevated for a period of two days, as did fraction 3 before a recovery was noticed (Figure 15). This suggests that the origin of fractions 3 and 5 may be different from that of the blood proteins (albumin and transferrin) of fractions 4 and 7. Fraction 6 was hardly detected in air control animals (Figure 5), but showed a significant increase in NO_2 exposed animals 8 hr and 24 hr post-exposure respectively ($P< 0.002$, $P< 0.001$). This fraction was elevated greater than ~2 -fold higher than air controls after 8 hr and maximally increased ~2.8 -fold by 24 hr NO_2 post-exposure. As of 48 hr, the increase seen at 24 hr had subsided to ~2 -fold and by 72 hr this fraction had subsided to levels of control (Figure 16). The results from NO_2 exposures showed significant differences in fraction 7 at the 8 hr, 24 hr, and 48 hr sacrifice times, when compared to air control ($P < 0.001$, $P< 0.001$, $P< 0.002$), this fraction has been identified as containing the plasma protein albumin. Fraction 7 was elevated ~ 11-fold at 8 hr after NO_2 exposure and this constituent remained similarly elevated ~10-fold at 24 hr after NO_2 exposure. By 48 hr after exposure, fraction 7 appeared to subside to a level that was ~7 -fold higher than control values (Figure 17). As of 72 hr after exposure to NO_2 the amount of fraction 7 in the lavage fluids had subsided significantly and by 96 hr after exposure, the amount of this constituent was virtually identical to that in control lavage fluid samples. When graphing the kinetic response of fractions 4, 6, and 7 it was found that these three constituents follow the same time course (Figure 18), which may indicate that they are derived from the same compartment, (i.e. the blood compartment).

The remaining two fractions (8 and 9) in Figure 12 were hardly detectable in air control animals (Figure 5) and showed a significant increase after NO_2 exposure when compared to the air control values (Figure 19). Fraction number 8 and fraction number 9 demonstrated similar kinetic patterns. This pattern can be described as increasing rapidly to near maximum values in 8 hrs, remaining high for 40 hrs and then decreasing to control levels in 48hrs (Figure 19). This pattern differed from that fractions 4,6, and 7 (the blood proteins) which only stayed elevated at maximum levels for 16 hrs (Figure 18). It also

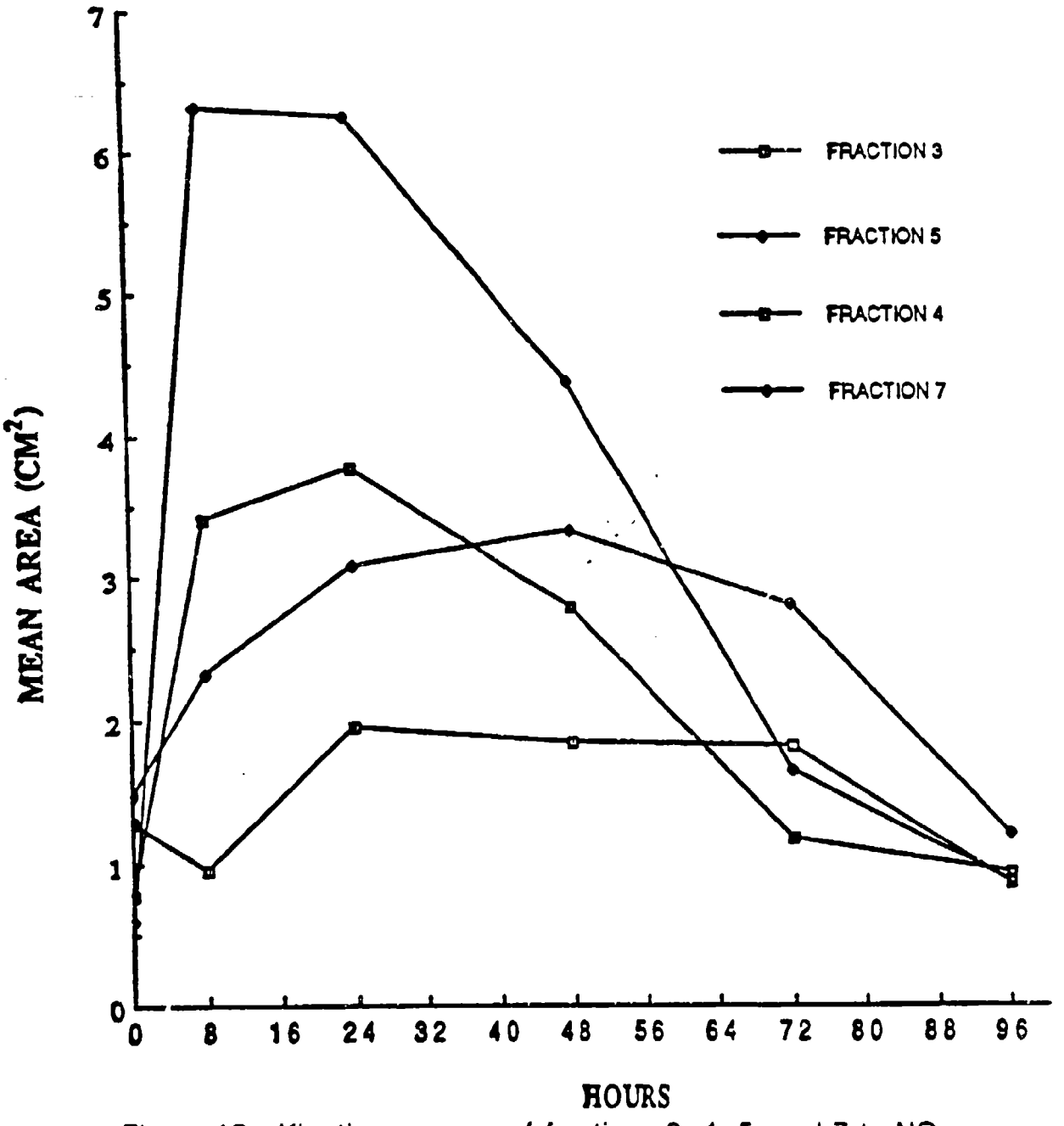

Figure 15: Kinetic response of fractions 3, 4, 5, and 7 to NO_2 exposure. Fraction 5 response to NO_2 was similar to fraction 3, while fraction 4 response was similar to fraction 7. Fractions 3 and 5 remained elevated for a period of two days. Fraction 5 showed an increase after 24 hr post-exposure that was significant. The response of fractions 3 and 5 were less than that of fractions 4 and 7.

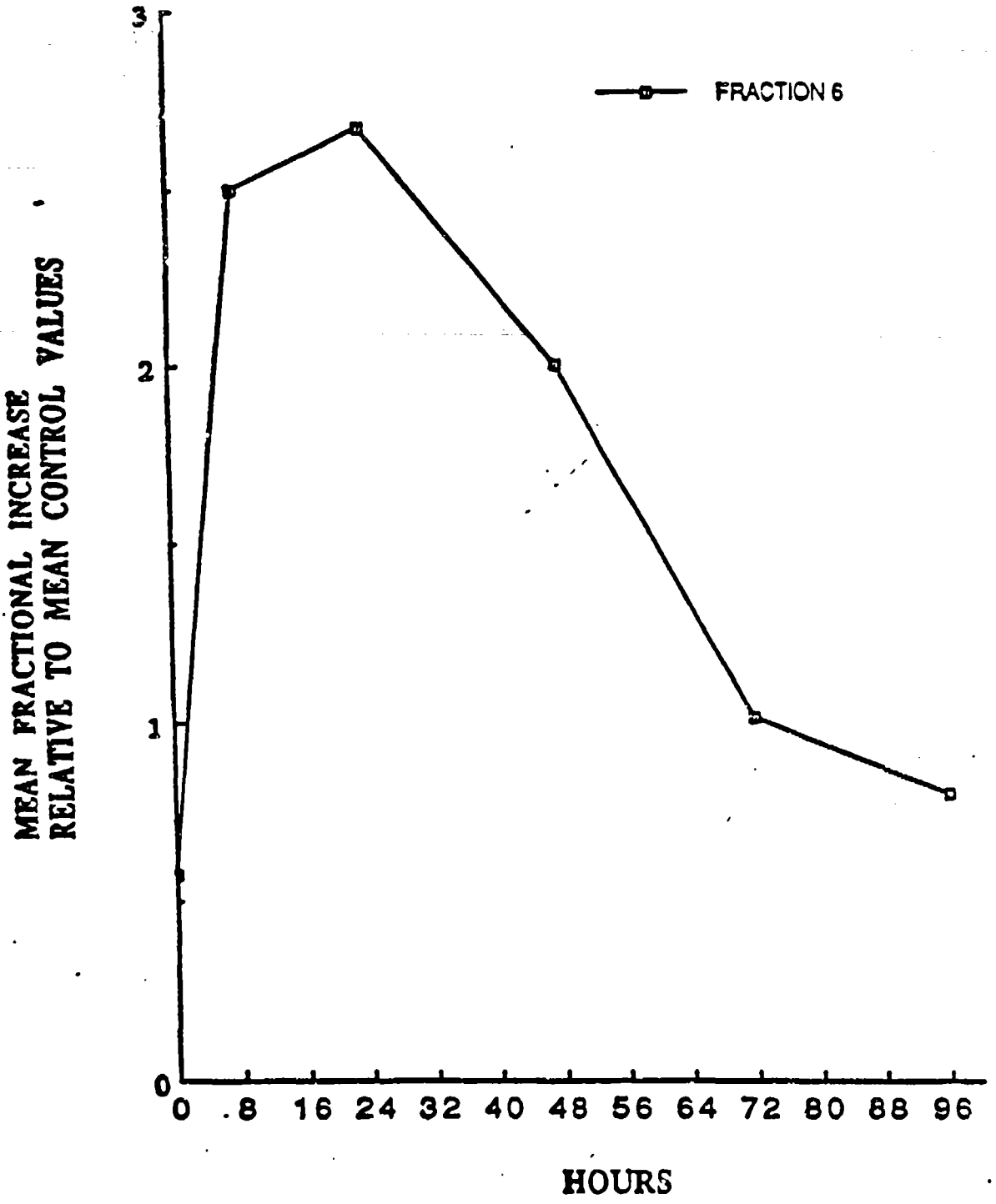

Figure 16: Kinetic response of Fraction 6 to NO_2 exposure. Fraction 6 was hardly detectable in air control animals, but showed significant increases at 8 hr and 24 hr NO_2 post-exposure.

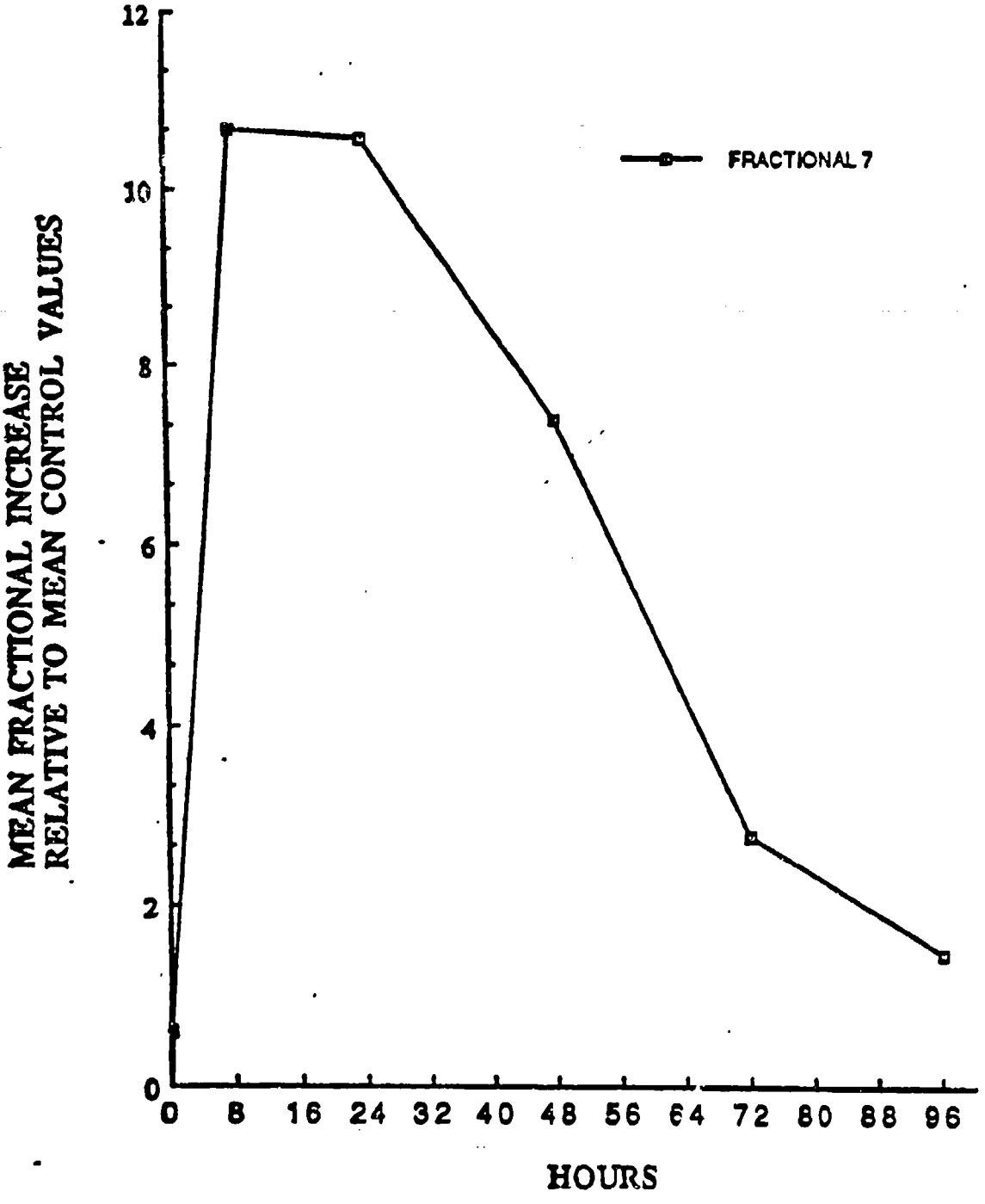

Figure 17: Kinetic response of fraction 7 to NO_2 exposure. Fraction 7 was elevated ~10 fold at 24 hr NO_2 post-exposure.

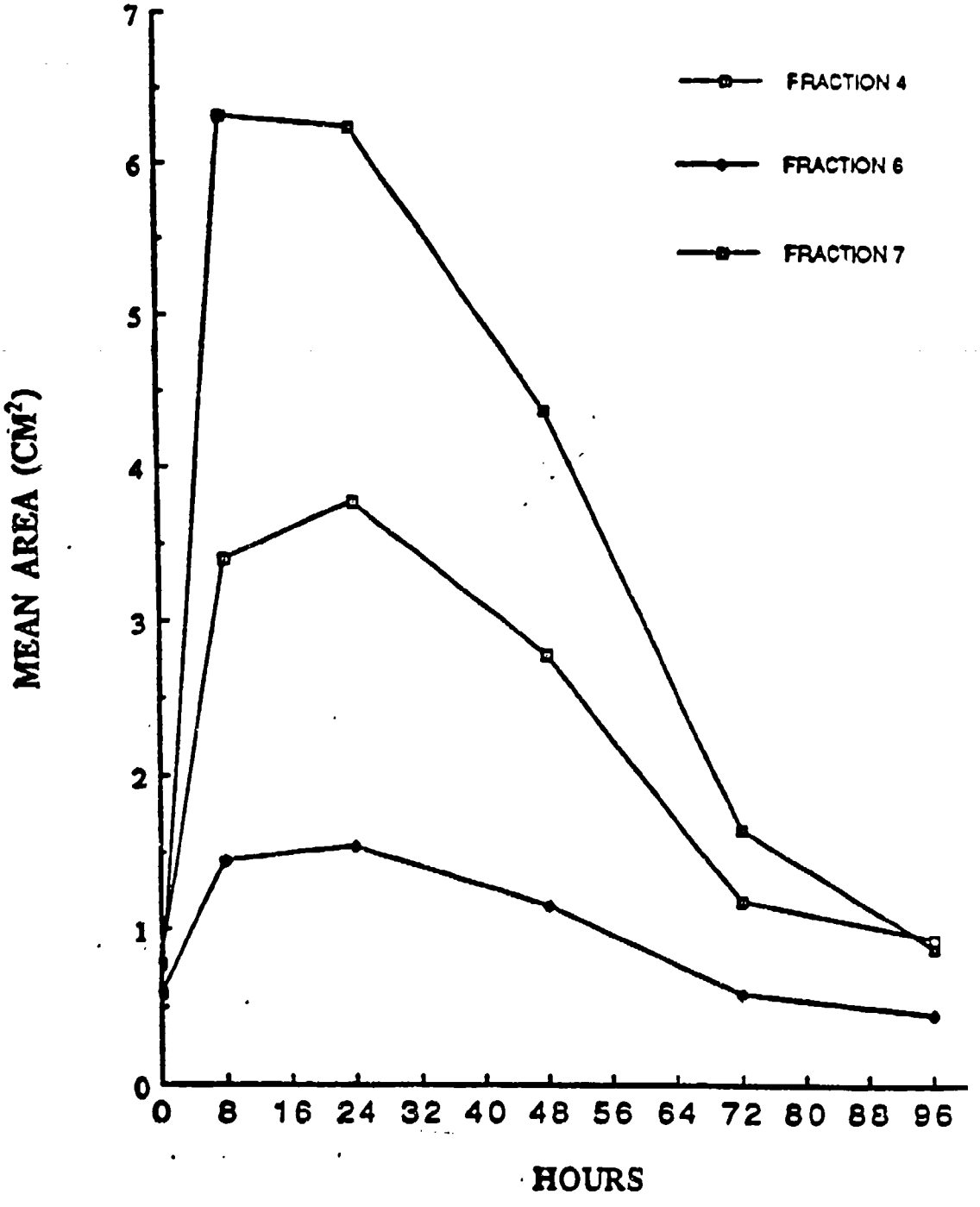

Figure 18: The kinetic response of fractions 4, 6, and 7 after exposure to NO_2. These kinetics indicate that these three constituents of BALF followed the same time course.

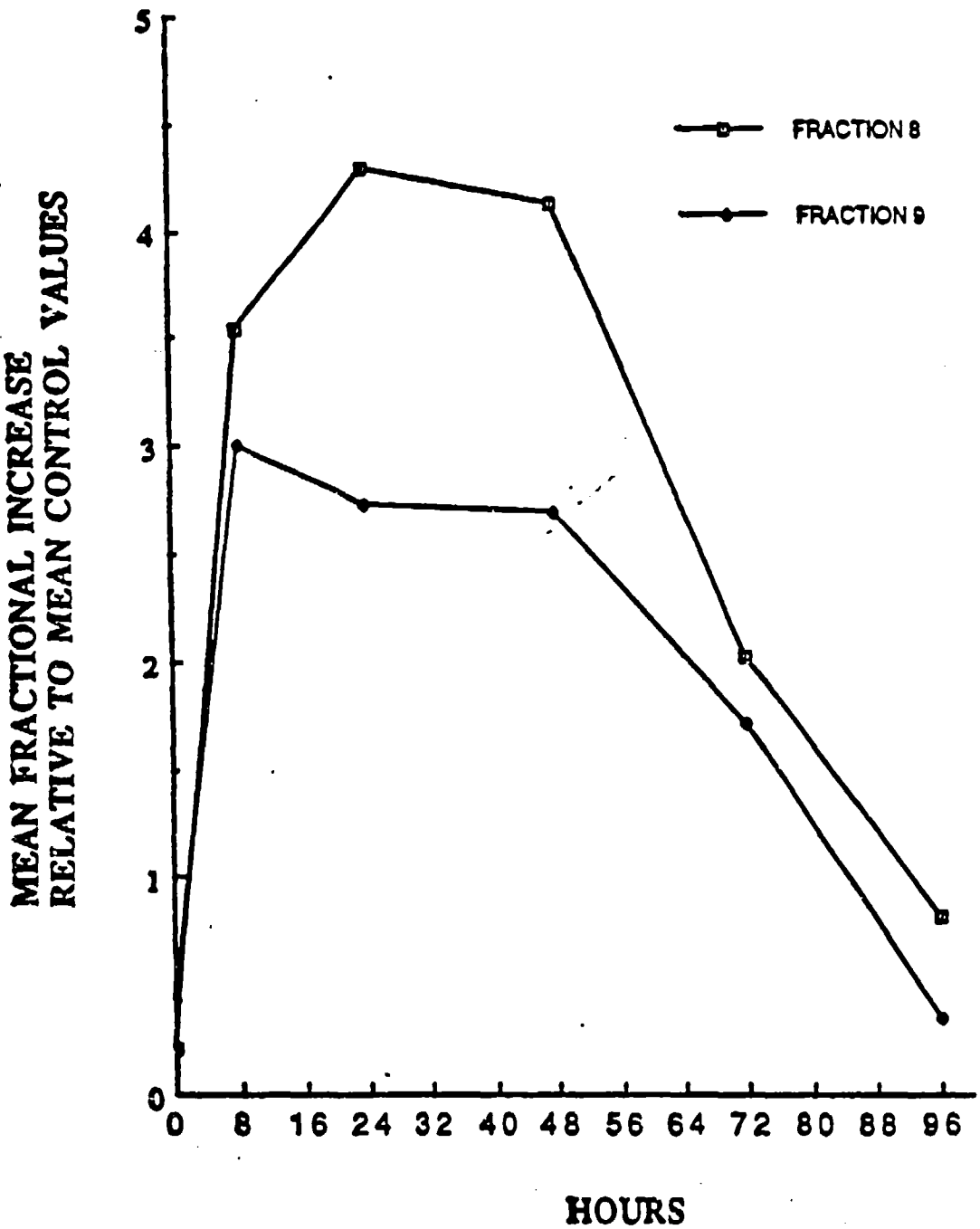

Figure 19: Kinetic response of fraction 8 and fraction 9 to exposure to 100 ppm NO_2 for 15 minutes. These two constituents were hardly detectable in control animals, but increased to levels that were significant in NO_2 exposed animals.

differed from that of fractions 3 and 5 which were slower to increase to maximum levels (they took 24 hrs) and which stayed elevated longer (through 72 hrs post-exposure) before decreasing to control levels (Figure 15). These three different kinetic responses suggest that three different sources may exist from which the lavage proteins are derived and/or translocated from due to a permeability leak. The detailed analysis described above demonstrates the usefulness of IEC in characterizing the kinetic response of lavage fluid constituents during an environmental insult.

IV. D. Kinetics of the Free Cell Response to NO_2

In a second component of the study, animals that were exposed to sham-air and NO_2 were sacrificed and lavaged to analyze the lung's free cell response as an index of lung injury. The lung free cells from the air control animals were counted by a hemocytometer and the viability of the cells was indexed as cell membrane integrity using the trypan blue exclusion technique (Life Technologies, Inc. Chagrin Falls, OH). Also cytocentrifuged slide preparations were made of the lavaged cell populations for cell differential analyses. This experiment indicated that, on average, >95% of the cells lavaged from the control lungs were viable, or at least had intact cell membranes, Table II. Cell differential analyses of control cells indicated that greater than 98% of the cells were alveolar macrophages (figure 20). The average percentage of polymorphonuclear leukocytes (PMN) in the control free cell populations was less than 1%. Small mononuclear cells were infrequently observed in the control free cell samples (~0.5%).

The viabilities of the lung free cells harvested from the NO_2 exposed animals were similar to those of cells lavaged from the air

Table II: Lavaged Cell Viabilities

Groups: N=4	Air 24 hr	NO_2 8 hr	NO_2 24 hr	NO_2 48 hr	NO_2 72 hr	NO_2 96 hr
X	95.5	92.1	92.3	97.2	98.1	95.1
S.E.M. ±	1.56	1.55	1.81	0.82	0.14	0.44

*No significant differences were observed in the average cell viability between air control and NO_2 exposed pupulations.

(N) Number of animals per group.
(X) Mean.
(S.E.M.) Standard Error of Mean.

Table III:Total Numbers of Lavaged Cells ($x10^{-7}$)

N=4	Air 24hr	NO_2 8hr	NO_2 24hr	NO_2 48hr	NO_2 72 hr	NO_2 96hr
X	1.35	2.0	1.2	5.7	6.1	1.9
S.E.M. ±	0.18	0.68	0.15	0.34	0.43	0.32

* There were noticeable increases in the total number of lavaged cells at NO_2 48 hr and 72 hr, but at 96 hr post-exposure NO_2 the number of cells retrieved were similar to those from control animals.

(N) Number of animals per group
(X) Mean
(S.E.M.) Standard Error of Mean

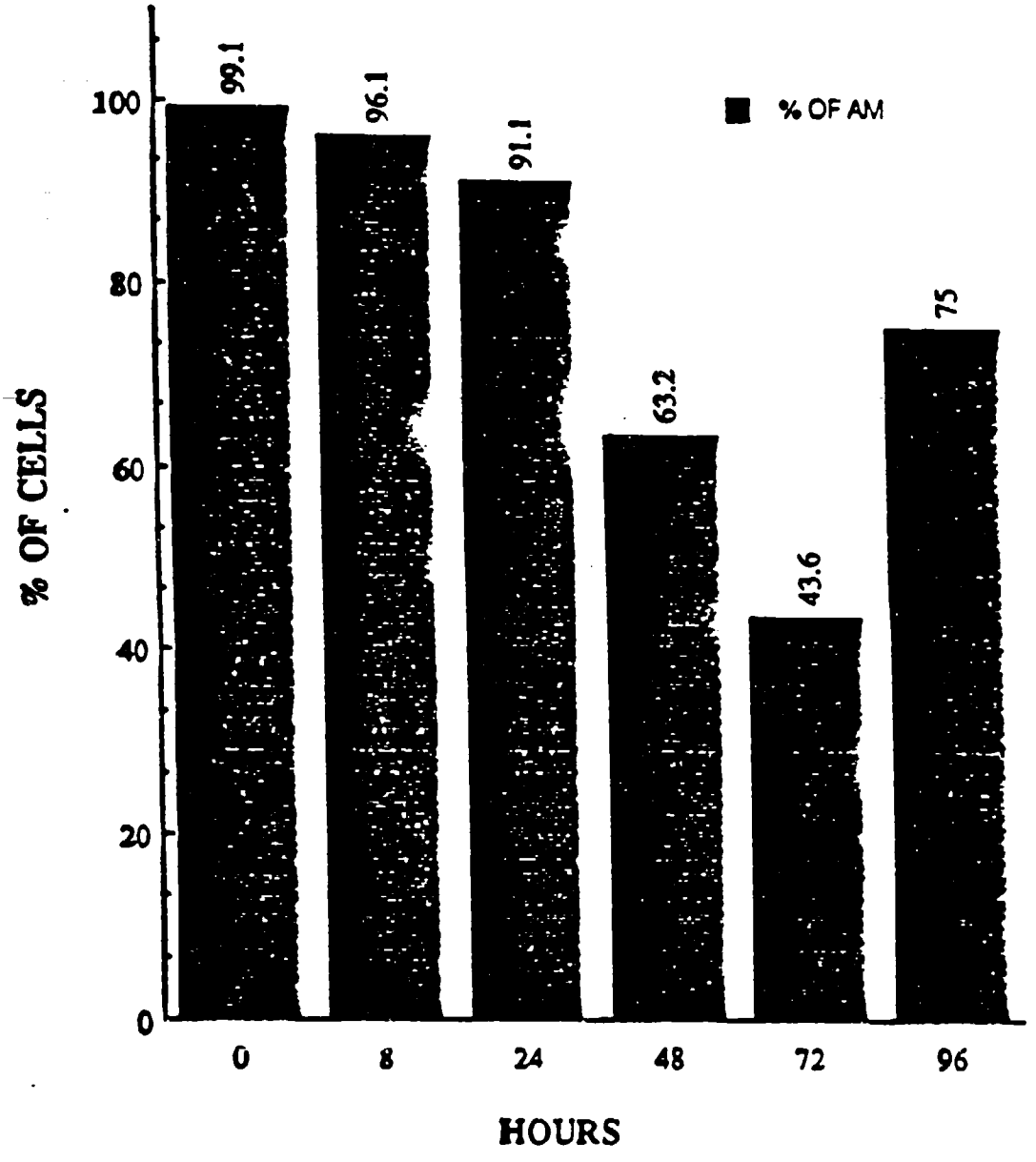

Figure 20: Shows the changes in the percentages of AM after exposure to 100 ppm NO_2 for 15 minutes. (0) Represents control values.

control animals ,Table II. When examining the number of lavaged cells, there were no significant increases at the 8 hr and 24 hr NO_2 post-exposure time points relative to control values. Significant numbers of lavaged cells were retrieved 48 hr and 72 hr after NO_2 exposure. At the 48 hr time point, the total number of lavaged cells were elevated ~4, and as of 72 hr post-NO_2 the number of lavaged cells remained similarly increased, Table III.

The cell differential analyses performed on animals exposed to NO_2 indicated that as of 8 hr post-exposure ~96% of the cells were alveolar macrophages (AM). Subsequently, a slight decrease occurred in the percentage of AM as of the 24 hr post-exposure time point. This decrease in the relative abundance of AM continued in animals sacrificed at 48 hr and 72 hr post-exposure when the percentages of AM at these times had decreased significantly to ~63% and ~43% of the free cell population respectively(figure 20). As of 96 hr the percentage of AM cells were ~75% , suggesting a recovery from the effects of NO_2 injury. The influx of PMN cells from the vasculature compartment into alveoli spaces, was first detected as of 8 hr post-exposure. This response was initially relatively mild, but it did continue in animals sacrificed at 24 hr. By 48 hr the percentage of PMN cells had increased ~31% compared to control animals. The results from animals sacrificed 72 hr after NO_2 exposure indicated that the percentage of PMN cells had increased to ~53.2%. There after, the percentage of PMN cells decreased to ~22% by 96 hr (Figure 21).

The numbers of AM increased considerably after NO_2 exposure. While there were no significant increases in AM numbers at the 8-24 hr NO_2 time points, as of the 48 hr post-exposure the absolute number of AM had increased from ~1.3×10^7 in control animals to ~3.6×10^7 in exposed animals, Table IV. The numbers of AM remained greater than the numbers observed with control animals, even after 72 hr NO_2, when the absolute numbers of AM were ~2.6×10^7 (Table IV). It was also found that the absolute number of AM diminished to a level comparable to control animals as of 96 hr after NO_2 exposure.

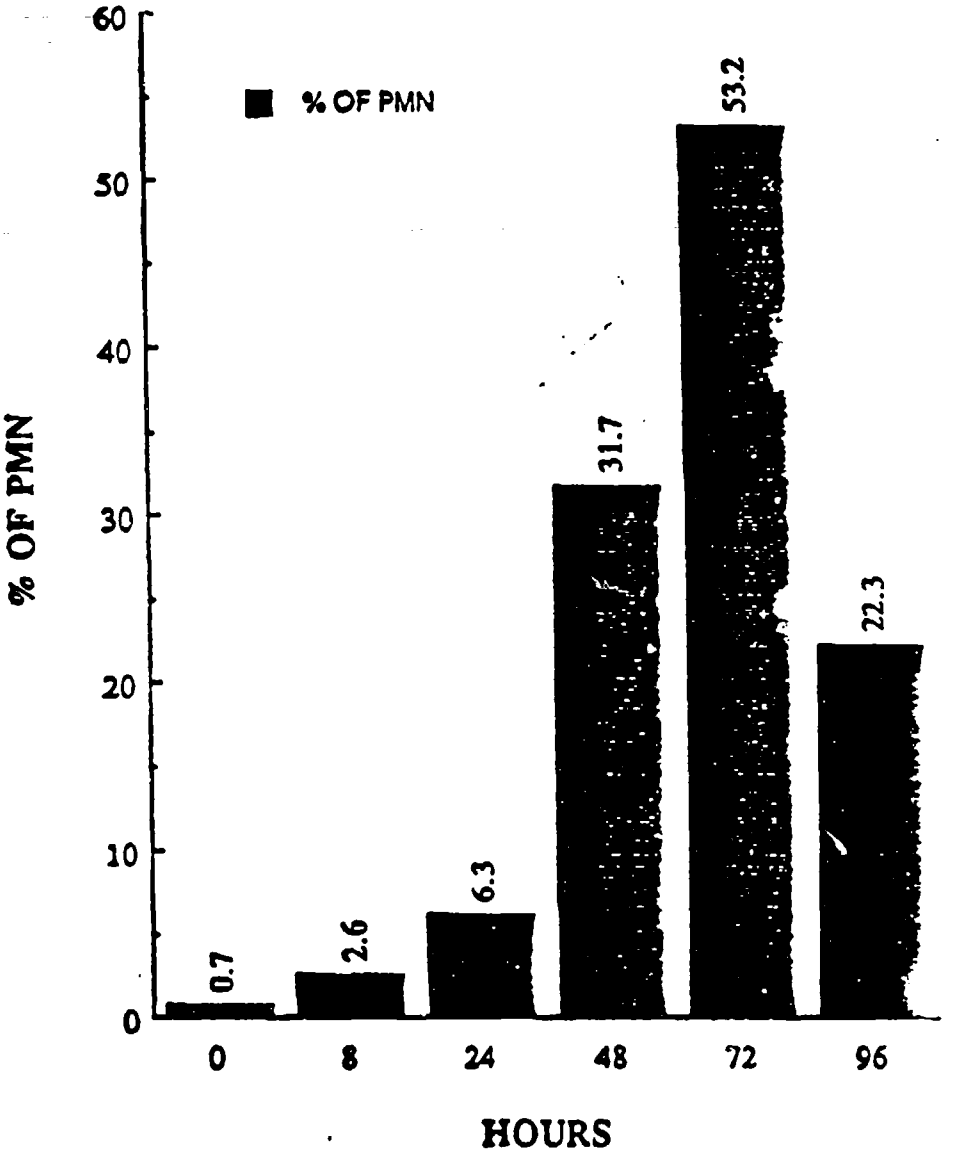

Figure 21: Shows the response of PMN cells to 100 ppm NO_2 for 15 minutes.
(0) Represent control values.

Table IV: Absolute Cell Population

	AM	PMN	MONO
AIR	1.3×10^7	9.4×10^4	6.7×10^5
NO_2 8 hr	1.9×10^7	5.2×10^5	2.2×10^5
NO_2 24 hr	1.0×10^7	7.5×10^5	3.0×10^5
NO_2 48 hr	3.6×10^7	1.8×10^7	2.7×10^6
NO_2 72 hr	2.6×10^7	3.2×10^7	1.9×10^6
NO_2 96 hr	1.4×10^7	4.2×10^6	3.8×10^5

Unlike with the AM, the PMN cells numerically increased as of 8 hr post-exposure to NO_2, and this inflammatory response continued to increase until it reached a maximal levels as of 72 hr after exposure (Table IV). By 96 hr after NO_2 exposure, the PMN response directionally subsided. There was also noticeable increase in mononuclear cells at the 48 and 72 hr post exposure times when AM numbers were also increased.

The kinetic responses of lung free cells to NO_2 exposure were generally slower than the kinetic responses of the BALF proteins. The BALF proteins showed maximum responses by 24 hr post-exposure (Figure 13) while the lung free cells took 48 hr to show a large response (Figures 20 & 21). Likewise, the recovery of free cells to control levels was slower than that of the proteins. By 96 hours the AM and PMN cells had not completely recovered to control levels (Figures 20 & 21).

V. DISCUSSION AND SIGNIFICANCE OF STUDY

V. A. Usefulness of HPLC Technique Compared to Other Techniques for Characterizing Pulmonary Edema.

Two of the main objectives of this study were: 1) to develop a more rapid, quantitative HPLC method for measuring various proteins in BALF, and 2) evaluate the utility of the new approach for determining changes in the protein constituents in the lung's ELF during pulmonary edema, as sampled by bronchoalveolar lavage. Several conventional approaches for assessing biochemical changes in BALF to index pulmonary edema do not provide specific information concerning the underlying nature of the permeability disturbances. Basically, these simple approaches are most useful for determining generalized permeability changes. Measurements of total protein or albumin in lavage fluid samples, for example, do not provide information that may be pertinent to the underlying nature of the permeability changes in the lungs, e.g., effective pore sizes.

The HPLC procedure developed in this study provides a means to quantitatively resolve a number of constituents that may be used to characterize the status of pulmonary edema. As examples, fraction 7 and fraction 4 have been identified as containing plasma proteins (albumin and transferrin) base on standards. These two fractions were elevated and responded similarly to 100 ppm NO_2 exposure, thus suggesting that these two constituents of the BALF were from similar origins, i.e., the blood compartment. It is also important to note that the sixth fraction , which was hardly detectable in control animals, also followed a similar kinetic course as fraction 4 and fraction 7 after exposure to 100 ppm NO_2. From this kinetic behavior, it is suspected that this unidentified protein was also derived from the blood compartment.

There are four other fractions that may contain proteins (3, 5, 8, and 9), which have not been identified in this study. These potentially were derived from the epithelial cells of the lung. All these fractions can be collected and subjected to further HPLC analysis by the reverse-phase chromatography system recently developed by Gurley et al, 1987.

The separation of various proteins found in rat lung lavage preparation by IEC can be useful in toxicological and pathological studies of permeability pulmonary edema. For example, protein in lavage fluid usually increases in the early hours of lung damage when edema fluid moves across the air-blood barrier carrying plasma derived proteins. However, protein increases in the ELF can also result from lung cells, either as metabolic products or as constituents that may be released after lung cells become damaged. Thus, IEC techniques may be useful in the study of proteins that are derived from Type I and Type II cells . Fraction 3 and fraction 5 followed a similar kinetic response, totally different from the kinetic course observed with fractions 4 and 7. This suggests that fraction 3 and fraction 5 are from different origins separate from the blood compartment and should be given close attention in future studies. It is tempting to speculate that the origin of fraction 3 and fraction 5 may be from damaged lung cells.

The most important observation in this work is the discovery of three new proteins that appear in the BALF after exposure to NO_2. The identification of these three fractions (6, 8, and 9) and an investigation of their relationships to edema should have a high priority in future work on the mechanisms of lung injury.

V. B. Current Shortcomings and Advantages of the Technique and Areas Requiring Further Study.

This newly developed technique offers both advantages and disadvantages as an approach for quantitating protein constituents in lavage fluids. One of the major disadvantages found with the technique was that the commercial IgG standard did not give a clear identification of immunoglobulin-G, possibly due to heterogeneous subclass composition of the reference standard. Although not a shortcoming, several of the BALF fractions resolved from the IEC have not yet been identified, so the full potential of the methods resolution cannot yet be taken advantage of.

The advantages of this procedure, however, are numerous. One advantage is the technique's sensitivity. With the present system, the column can be loaded with a small amount of lavage fluid (~300

µl or more) and then the fractions can be collected and prepared for further studies using other analytical systems, e.g., reverse-phase chromatography, high performance capillary electrophoresis, and amino acid analyses, to mention only a few approaches that may be employed in future investigations. Compared to the current HPLC system developed by Gurley et al (1988, 1989), the IEC technique requires a shorter run duration (~30 min) than the reverse-phase protocol, which requires ~200 min. The shorter run durations will provide researchers the capability to assess more samples on a daily basis

Another Advantage of IEC is its sensitivity to the detection of new components in BALF following lung injury. IEC offers the pulmonary biologist a preparative method for the isolation and fractionation of these new BALF components. Thus, it should serve as an important new tool in the collection of methods used to study pulmonary biology.

V. C. Insight that the New Technique Has Provided In Characterizing the Kinetics of NO_2-Induced Pulmonary Edema.

This new IEC-HPLC technique was found to provide sufficient fractionation of BALF constituents to be of use in investigating the pulmonary edematous responses to NO_2 . Some of the constituents that eluted from the ion exchange column are thought to derive from the blood compartment of the rat. The other fractions, which were resolved by IEC, could have been derived from origins other than the blood, e.g., damaged lung cells and the lung interstitial region. Results from standards and preliminary studies identified fraction number 7 as albumin, which is a plasma protein. Albumin was the most abundant blood constituent found in lavage fluid, and it responded more rapidly to NO_2 than fractions 3 and 5, which have not yet been identified. This fraction also reached a maximum of 11-fold increase after only 8 hr exposure. This response remained elevated for one day and started to subside by the second day. By day four the albumin constituent had recovered to levels observed with air control animals. The kinetic response of fraction 4 (which contains the blood protein transferrin) was similar to the albumin fraction, as

was fraction 6, which would indicate that all three of these fractions (4, 6, and 7) were derived from plasma. The origin of fractions 3 and 5 is not known, but their slow kinetic response to NO_2 exposure suggests they are derived from some origin other than the blood compartment. Likewise, tne different kinetic responses of fractions 9 and 8 suggest these two new proteins are derived from yet a third source.

VI. CONCLUSION

The hypothesis that IEC could be useful in resolving and quantifing various blood protein in BALF has been substantiated. Secondly, the new technique has also been shown to offer the ability to characterized constituent changes in BALF following the inhalation of a toxic agent known to produce permeability changes in the lung. Thirdly, the new HPLC system has demonstrated an ability to quantify BALF constituent changes both rapidly and reprodi ɔly. Comparison of the lung free cell response to the protein changes in lavage fluid has the potential for revealing new insights into the mechanisms of pulmonary edema and the roles these cells and proteins have in the .ung injury resulting from the edema.

VII. REFERENCES

1 Barrios, R., Inoue, S., and Hogg, J.: Intercellular junctions in "Shock Lung" a freeze fracture study. Int Acad. of Path. Vol 36; 628-635. (1977)

2 Brown, E.S.: Lung area from surface tension effects. Proc. Soc. Exp. Biol. Med. Vol. 95; 168-170. (1957)

3 Burri, P.H: In Current Problems in Clinical Biochemistry. The Cells of the Alveolar Unit (Favez, G., Junod, A., and Leuenberg, T., Eds.), Vol. 13; 11-22, Huber, Bern. (1983)

4 Crapo, J.C., Barry, B.E., Gehr, P., Bachofen, M., and Weibel, E.R: Cell characteristics of the normal human. Amer. Rev. Respir. Dis. Vol. 125; 740-745. (1982)

5 Curry, F.C. and Michel, C.C: A fiber matrix model of capiliary permeability. Microvasc. Res. Vol. 20; 96-99. (1980)

6 Evans, M. J., Dekker, N.R., Carbral, Anderson, L.J., and Freeman. G: Quantitation of damage in acute oleic-induced lung injury. Amer. Rev. Respir. Dis. 845-850. (1978)

7 George, G., and Hook, E.R: The pulmonary extracellular lining. Environ. Health Perspect. Vol. 55; 227-237.(1984)

8 Green, G.M. Jakob, G.j., Low, R.B., Davis, G.S: Defense mechanisns of the respiratory membrane. Amer. Rev. Respir. Dis., Vol. 115, 479-514. (1977)

9 Gurley, L.R., Valdez, J.G., London, J.E., Dethloff, L.A., Lehnert, B E.: An HPLC procedure for the analysis of proteins in lung lavage fluid. Analytical Biochem. Vol. 172; 465-478. (1988)

10 Gurley, L.R., London, J.E., Dethloff, L.A., Stavert, D.M., Lehnert, B.E: Analysis of proteins in bronchoalveolar lavage fluids during pulmonary edema resulting from nitrogen dioxide and cadmium expcsure. In: Techniques in Protein Chemistry (T. Hugli, ed.) Academic Press, Inc., 479-489 (1989)

11 Hoffman, R.M., Claypool, W.D., Katyal, S.L., Singh, G., Rogers, R.M., and Dauber, J.H: Augmentation of rat alveolar macrophage migration by surfactant proteins. Amer. Rev. Respir. Dis. Vol. 135; 1358-1362. (1987).

12 Humbert, F., Grandchamp, A., Pricam,C., Perrelet, A: Morphological changes in tight junctions of necturus maculosus proximal tubules undergoing saline diuresis. J Cell Biol. Vol. 69; 90-97. (1976)

13 Inoue, S., Nichel, R.P., Hogg, J.C: Zonulae occludentes in alveolar epithelium and capillary endothelium of dog lungs studies with the freeze fracture technique. J. Ultrastruc. Res. Vol. 56; 215-225. (1976)

14 Jacobs, A: Low molecular weight intracellular iron transport compounds. Blood. Vol. 50; 433-439. (1977)

15 Juers, J.A., Rogers, R.M., McCurdy, J.B., and Cook, W.W: Enhancement of bactericidal capacity of alveolar macrophages by human alveolar lining material. J. Clin. Invest. Vol. 58; 271-275. (1976)

16 Kuhn, C: In Lung Biology in Health and Disease. Biochemical Basis of Pulmonary Function (Crystal, R.G., Ed.), Vol. 2; 3-48, Dekker, New York. (1976)

17 LaForce, F.M., and Boose, D.S: Subletal damage of esherichia coli by lung lavage. Amer. Rev. Respir. Dis. Vol. 124; 733-737. (1981)

18 Lehnert, B.E., and Morrow, P.E: Preservation of Fcγ receptor-mediated particle phagocytosis and binding with rat alveolar macrophages adhered to a plastic substrate in a serum free system. Immunol. Commun. Vol. 13; 313-323. (1984)

19 Macklem, P.T., Proctor, D.F., and Hogg, J.C: The stability of peripheral airways. Resp. Physiol. Vol. 8; 191-203. (1970)

20 Rombout, P.J.A., Doman, J.A.M., Marri, M., and Van Esch, G.J: Infuence of exposure regimen on nitrogen dioxide-induced morphological changes in the rat lung. Environ. Res. Vol. 41; 466-480. (1986)

21 Renkins, E.M: Capillary transport of macromolecules, pores, and other endothelial pathways. J. Appl. Physiol. Vol. 58; 315-325. (1985)

22 Soloman, A.K: Characterization of biological membranes by equivalent pores. J. Gen. Physiol. Vol. 51; 335-364. (1965)

23 Sorokin, S.R: A morophological and cytochemical study on the great alveolar macrophage. J. Appl. Physiol. Vol. 6; 230-237. (1966)

24 Schneeberger, E.E.and Karnovsky, M.J: The ultrastructural basis of alveolar-capillary membrane permeabilty to peroxidase used as a tracer. J. Cell Biol. Vol. 37; 781-793. (1968)

25 Starling, E.H., (1896). On the absorption of fluids from the connective tissue spaces. J. Physiol. (Lond) 2-247. (1896)

26 Stavert, D.M., Archuleta, D.C., Holland, L.M., Lehnert, B: Nitrogen dioxide exposure and development of pulmonary emphysema. Toxicol. Environ. Health Vol.17; 249-267. (1986)27 Stavert, D.M., Lehnert, B.E: Potentiation of the expression of nitrogen dioxide-induced lung injury by post exposure exercise. Environ. Res. Vol. 48; 87-99. (1989)

28 Stavert, D.M., Lehnert, B.E: Nitric oxide and nitrogen dioxide as inducers of acute pulmonary injury when inhaled at relatively high concentrations for brief durations. Inhalation Toxicology.(in press, 1990)

29 Styla, M., Wahl and Berierualtes: Antibody purification by high performance ion exchange chromatography. J. of Immunol. Meth. Vol. 75; 75-82. (1984)

Further Development of a Kinetic Model of Nitric Oxide-Induced Methemoglobin Formation and the Elimination of Methemoglobin

Previously, we developed a simple first order model of the formation of methemoglobin (MetHb) during the inhalation of nitric oxide (NO) and the elimination of MetHb after cessation of exposure to NO. As a point of reference for a subsequent discussion of further work we have undertaken is this area, a summary of our original model follows.

KINETICS OF METHEMOGLOBIN FORMATION AND ELIMINATION AS A FUNCTION OF INHALED NITRIC OXIDE CONCENTRATION AND MINUTE VENTILATION

The Toxicologist 9:A144, 1989

INTRODUCTION

Nitric oxide (**NO**) is a major oxide of nitrogen that can be produced during combustion processes. Recent studies in our laboratory indicate that this nitrogen oxide species is essentially non-toxic to lung tissue, even when inhaled at high mass concentrations. However, the inhalation of **NO** does result in the formation of methemoglobin (**MetHb**), which in turn reduces the oxygen carrying capacity of the blood.

Little experimental information is currently available as to the rates at which **MetHb** accumulates relative to inhaled **NO** concentration and minute ventilation. Additionally, surprisingly little data presently exists as to the rate by which **MetHb** is removed from the blood following **NO** exposure. Thus, the present study was undertaken with the Fischer 344 rat to obtain such information. The resulting data base was then used to develop an initial kinetic model for **MetHb** formation and elimination as a function of **NO** exposure concentration and minute ventilation.

METHODS

MetHb Kinetic Studies: Adult Fischer 344 rats were anesthetized with ethrane and catheters were placed into their middle caudal arteries. 30 min thereafter, 20 μl of arterial blood was sampled from each resting animal and analyzed for **% MetHb** saturation (Radiometer OSM-3). The rats were then exposed to 1000 ppm **NO** for 23 min or to 200 ppm NO for 120 min. Blood samples were taken and analyzed at various times during and after the **NO** exposures. the total amount of blood cumulatively taken from each animal in the 1000 ppm **NO** group was 0.4 ml, and 0.28 ml was obtained from rats in the 200 ppm **NO** exposure group.

MetHb Kinetic During Increased Minute Ventilation (VE): Prior to **NO** exposure, rats were placed into partial body flow plethysmographs. Pressure fluctuations within the plethysmographs were conditioned and amplified and analyzed with a Buxco pulmonary mechanics computer. The rats were exposed to 500 ppm **NO** for 15 min or to 500 ppm **NO** in combination with 5% CO_2 for 15 min. Blood samples were collected during the exposures and up to 1 hr thereafter for **% MetHb** saturation measurements.

RESULTS

Patterns of MetHb Formation and Elimination: The patterns of **MetHb** accumulation and elimination obtained during and after the exposures to 1000 ppm **NO** x 23 min and exposures to 200 ppm **NO** x 120 min are illustrated in Figures 1 and 2. The 1000 ppm **NO** exposure resulted in the formation of ~60% **MetHb** whereas ~25% **MetHb** saturation resulted from the 200 ppm **NO** exposure.

The **% MetHb** saturations of arterial blood collected during and after exposure to 500 ppm **NO** for 15 min or to 500 ppm **NO** in combination with 5% CO_2 are illustrated in Figure 3. The inhalation of CO_2 brought about an approximately 1.6-fold increase in minute ventilation, Figure 4, which was attributable to increases in both tidal volume and breathing frequency, Figures 5 and 6. Importantly, the addition of CO_2 to the exposure atmosphere resulted in an ~1.6-fold increase in the **% MetHb** formed during the 500 ppm **NO** exposure relative to that formed during normal $\dot{V}E$ conditions (~25% **MetHb** vs ~15% **MetHb**), Figure 3.

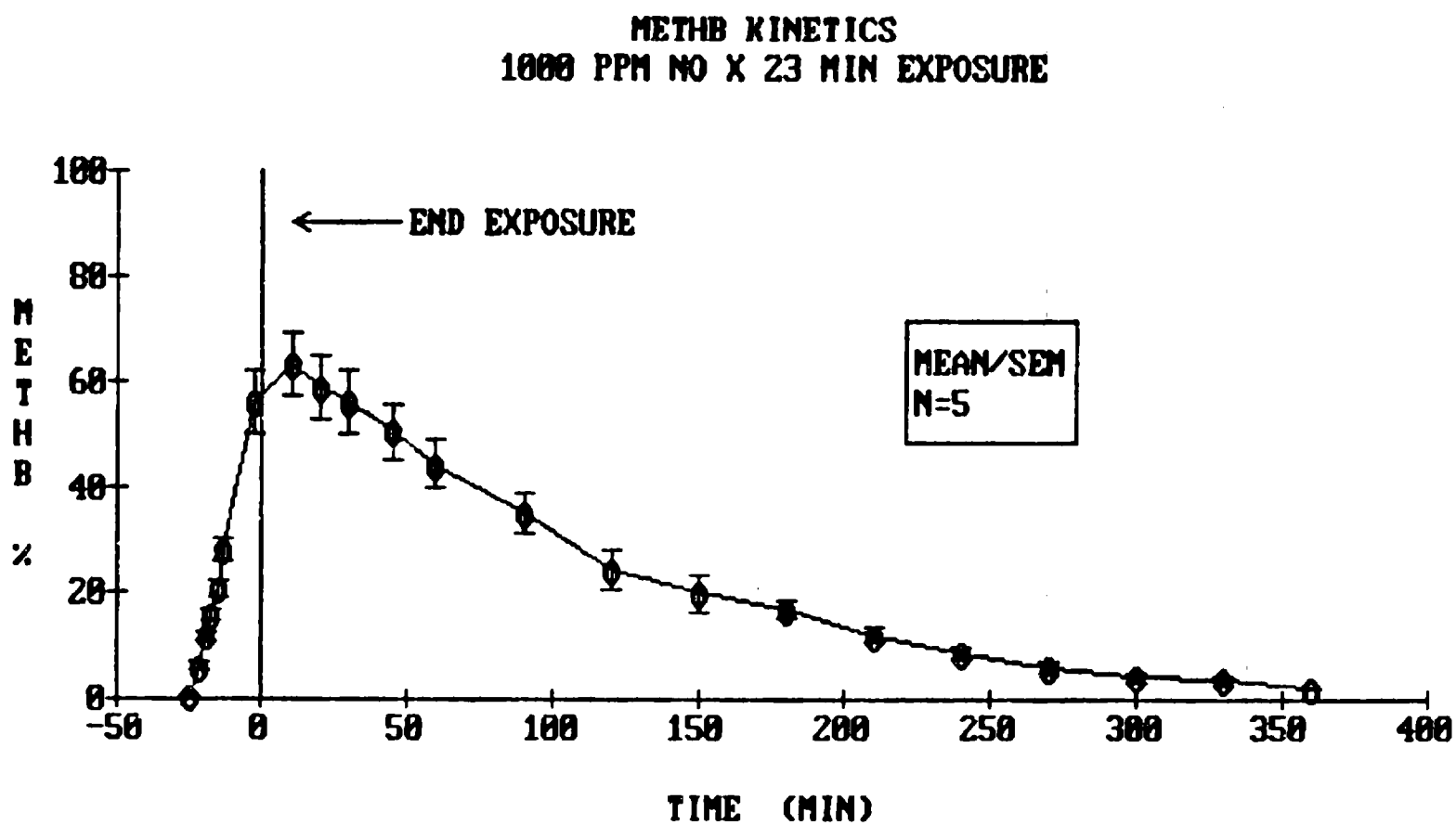

Figure 1: Methemoglobin saturation of arterial blood samples collected from rats during and after inhalation exposure to 1000 ppm NO for a 23 min period of time. Each point represents the mean and standard error of the mean for N = 5 animals.

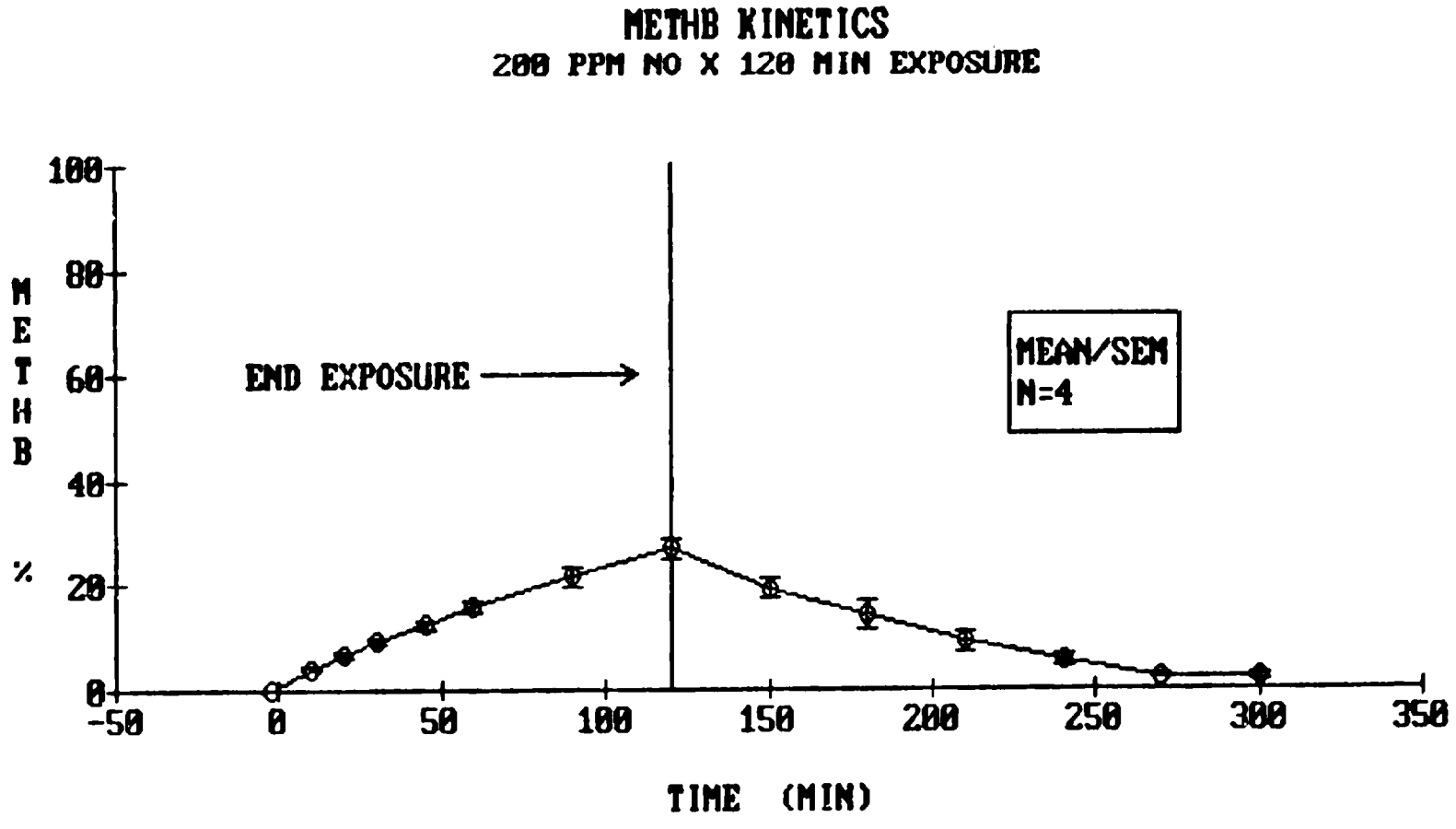

Figure 2: Methemoglobin saturation of arterial blood samples collected from rats during and after inhalation exposure to 200 ppm NO for a period of 120 min. Each point represents the mean and standard error of mean for N = 4 animals.

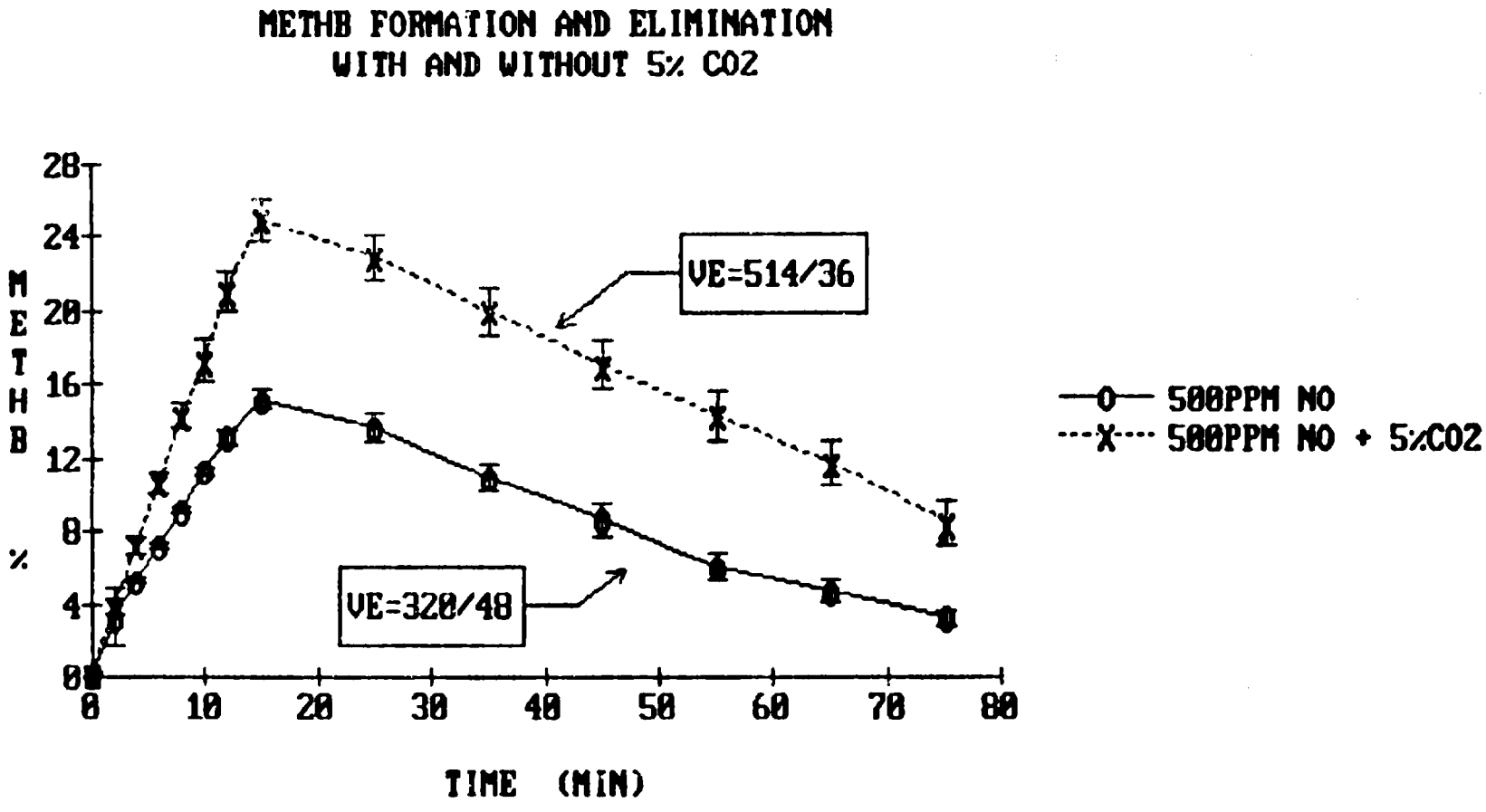

Figure 3: Methemoglobin saturation of arterial blood collected during and after exposure to 500 ppm NO for 15 min or to 500 ppm NO in combination with 5% CO_2 for 15 min. Each point represents the mean and standard error of the mean on 4 or 5 animals.

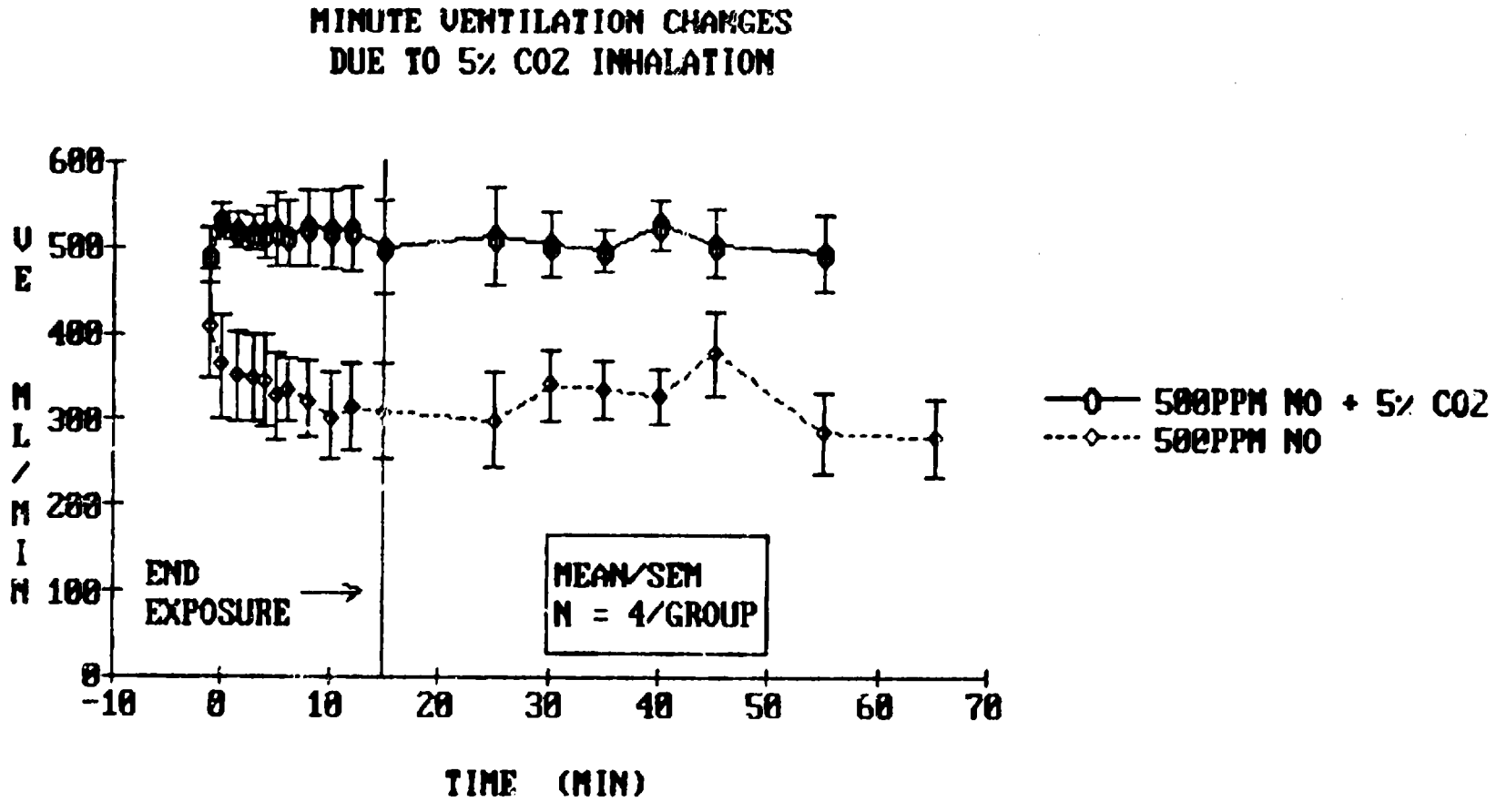

Figure 4: Minute ventilation ($\dot{V}E$) measured on rats during and after exposure to 500 ppm NO or 500 ppm NO in combination with 5% CO_2. Each point represents the mean and standard error of the mean of 4 or 5 animals.

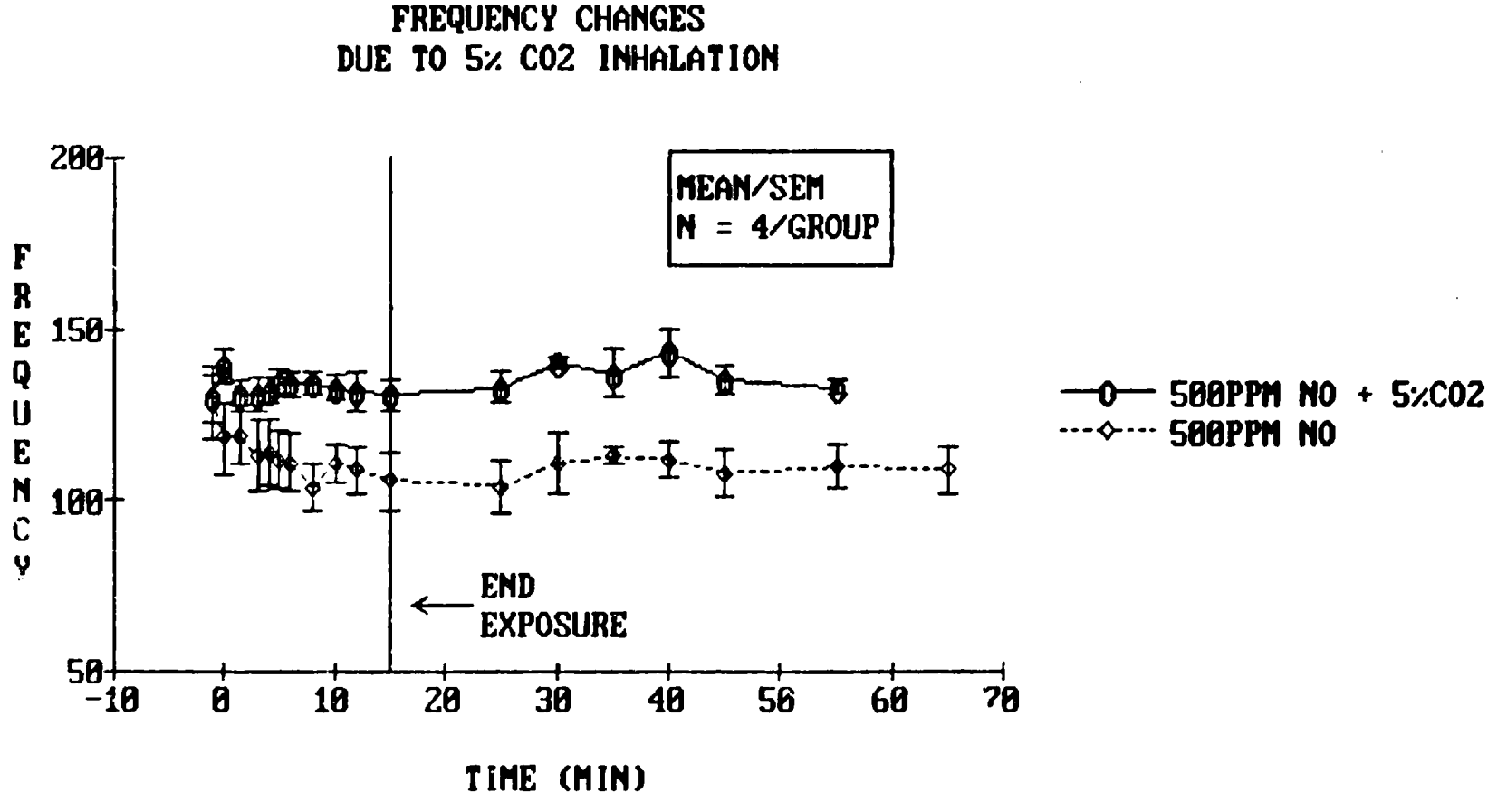

Figure 5: Breathing frequency (f) measured on rats duirng and after exposure to 500 ppm NO or 500 ppm NO in combination with 5% CO_2. Each point represents the mean and standard error of the mean of 4 or 5 rats.

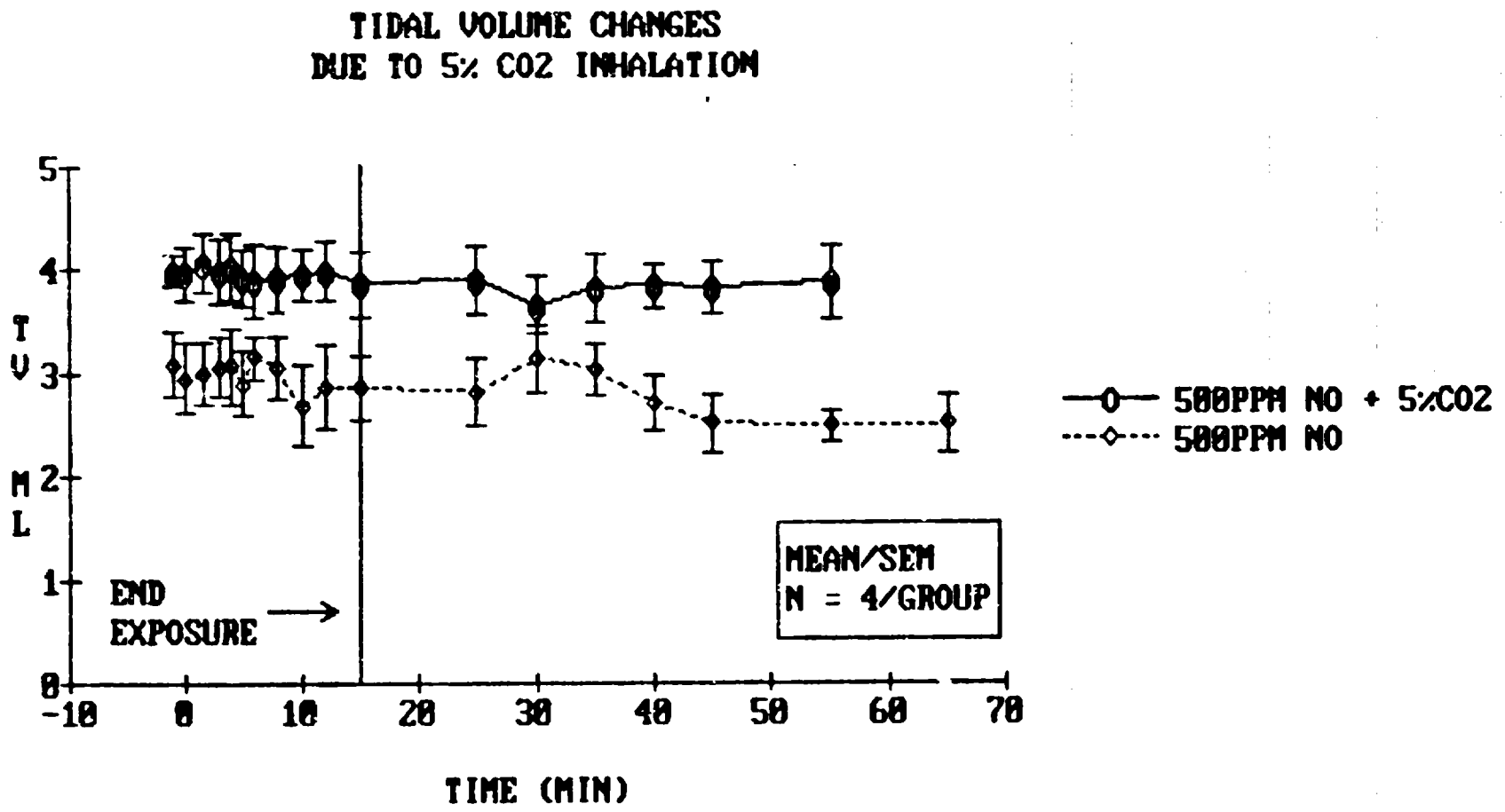

Figure 6: Tidal volume (V_t) measured on rats during and after exposure to 500 ppm NO or 500 ppm NO in combination with 5% CO_2. Each point represents the mean and standard error of the mean of 4 or 5 rats.

Model for Methemoglobin Formation and Elimination in the Rat: Assessments of the elimination kinetics of **MetHb** following cessation of the exposures to 1000, 500, and 200 ppm **NO** indicated that **MetHb** elimination followed a pattern typical of a simple first order process, Figure 7. Given the similar constants for the rate of **MetHb** elimination, or K_{out}, that were estimated from least squares analyses of the actual experimental data for each exposure, the data from all exposures (excluding those involving CO_2) were pooled and reanalyzed to better estimate the actual value for K_{out}, Figure 8. This value was found to be -0.00903 **% MetHb** · min^{-1}, $r = 0.95$ ($P < 0.01$).

In order to model the formation of **MetHb** during the exposures to **NO**, the following model was considered:

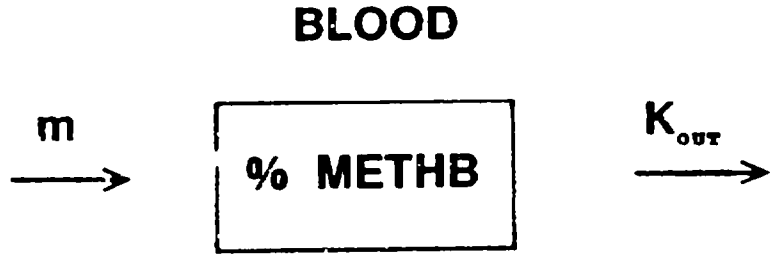

where m is analogous to a constant rate of infusion of **MetHb** into the blood, or, in other words, the % increase in **MetHb** in the blood · min^{-1}. During exposure to NO, actual values for **% MetHb** are measured values and K_{out} was estimated as previously described. m was considered to have a unique value for each exposure concentration considered; $\dot{V}E$ was assumed to be constant in all studies not involving concurrent CO_2 exposure.

The following equation was used to determine m for each exposure concentration:

$$\%\ \text{METHB}_{(t)} = \frac{m}{K_{out}} (1 - e^{-K_{out}(t)}), \text{ where}$$

% MetHb$_{(t)}$ is the percent blood saturation with **MetHb** at any given time during the **NO** exposures. It will be noted that the above equation concurrently accounts for the removal of some **MetHb** during the actual exposure period. (After cessation of the exposure, reductions in **MetHb** are simply described by **% MetHb**$_{(t)}$ = **% MetHb** $_{\text{immediately post exposure}} \cdot e^{-K_{out}(t)}$. Values ascertained for m for each **NO** concentration are shown in Table I and Figure 9. These data could satisfactorily be described by the following equation that relates the rate of **MetHb** accumulation to **NO** exposure concentration under normal ventilating conditions: $\uparrow$ **in % MetHb** $\cdot$ **min**$^{-1}$ = **-0.189 + [0.00313 x NO exposure concentration]**, r = 0.98, Figure 8. Thus, the rate of **MetHb** accumulation can be predicted with foreknowledge of **NO** exposure concentration and the value for K_{out}.

Predicted values for **% MetHb** that were derived from the kinetic model are compared to measured values obtained from animals exposed to 1000, 500, 200 ppm **NO** in Tables II-IV.

TABLE I

Estimated Values For "m"

1000 ppm NO: $m = 3.07684$ % MetHb $\cdot$ min^{-1} ($t = 20$ min)

500 ppm NO: $m = 1.15188$ % MetHb $\cdot$ min^{-1} ($t = 12$ min)

200 ppm NO: $m = 0.34324$ % MetHb $\cdot$ min^{-1} ($t = 60$ min)

500 ppm NO with a 1.6 Fold ↑ in V_E: $m^* = 1.8465$ % MetHb $\cdot$ min^{-1} ($t = 12$ min)

( ): Exposure times at which m was estimated.
*: Estimated value for m is 1.6 times greater than that estimated for the inhalation of 500 ppm under resting conditions.

TABLE II

Predicted Values for % MetHb During and After Exposure to 1000 ppm NO

During Exposure	Predicted*	Measured % MetHb
t = 6 min	17.9%	16.0%
t = 8 min	23.7%	20.7%
t = 10 min	29.4%	28.4%
t = 20 min	56.3%	56.3%
After Exposure		
t = 10 min	70.1%	58.8%
t = 50 min	48.8%	44.5%
t = 120 min	26.0%	24.3%
t = 200 min	12.6%	12.3%
t = 300 min	5.1%	3.8%

*Predicted post-exposure values were determined using the zero time post exposure value for % MetHb extrapolated from least squares fit analyses of all post-exposure data.

TABLE III

Predicted Values for % MetHb During and After Exposure to 500 ppm NO

During Exposure	Predicted*	Measured % MetHb
t = 2 min	2.3%	3.4%
t = 6 min	6.7%	7.3%
t = 8 min	8.9%	9.1%
t = 12 min	13.1%	13.1%
t = 15 min	16.2%	15.1%
After Exposure		
t = 10 min	13.9%	13.6%
t = 20 min	12.7%	10.9%
t = 40 min	10.6%	6.1%
t = 60 min	8.8%	3.3%

*Predicted post-exposure values were determined using the % MetHb value measured immediately upon the cessation of the NO exposure.

TABLE IV

Predicted Values for % MetHb During and After Exposure to 200 ppm NO

During Exposure	Predicted*	Measured % MetHb
t = 10 min	3.3%	4.2%
t = 30 min	9.0%	9.2%
t = 90 min	21.1%	21.5%
t = 120 min	25.1%	26.9%
After Exposure		
t = 30 min	20.5%	19.1%
t = 90 min	11.9%	9.1%
t = 120 min	9.1%	5.8%
t = 180 min	5.2%	2.5%

*Predicted post-exposure values were determined using the % MetHb values measured immediately upon the cessation of the NO exposure.

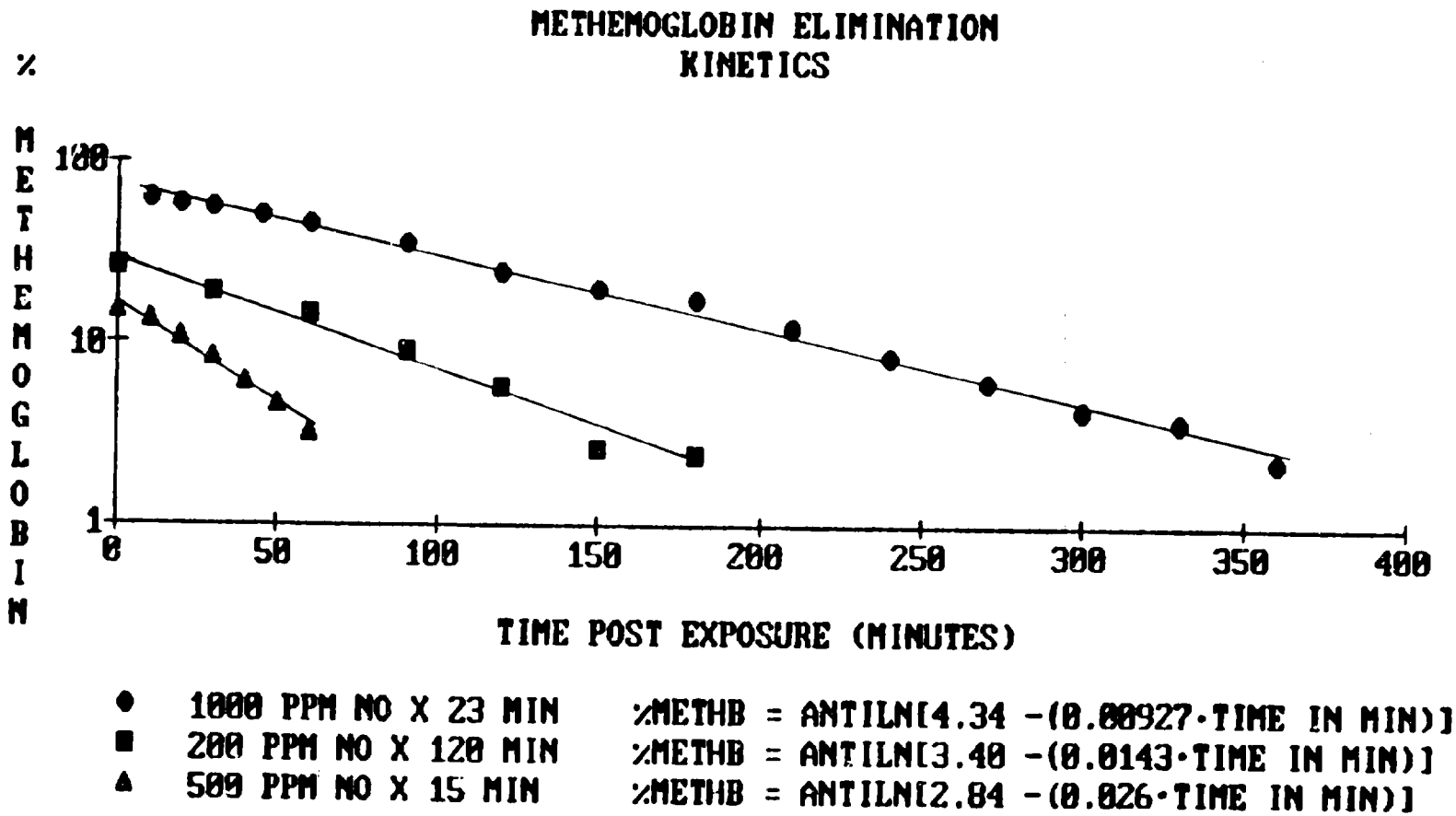

Figure 7: Log plot of % MetHb upon cessation of the 1000 ppm, 500 ppm, and 200 ppm NO exposures.

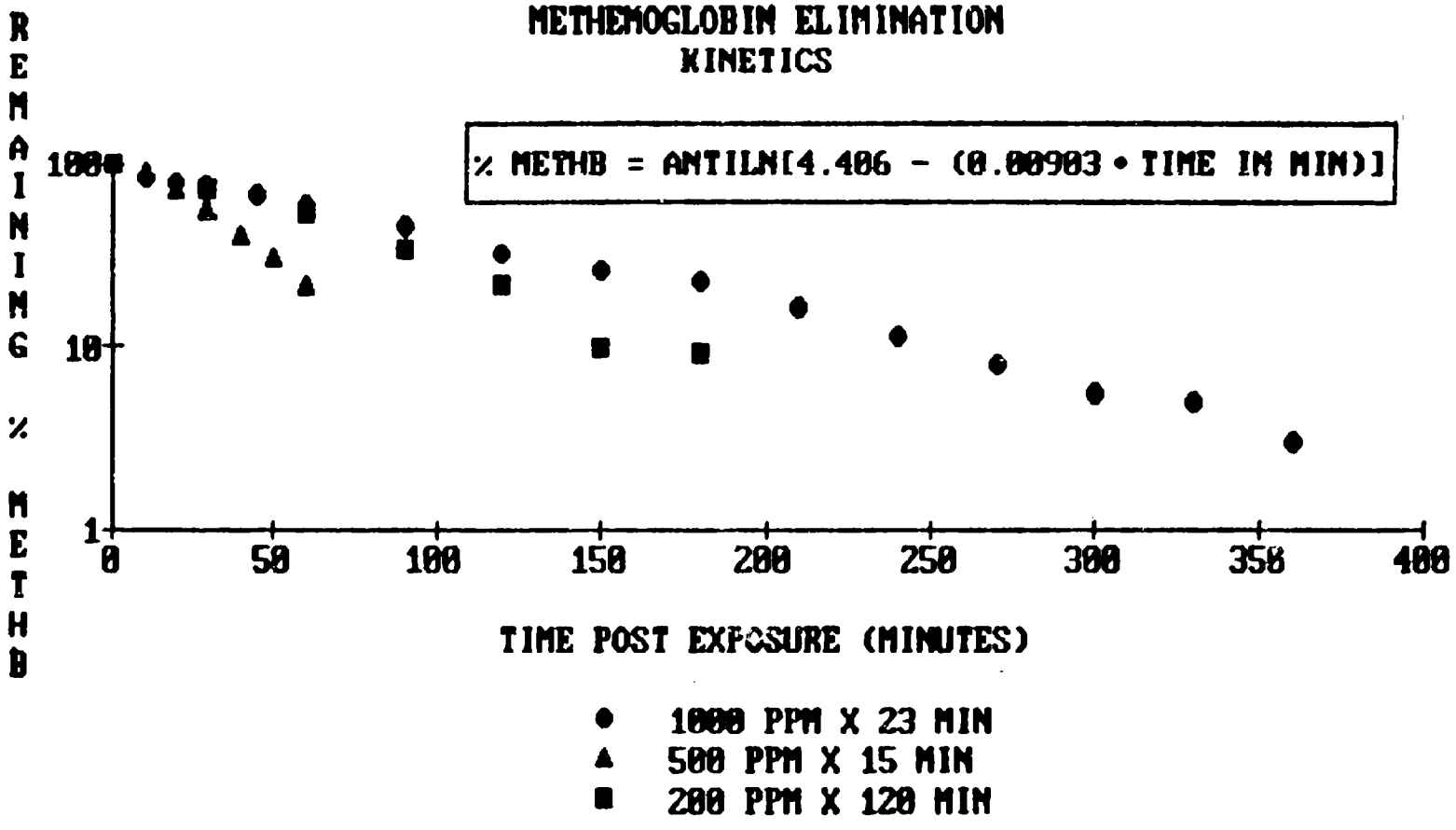

Figure 8: Pooled values plotted represent the percentages of the initial % MetHb at t = 0 post exposure that remained at subsequent post exposure times.

For a given exposure to **NO**, m can be related to the product of **NO** concentration and minute ventilation, which in turn, can be used to predict delivered dose. Accordingly, alterations in m should be proportional to $\dot{V}E$ at a fixed exposure concentration. The results of our studies support such a relationship. As shown in Figure 9 and Table I, a 1.6 fold increase in $\dot{V}E$ due to CO_2 inhalation appeared to have the same effect on m as would an increase in **NO** exposure concentration inhaled under normal conditions. In that **NO** Exposure Concentration = [m - (-0.189)]/0.00313, a 1.6 fold increase in $\dot{V}E$ is equivalent to exposing the animals to ~650 ppm **NO**, Figure 9, under resting conditions.

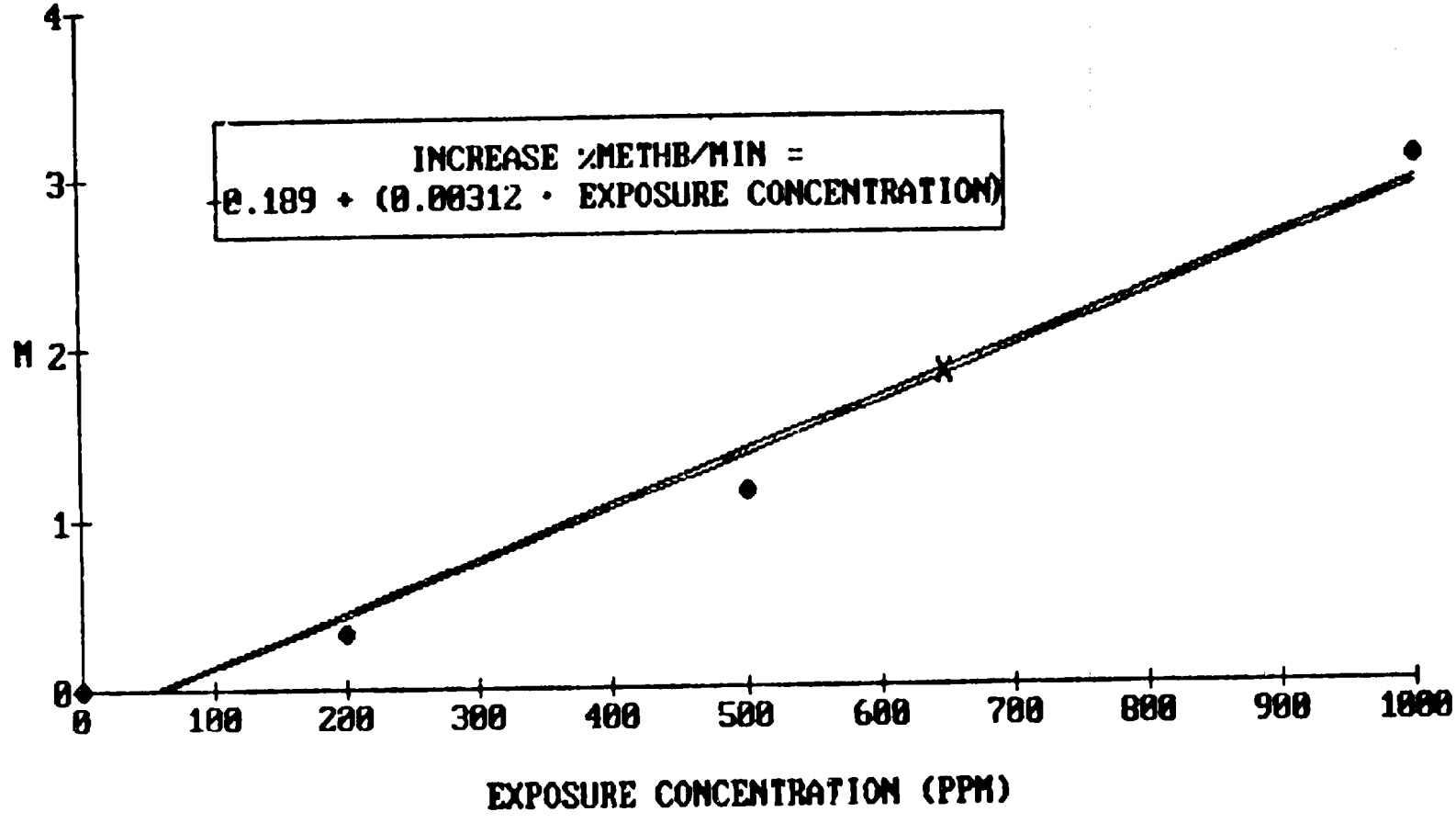

Figure 9: Values for m as related to exposure concentration. X: value for m when minute ventilation was increased 1.6 fold.

SUMMARY

A model has been developed to relate **NO** exposure concentrations to the rate of **MetHb** formation in the rat. The model indicates that the rate of **MetHb** formation is proportional to **NO** exposure concentration. Additionally, the rate of **MetHb** accumulation most simply models as the product of minute ventilation and exposure concentration; increasing minute ventilation during the inhalation of a given concentration of **NO** results in a proportional increase in the rate of **MetHb** formation. The model also accounts for the removal of **MetHb** both during and after **NO** exposures. Future **NO** exposure studies with simultaneous ventilatory measurements should more closely refine estimates for m and K_{out}.

In the original model K_{OUT} was estimated as a pooled value from all collected MetHb elimination data, without considering how the saturation level of MetHb achieved in a given exposure to NO may have impacted on this parameter. While the previously described model rather closely approximated the actual experimental data, the MetHB elimination data shown in Figure 10 has suggested to us that K_{OUT} may actually be a function of the % saturation of MetHB achieved during an exposure to NO in that the rate of MetHb elimination appears to diminish as the maximal %MetHb attained increases. Such a relationship is further suggested by the data shown in Figure 11, where the various K_{OUT}s obtained after several different NO exposure regimens are plotted against the natural log of the maximal percentage of MetHb saturation achieved during each exposure. It would appear, accordingly, that K_{OUT} may be more suitably modeled as a continuously changing variable during the accumulation of MetHb during NO exposure.

From the data shown in Figure 11, it was estimated that:

$$-K_{OUT} = (0.01) \ln \%MetHb + (-0.05), \text{ or}$$
$$K_{OUT} = (-0.01) \ln \%MetHb + (0.05).$$

We next solved for "m" during the NO exposure-MetHb accumulation phase, while considering K_{OUT} as being a continuously changing parameter that varys with the %MetHb present at a given time. The accumulation of MetHb during three exposure conditions was modeled using Newton's method. The exposure conditions were: 1000 ppm NO x 23 min (3.035), 500 ppm x 15 min (1.221), and 200 ppm x 120 min (0.486). The values in the parentheses are for "m". The results of this change in the model relative to fitting the actual experimental data are summarized in Figure 12. The fits are nearly exact, and they are well within the error of the actual MetHb measurements.

Some problems with the model persist and require further investigation. For example, use of continuously changing K_{OUT}s for the MetHb elimination component of the model have as yet to be evaluated, but the inclusion of such a feature in the model may be useful. In the initial form of the model, K_{OUT} was assumed to be a first order process, and this assumption resulted in reasonably good fits between the model's results and the empirically-derived data. However, if K_{OUT} is an unvarying constant, one interpretation of the data summarized in Figure 10 is that the mechanism(s) underlying the removal of MetHb following cessation of NO exposure may be increasingly compromised with increasing maximal %MetHb achieved during an exposure. Given our original assumption that the rate of removal of MetHb is first order, which was based on our initial

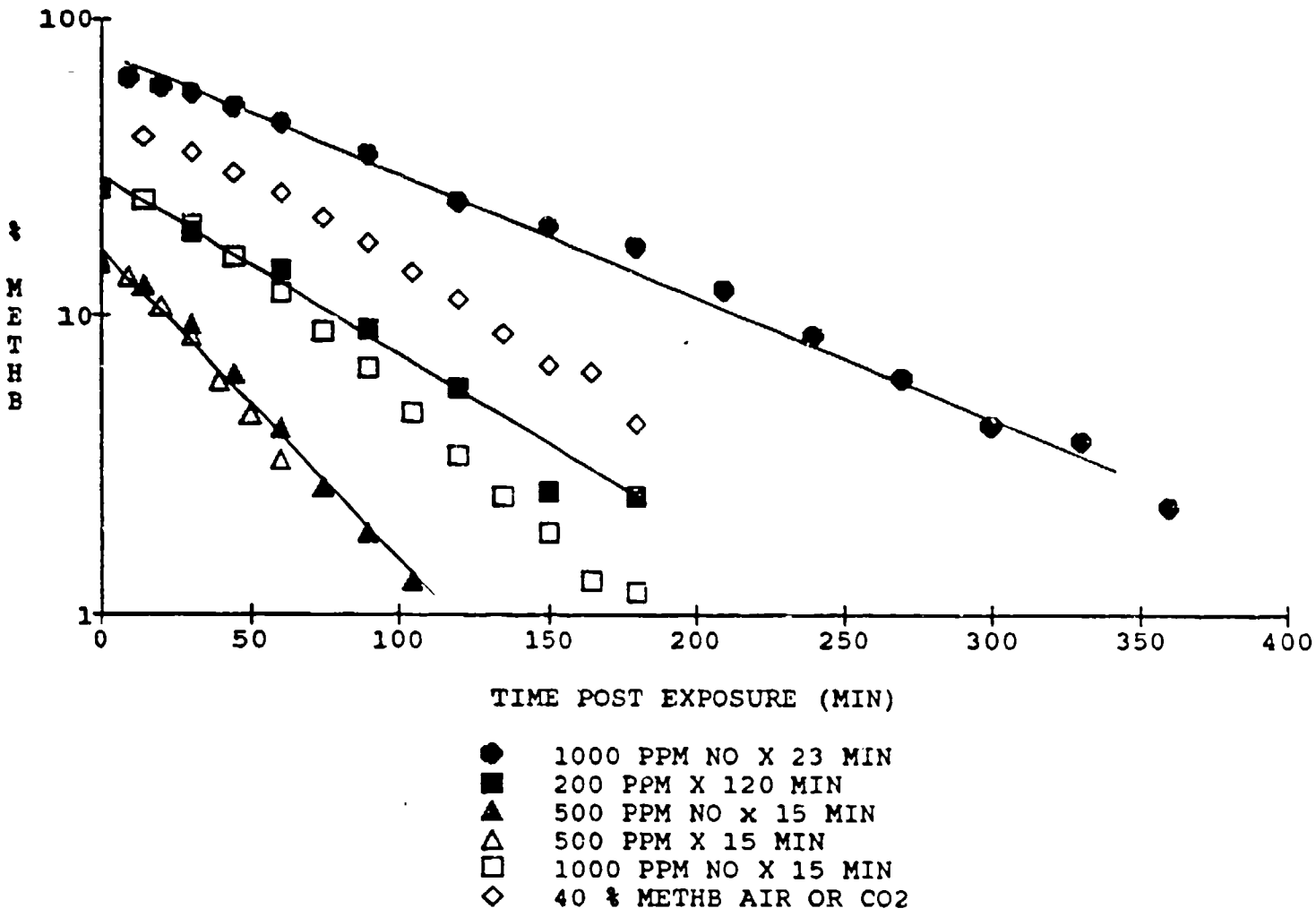

Figure 10: Elimination kinetics of MetHb modeled as a simple first order process.

Figure 11: Plot of -K_{OUT} (slopes) versus the natural log of the maximal MetHb concentrations achieved during several NO exposure studies. The line describing the data was determined by linear regression.

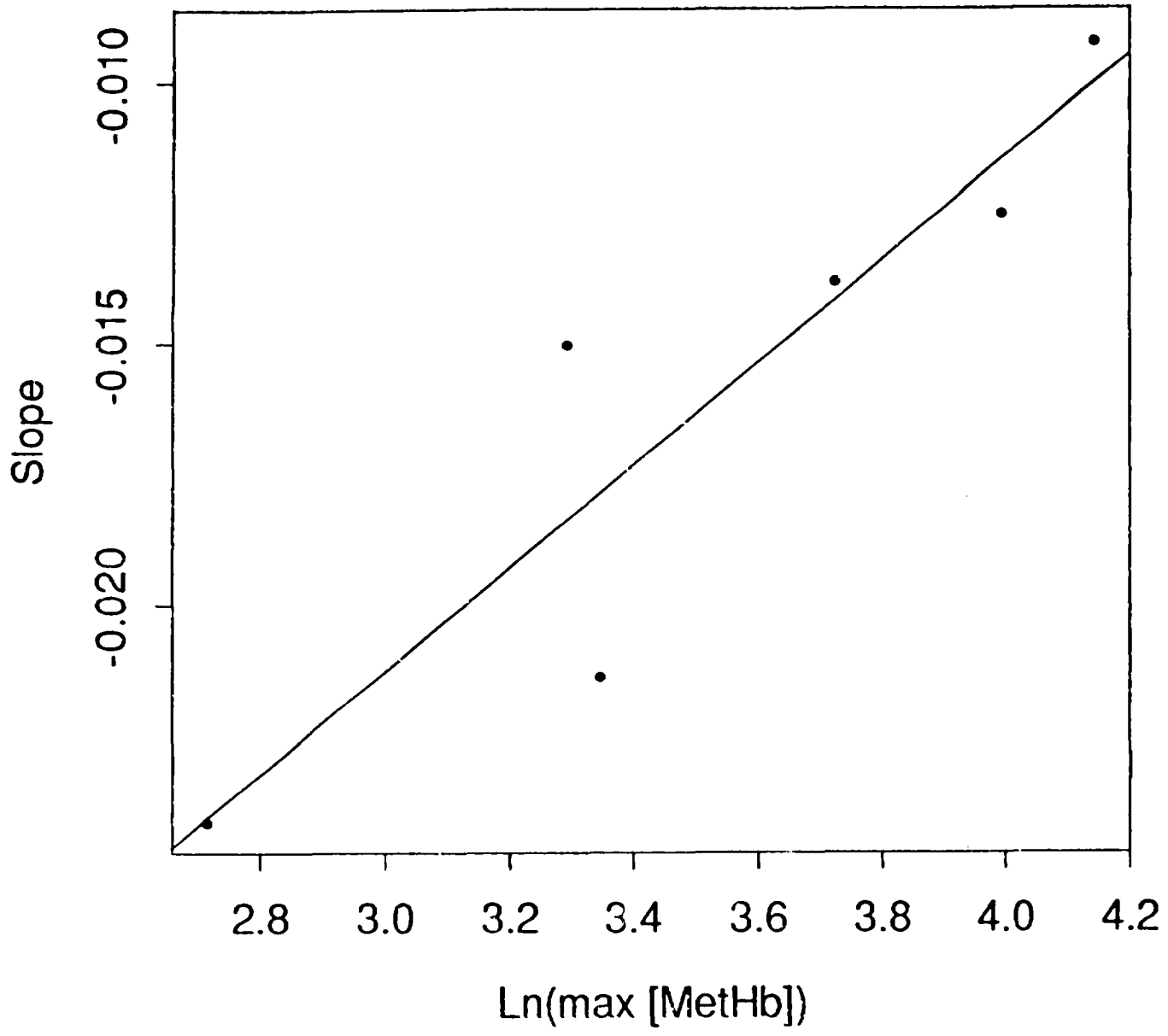

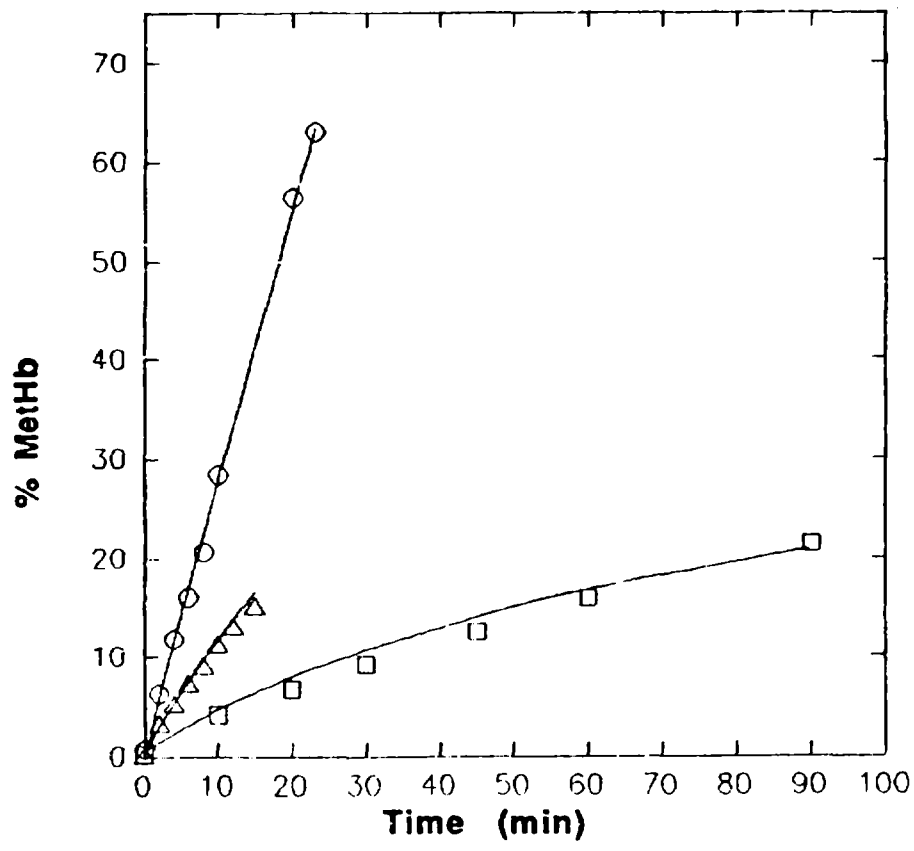

Figure 12: Model fits (lines) of the accumulation of MetHb (experimental data:symbols) during exposure to NO. Circles: 1000 ppm NO; Triangles: 500 ppm NO; Squares: 200 ppm NO.

analyses of MetHb elimination data collected as of the time of development of our first model, a persistence in the "poisoning" of the MetHb elimination mechanism would be predicted. However, we have been unable to demonstrate such an effect. Figure 13 summarizes the results from a study in which rats were exposed to 1000 ppm NO to bring about an ~65% MetHb saturation level in their blood. After a post-exposure period during which MetHb was allowed to decrease to a saturation level of <5%, the rats were re-exposed to NO to raise their %MetHb to ~20%, and the rate of MetHb elimination thereafter was monitored. No evidence was found to support a persistent retardation in MetHb elimination due to the animals having had a recent history of a high percentage of MetHb saturation. We are reaching the conclusion that K_{OUT} during the elimination of MetHb should not be modeled as a simple first order process. Indeed, more recent data, such as those summarized in Figure 14, strongly suggest K_{OUT} cannot be simply viewed so simplistically.

It should be noted that the above modifications to the model were made in collaboration with Dr. Richard Posner, a postdoctoral fellow in the Life Sciences Division at the Los Alamos National Laboratory.

Recent Reports, Publications Emanating From This Project

Stavert, D.M., Lehnert B.E.: Nitric oxide and nitrogen dioxide as inducers of acute pulmonary injury when inhaled at relatively high concentrations for brief durations. *Inhalation Toxicology* 2:53-67, 1990.

Lehnert, B.E.: Toxicology of nitric oxide and nitrogen dioxide. In: *Handbook of Hazardous Materials.* (M. Corn, ed.) Academic Press, San Diego, CA (in press), 1991.

Martinez, M., Archuleta, D., Stavert, D.M., Lehnert, B.E.: Nitrogen dioxide (NO_2) induced acute lung injury relative to increased minute ventilation during NO_2 exposure. 1991 Society of Toxicology Annual Meeting, Dallas, TX, February 25-March 1, 1991. *The Toxicologist* 11(1):A340, 1991.

Lehnert, B.E., Stavert, D.M.: Potentiation of lung injury by exercise following the inhalation of toxic gases: Evidence consistent with a postulated mechanism. 1991 Society of Toxicology Annual Meeting, Dallas, TX, February 25-March 1, 1991. *The Toxicologist* 11(1):A336, 1991.

Lehnert, B.E., Stavert, D.M., Ellis, T., Session, W.S., Gurley, L.R.: Kinetics of lung free cell and bichemical changes in lavage fluids following exposure to a high concentration of nitrogen doxide (NO_2). 1992 Annual Meeting of the Society of Toxicology, Seattle, WA, 1992.

Figure 13: Lack of an effect of an initially high saturation MetHb level on the rate of removal of MetHb achieved by as second NO exposure. If the initially high MetHb level persistently compromises MetHb elimination, the rate of MetHb elimination observed after the second exposure should be prolonged, e.g., ~ the same as that observed with the high MetHb level.

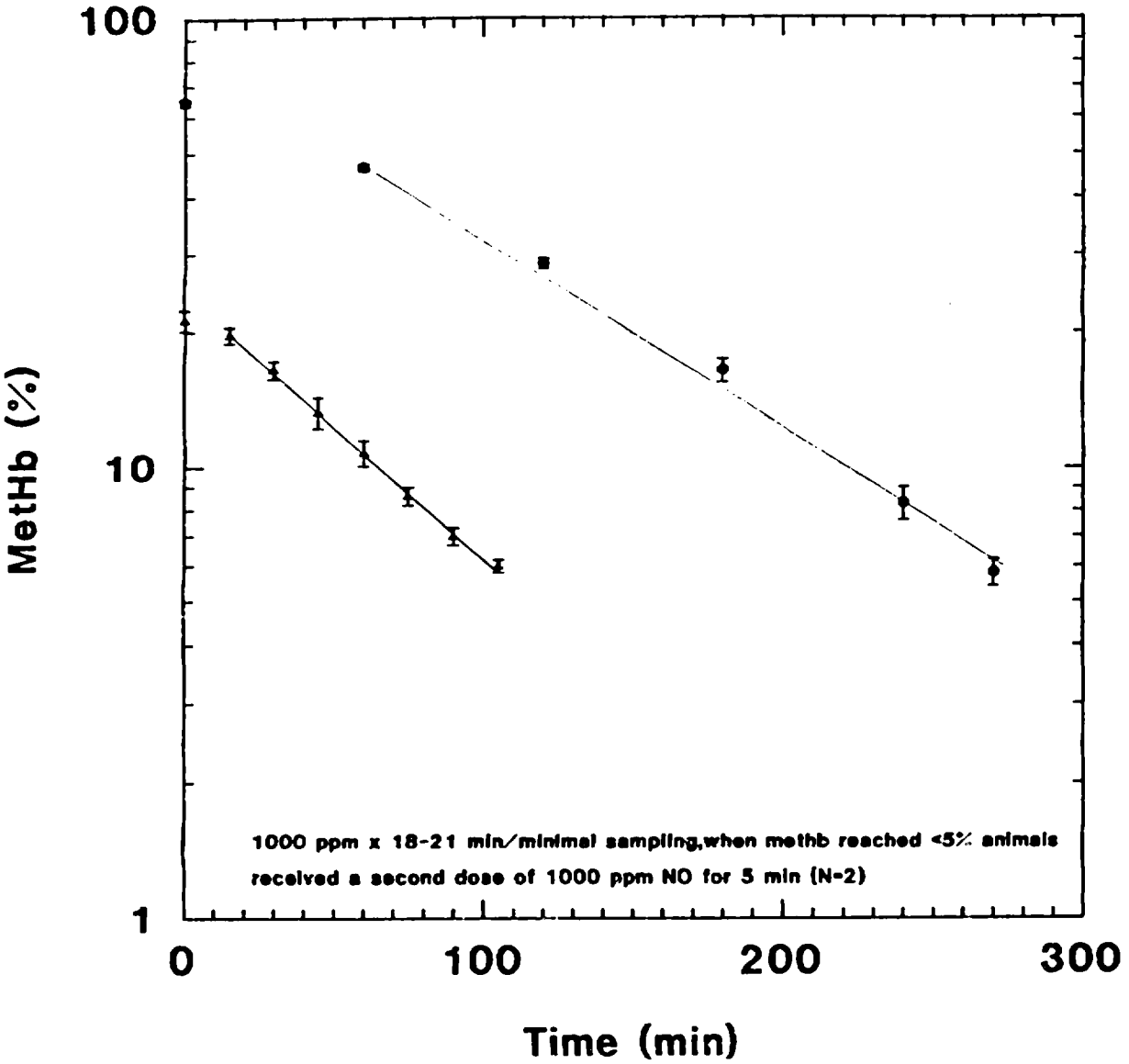

Figure 14: Complexity of the pattern of MetHb elimination when examined over a prolonged period after the exposure of rats to 1000 ppm NO for 18-25 min.